CENTRAL REGION
APPLIED RESEARCH PAPERS
NO. 9

April 1993

NATIONAL WEATHER SERVICE CENTRAL REGION SERIES OF CENTRAL REGION APPLIED RESEARCH PAPERS (CRARP)

The NWS Central Region Applied Research Paper (CRARP) series is an informal medium to compile and distribute a small part of the on-station research efforts being performed by the operational personnel of the Central Region. As the National Weather Service becomes more involved in using high technology to sample, describe, and forecast the weather, this medium has been made available to encourage the transfer of useful knowledge and skills to other NWS offices. Many times on-station research efforts and case studies are only circulated locally due to the time and effort required to put the study into "publishable" form (both text and graphic). The following CRARP compilations are a vehicle to distribute scientific and operational information to other NWS offices without forcing the authors to perform the time-consuming work typically required to "pretty up" the figure.

The first three were published as Technical Memoranda: (1) CR 88 "Central Region Applied Research Papers 88-1 through 88-7," (2) CR 97 "Central Region Applied Research Papers 97-1 through 97-6," and (3) CR 99 "Central Region Applied Research Paper 99-1 through 99-7." Central Region Applied Research Papers Nos. 3 and 4 were a first attempt at starting a new series numbering system. However, due to an editorial error, CRARP No. 6 served as the beginning point for accurately reflecting the numbering for this series.

NWS CR 88	Central Region Applied Research Papers 88-1 through 88-7, May 1988.
NWS CR 97	Central Region Applied Research Papers 97-1 through 97-6, July 1989.
NWS CR 99	Central Region Applied Research Papers 99-1 through 99-7, November 1989.
CRARP No. 3	Central Region Applied Research Papers 3-1 through 3-7, July 1990.
CRARP No. 4	Central Region Applied Research Papers 4-1 through 4-5, December 1990.
CRARP No. 6	Central Region Applied Research Papers 6-1 through 6-7, May 1991.
CRARP No. 7	Central Region Applied Research Papers 7-1 through 7-4, November 1991.
CRARP No. 8	Central Region Applied Research Papers 8-1 through 8-6, September 1992.

TABLE OF CONTENTS

CENTRAL REGION APPLIED RESEARCH PAPER 9-1

AN ANALYSIS OF THE SOUTH CENTRAL NEBRASKA FLASH FLOOD OF JULY 8-9 1991

Brian P. Walawender[1]
National Weather Service Office
North Platte, Nebraska

1. Introduction

On the night of July 8 and the morning of July 9, 1991, two to five inches of rain fell over parts of south central and east central Nebraska and southwest Iowa. The heaviest rain occurred along the Platte River Valley from Grand Island to Plattsmouth (Figure 1). Most of this rain fell in a two to three hour period. The heavy rain was produced by a quasi-stationary mesoscale convective system (MCS). This paper will explore the synoptic and mesoscale factors which led to the development of this quasi-stationary MCS.

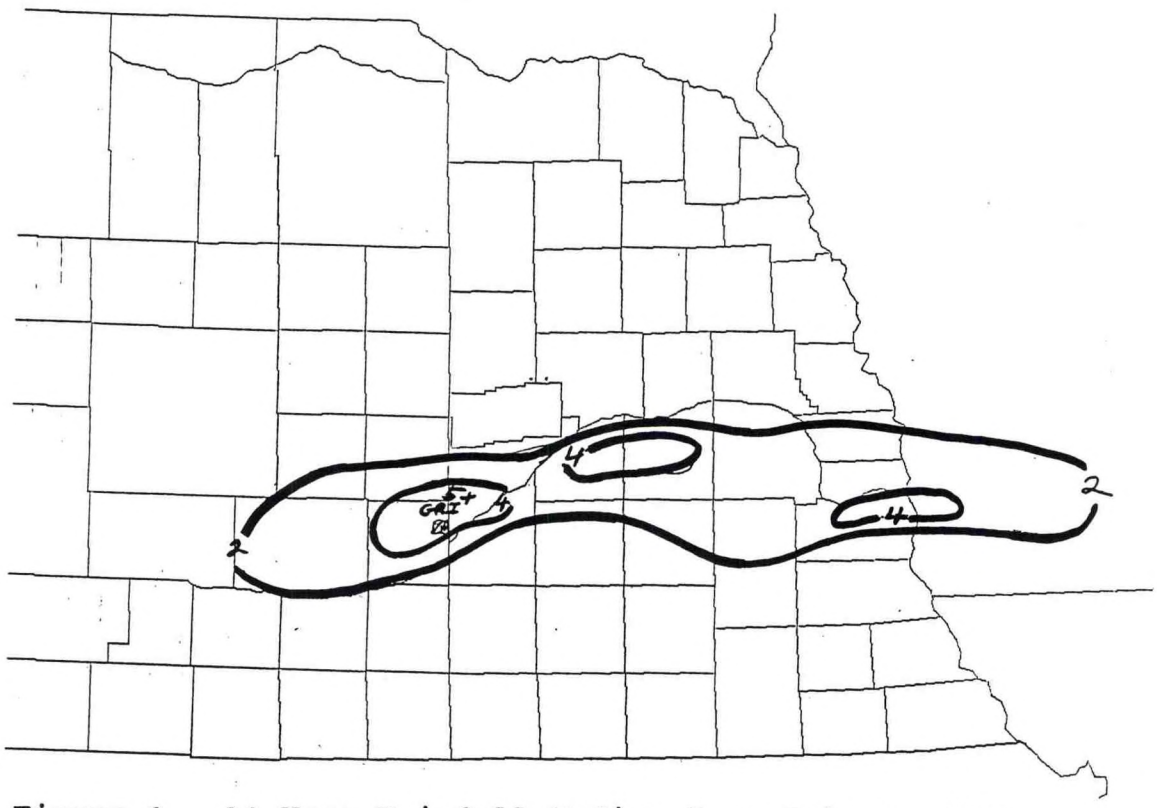

Figure 1. 24 Hour Rainfall Ending 7 am July 9, 1991

[1]Current Affiliation: National Weather Service Forecast Office Topeka, KS

2. The Case Study

A. Surface Data

At 0000Z July 9, 1991, a stationary east-west frontal boundary extended across northern Colorado into southeast Kansas. A weak mesolow was located along the frontal boundary near Dodge City (DDC). A 1018 mb high was located over northern Iowa near Mason City (MCW). A moist axis of 60°F plus dew points were located along the front across Kansas.

At 0300Z, the frontal boundary had moved little as the high remained centered near MCW. The weak mesolow also remained quasi-stationary along the front near DDC.

By 0600Z, some changes had taken place. The high had shifted eastward into Minnesota allowing the frontal boundary to shift northward over eastern Kansas. At 0600Z, the frontal boundary (Figure 2) was on an Akron (AKO) to Goodland (GLD) to Salina (SLN) to Kansas City (MCI) line. The mesolow had also shifted northeast to SLN at 0600Z. Temperatures to the south of the frontal boundary remained very warm, in the 80s, with cooler 60s to the north of the boundary.

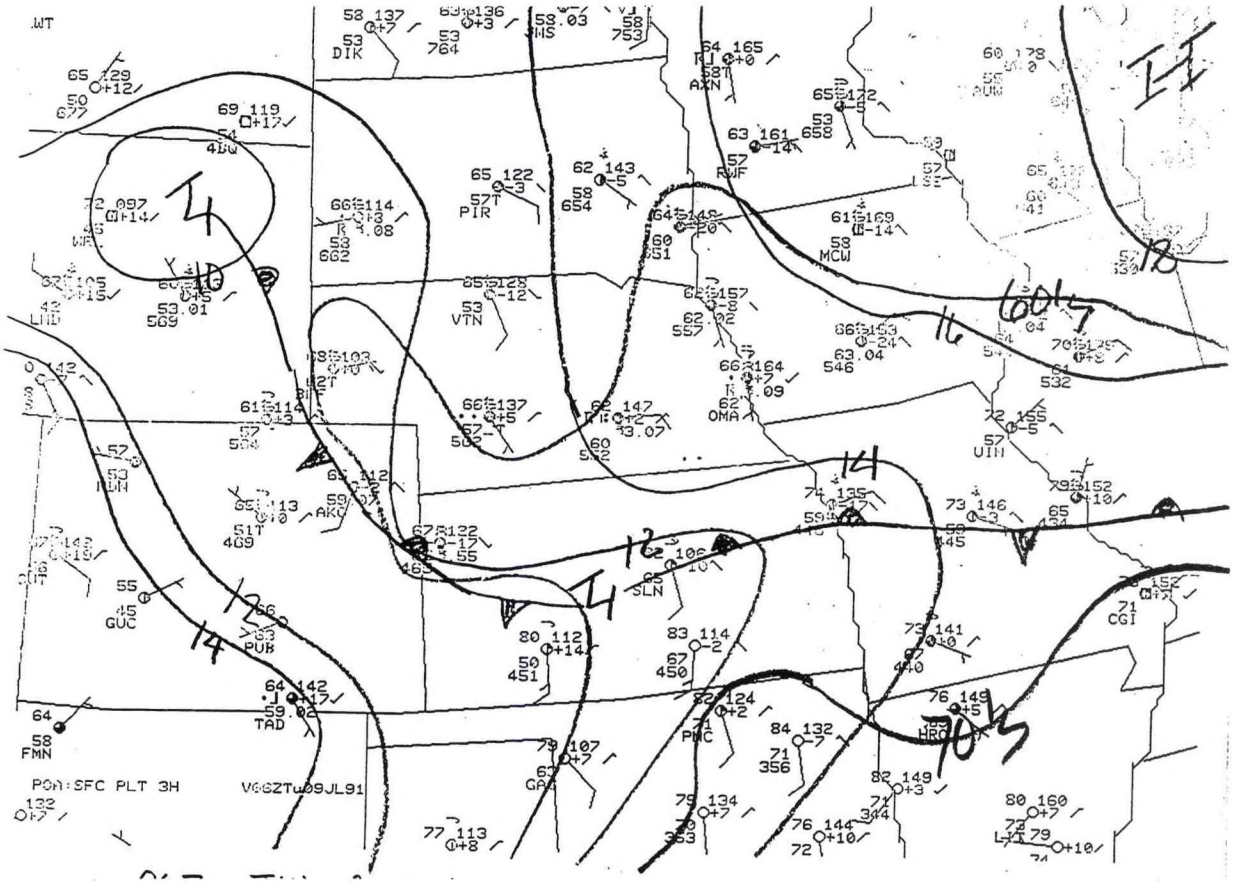

Figure 2. 0600Z July 9, 1991 Surface Map.

B. Sounding Data

The 0000Z radiosonde data (Figure 3) from North Platte (LBF) showed a frontal inversion at 780 mb with directional shear mainly confined to the layer from 800 to 700 mb. Wind speeds were relatively weak below 400 mb (under 35 kts). The sounding was quite moist with a precipitable water of 1.29 inches. Using conventional stability parameters the sounding was relatively stable (LBF Showalter index +2). However, the air mass to the south of the boundary was quite unstable (Topeka (TOP) Showalter index -5).

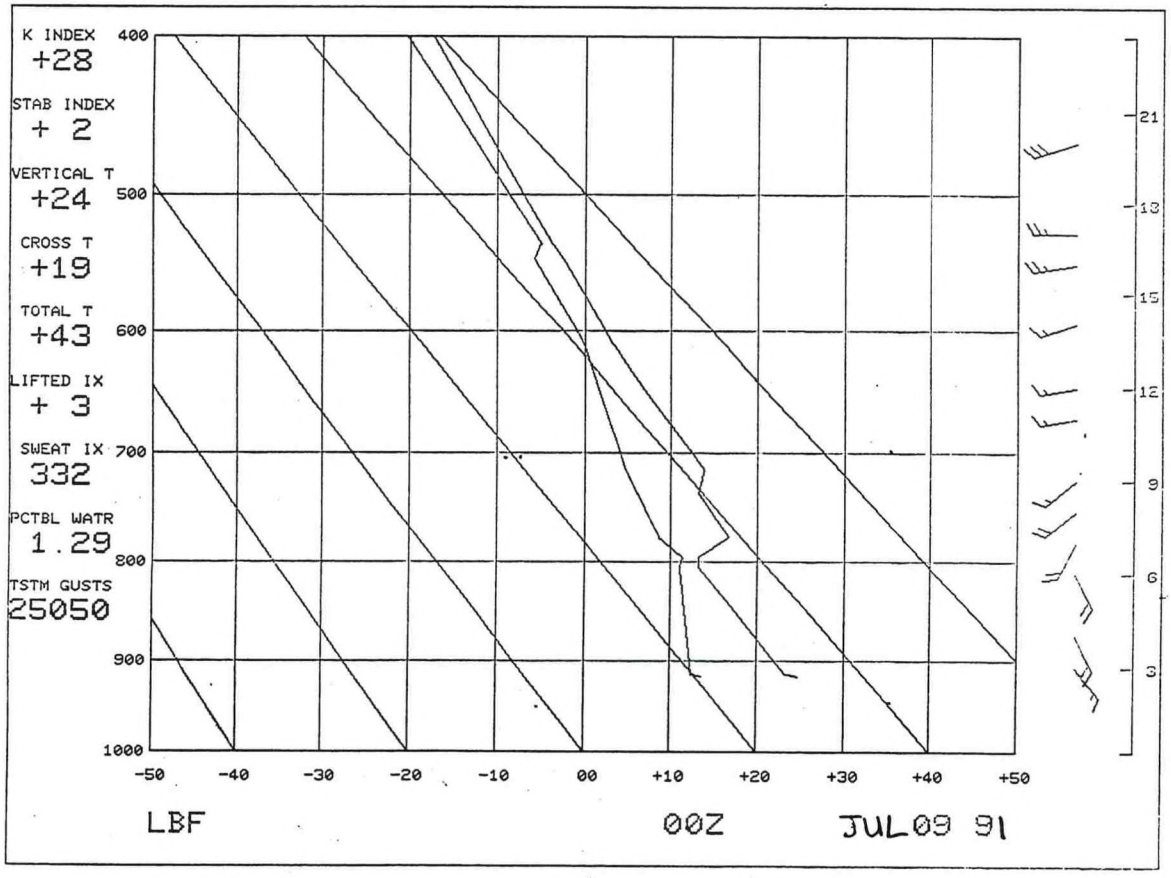

Figure 3. 0000Z July 9, 1991 North Platte (LBF) sounding.

C. Upper Air Data

The 0000Z 850 mb analysis (Figure 4) showed a ridge from northern Minnesota to southern Louisiana. Strong warm air advection was taking place to the west of the ridge over southern Nebraska and northern Kansas. The 850 mb frontal boundary was

located slightly east and north of the surface front from Rapid City (RAP) to between DDC and LBF to Topeka. A moist axis of 12°C dew points extended from southern Texas into northeast Kansas. The 850 mb theta-e analysis showed a ridge across southern Kansas and central Missouri from DDC to St. Louis (STL).

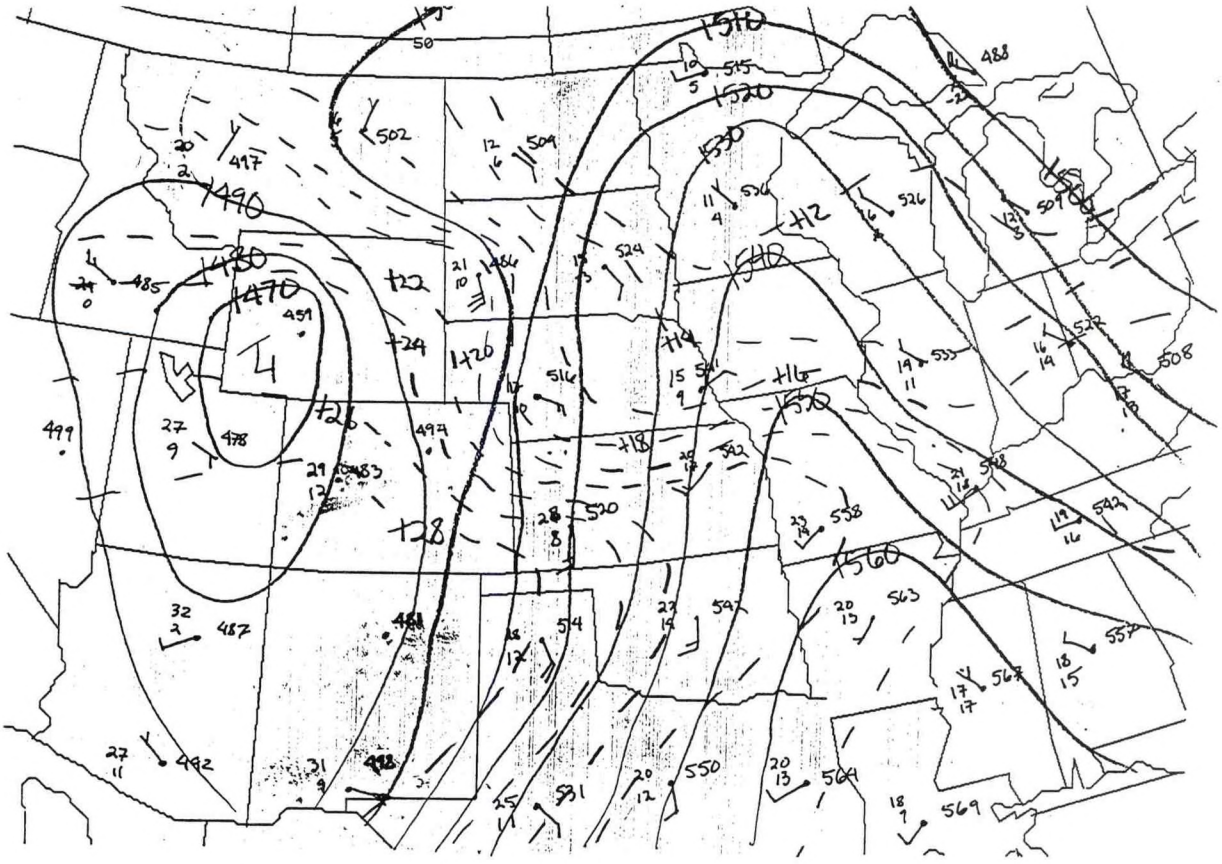

Figure 4. 0000Z July 9, 1991 850 mb Analysis.

The 0000Z 700 mb analysis showed a weak flow pattern over the Central Plains with a weak short wave trough extending from Glasgow (GGW) to Denver (DEN). At 700 mb the frontal boundary was evident over southern South Dakota and Nebraska from RAP to Omaha (OMA).

The 0000Z 500 mb pattern over the Northern Plains was zonal. A weak short wave trough was located over the Rockies from GGW to Lander (LND). A pool of nearly saturated air (dew point depression < 5°C) extended from northern New Mexico into eastern Nebraska.

The 0000Z 250 mb analysis showed a 75 kt jet from northeastern Wyoming into the Great Lakes region. This placed Nebraska in the favored right rear quadrant of the jet max.

The 850/500 mb thickness analysis (Figure 5) had a strong gradient oriented northwest to southeast from northwestern South Dakota to northeastern Nebraska. A diffluent thickness pattern was located over south central and southeastern Nebraska, eastern Kansas and western Missouri.

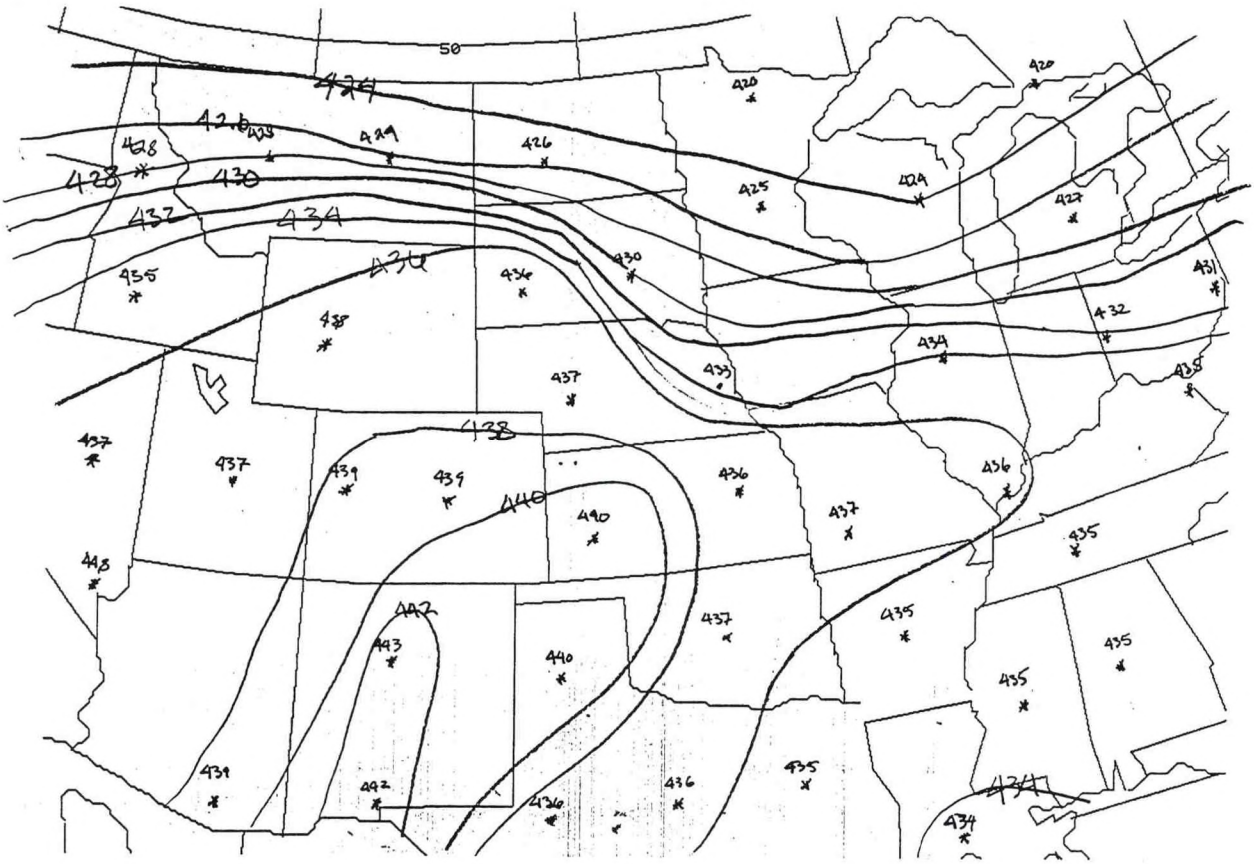

Figure 5. 0000Z July 9, 1991 850-500 mb Thickness Analysis

D. Satellite Imagery

1. Water Vapor

The 0300Z water vapor satellite imagery (Figure 6) showed a deep "Mexican connection" of mid- and high-level moisture, as described by Scofield and Robinson (1990). Moisture was flowing northward from the eastern Pacific through Mexico and New Mexico into Colorado, Kansas, and Nebraska.

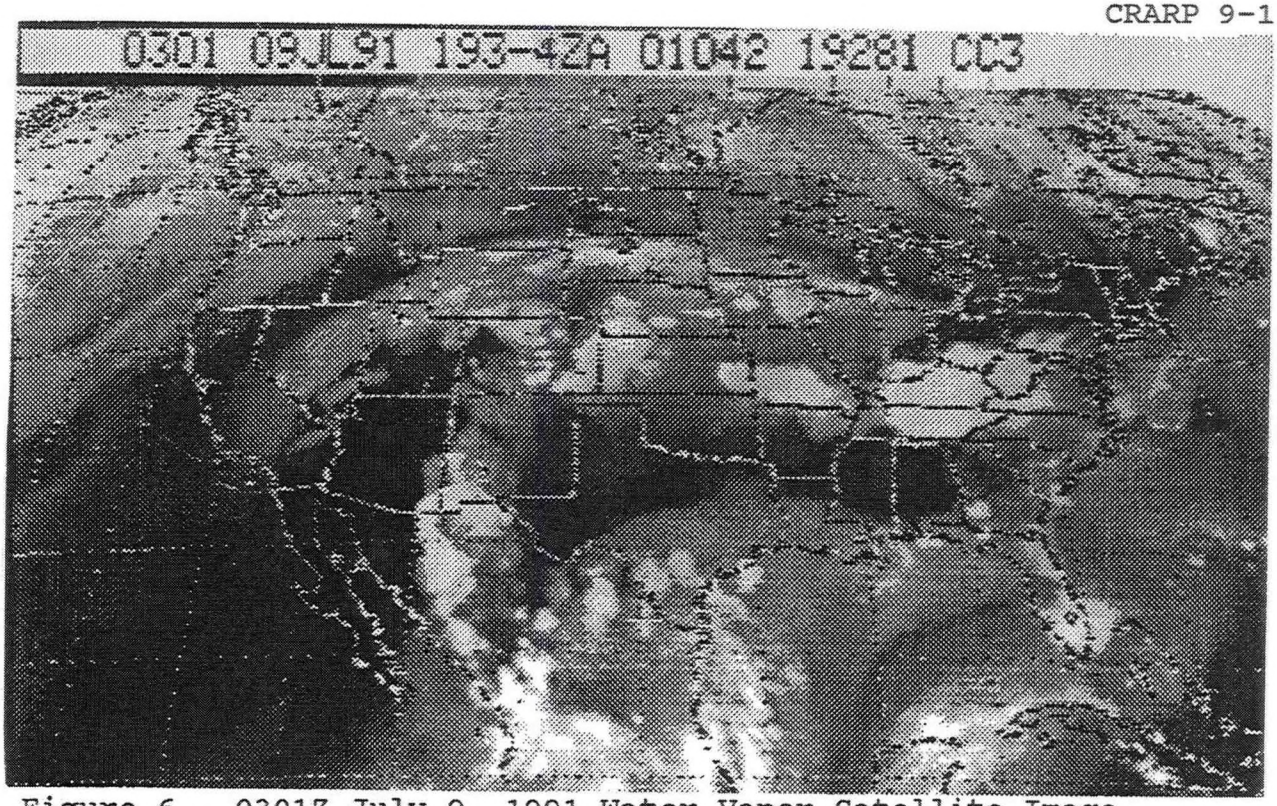

Figure 6. 0301Z July 9, 1991 Water Vapor Satellite Image.

2. IR (Pre MCS Stage)

At 0200Z, deep convection was occurring along the stationary frontal boundary in northeast Colorado and southeast Kansas. By 0300Z (Figure 7), the convection over southeast Kansas had weakened and the convection over northeast Colorado had moved into northwest Kansas and extreme southwest Nebraska. Convection had also begun to develop over south central Nebraska. At 0400Z, the complex of storms over northwest Kansas had slowed as it moved into north central Kansas. The convection over south central Nebraska continued to slowly intensify showing little movement. By 0500Z, the convection over south central Nebraska had exploded into a MCS and expanded into southeast Nebraska (Figure 8). The complex over north central Kansas was weakening and was moving towards the southern Nebraska complex.

3. IR (MCS Stage)

At 0600Z (Figure 9), the MCS continued to develop and expand rapidly covering all of southeast and south central Nebraska. The MCS had shown little movement since 0600Z. The enhancement of the complex since initiation had remained in the black on the MB scale (-58 to -62°C) with isolated patches of repeat gray (-62 to -80°C). Between 0600Z and 0800Z, the MCS showed little change in enhancement and very little movement. After 0800Z, the complex began to dissipate.

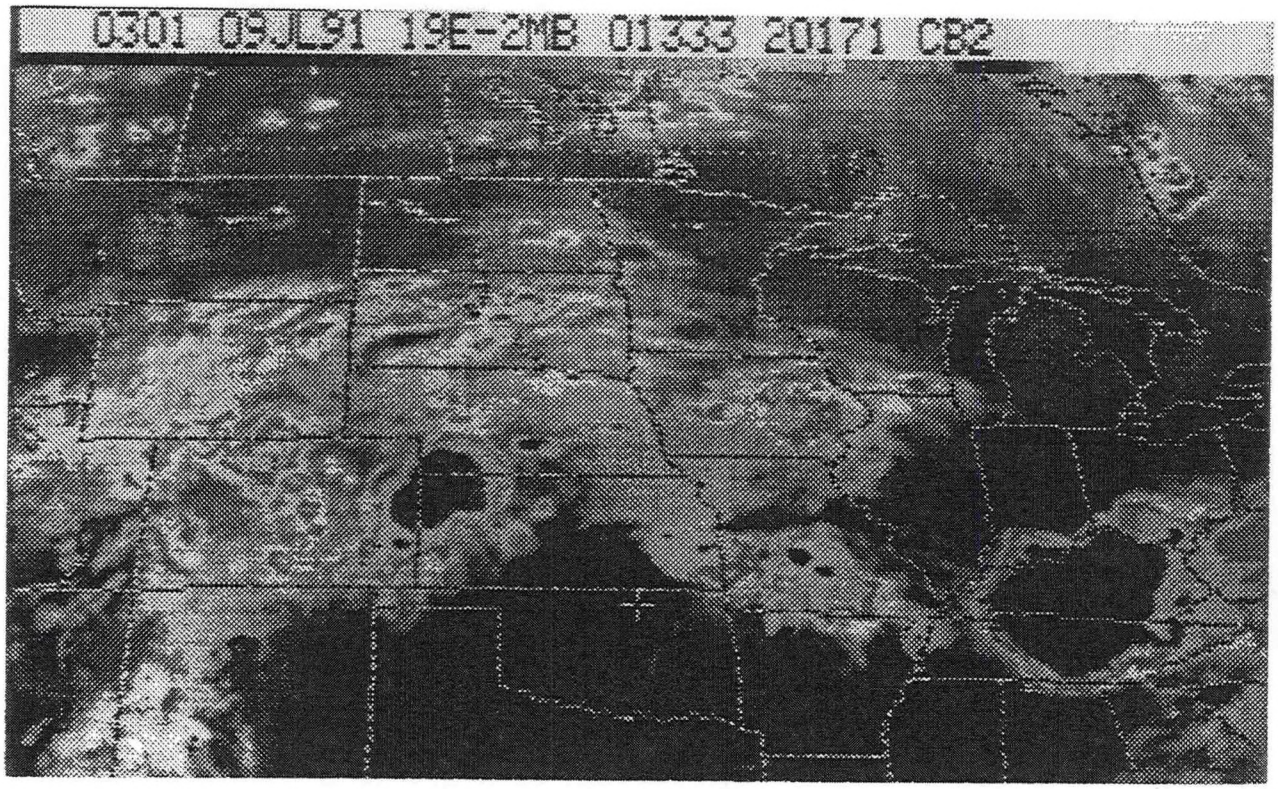

Figure 7. 0301Z July 9, 1991 IR Satellite Image (MB enhancement).

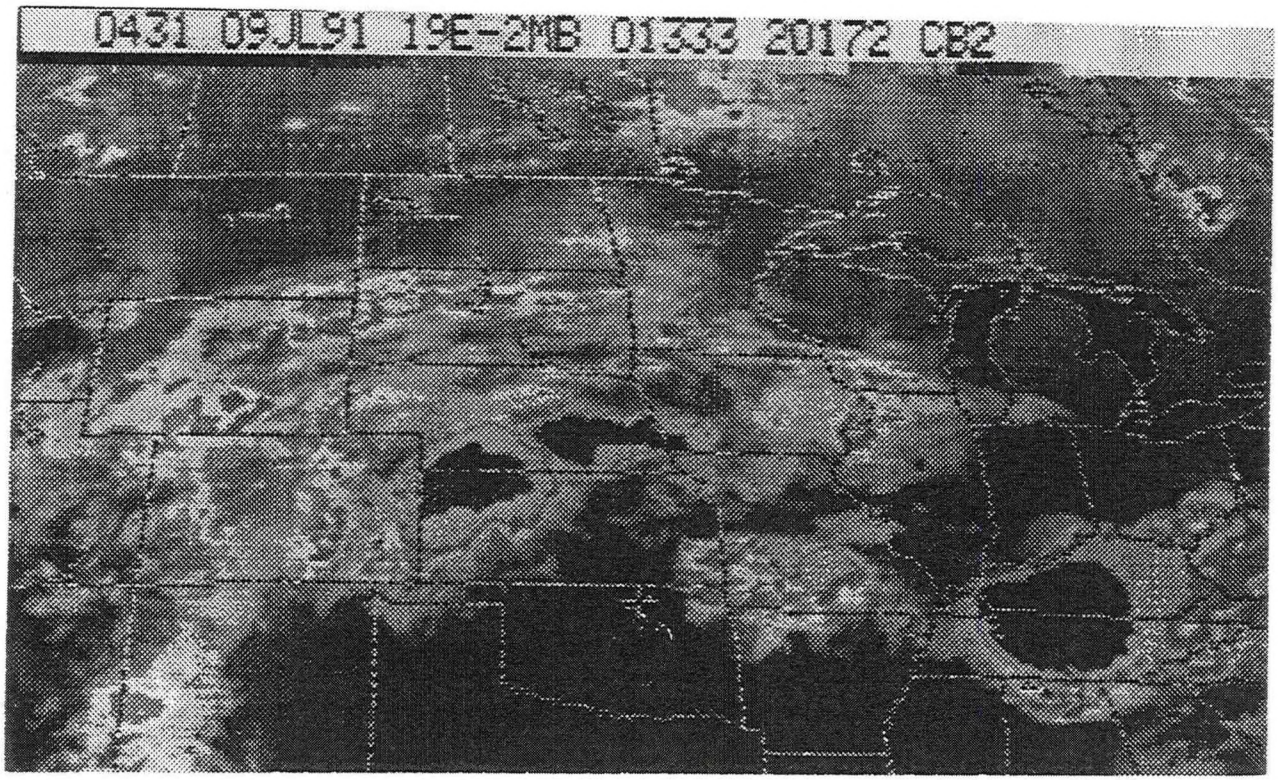

Figure 8. 0431Z July 9, 1991 IR Satellite Image (MB enhancement).

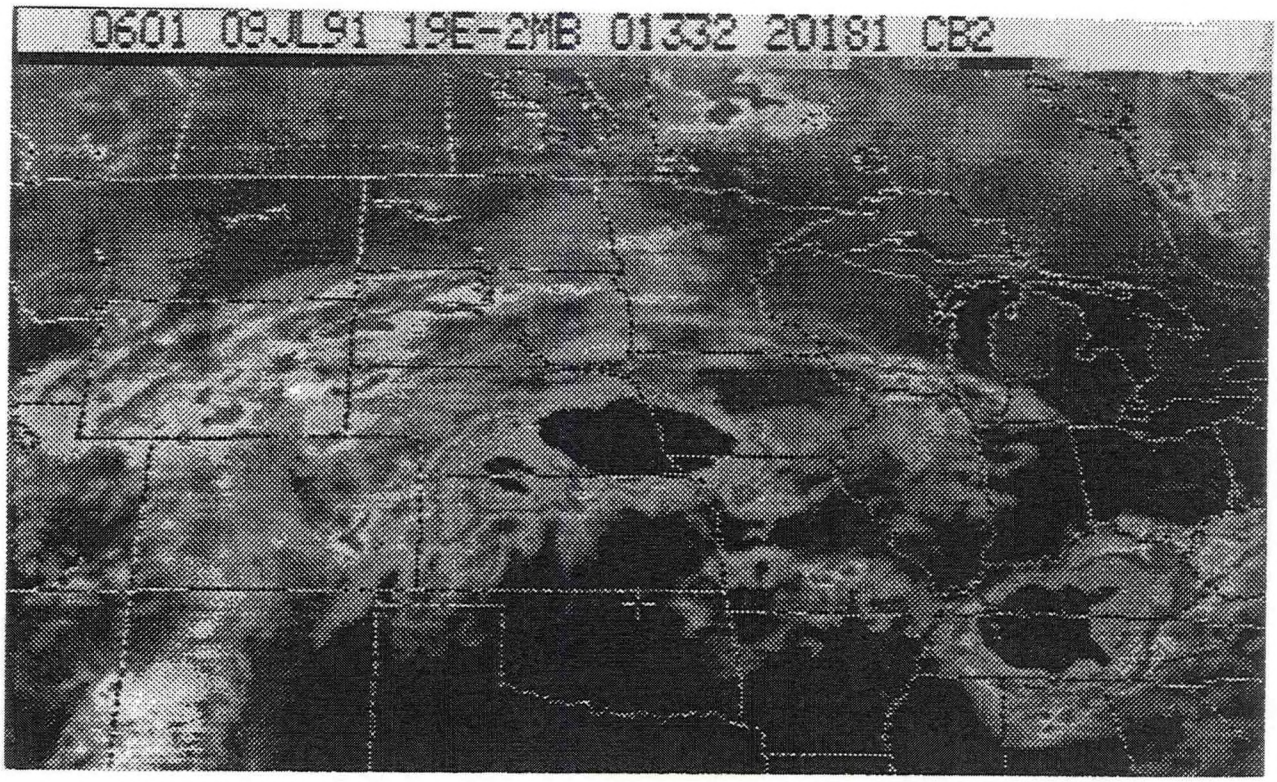

Figure 9. 0601Z July 9, 1991 IR Satellite Image (MB enhancement).

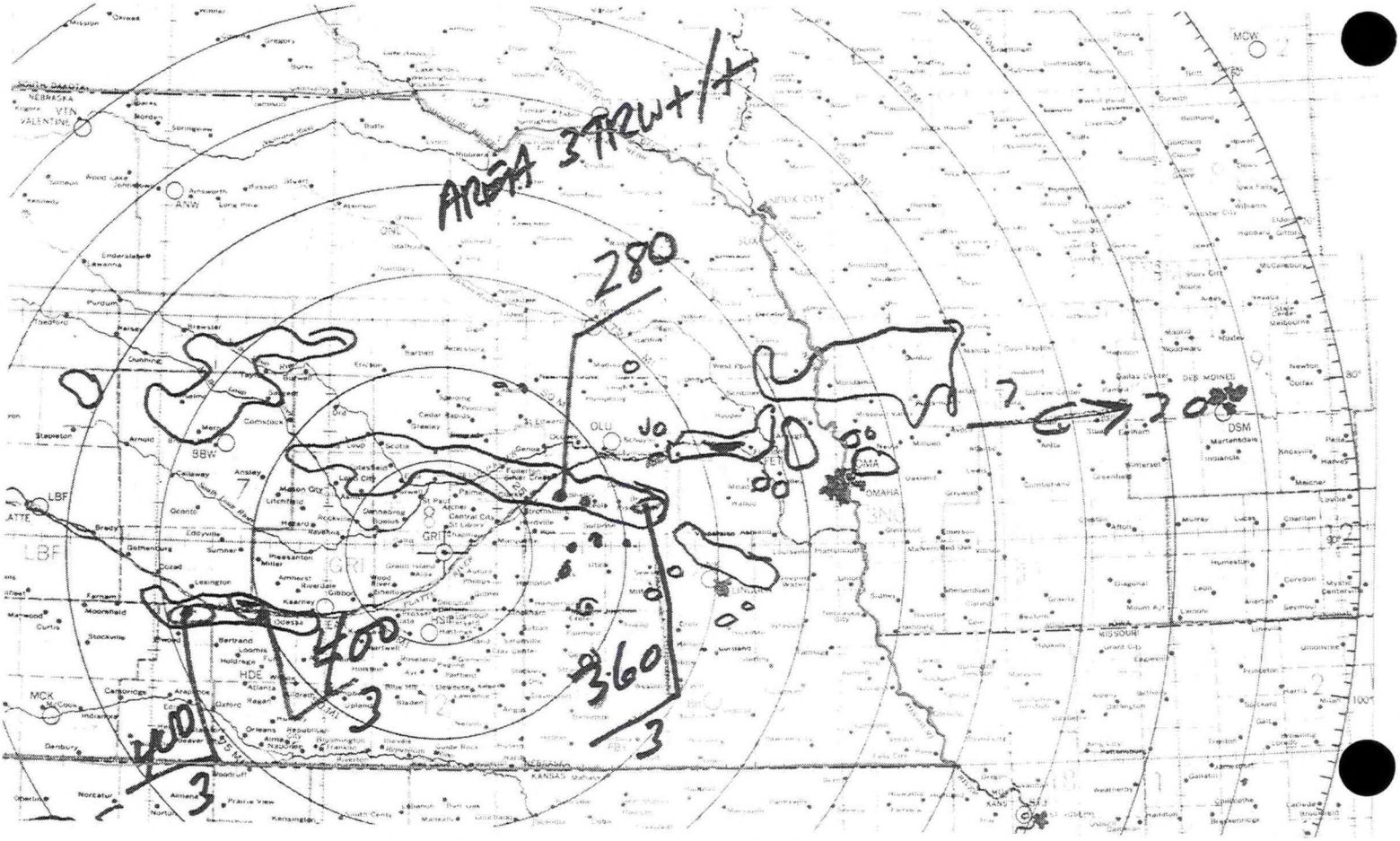

Figure 10. 0234Z July 9, 1991 Grand Island (GRI) Radar Overlay.

E. Radar

Grand Island (GRI) recorded the first echoes around 0230Z (Figure 10) about 50 to 75 miles west of GRI. The echoes were VIP 3 with tops of 40,000 feet, and were moving from 270 at 30 kts. By 0330Z, the area of echoes had expanded and intensified to VIP 5. The echoes were 25 to 50 mi west of GRI and continued to move from 260 at 30 kts. From 0430Z to 0730Z (Figure 11), the MCS remained quasi-stationary over south central Nebraska with new cells developing along the western flank of the complex (about 50 miles west of GRI). The cells would then move east at 20 kts through the complex. After 0730Z, the complex began to shift eastward and weaken.

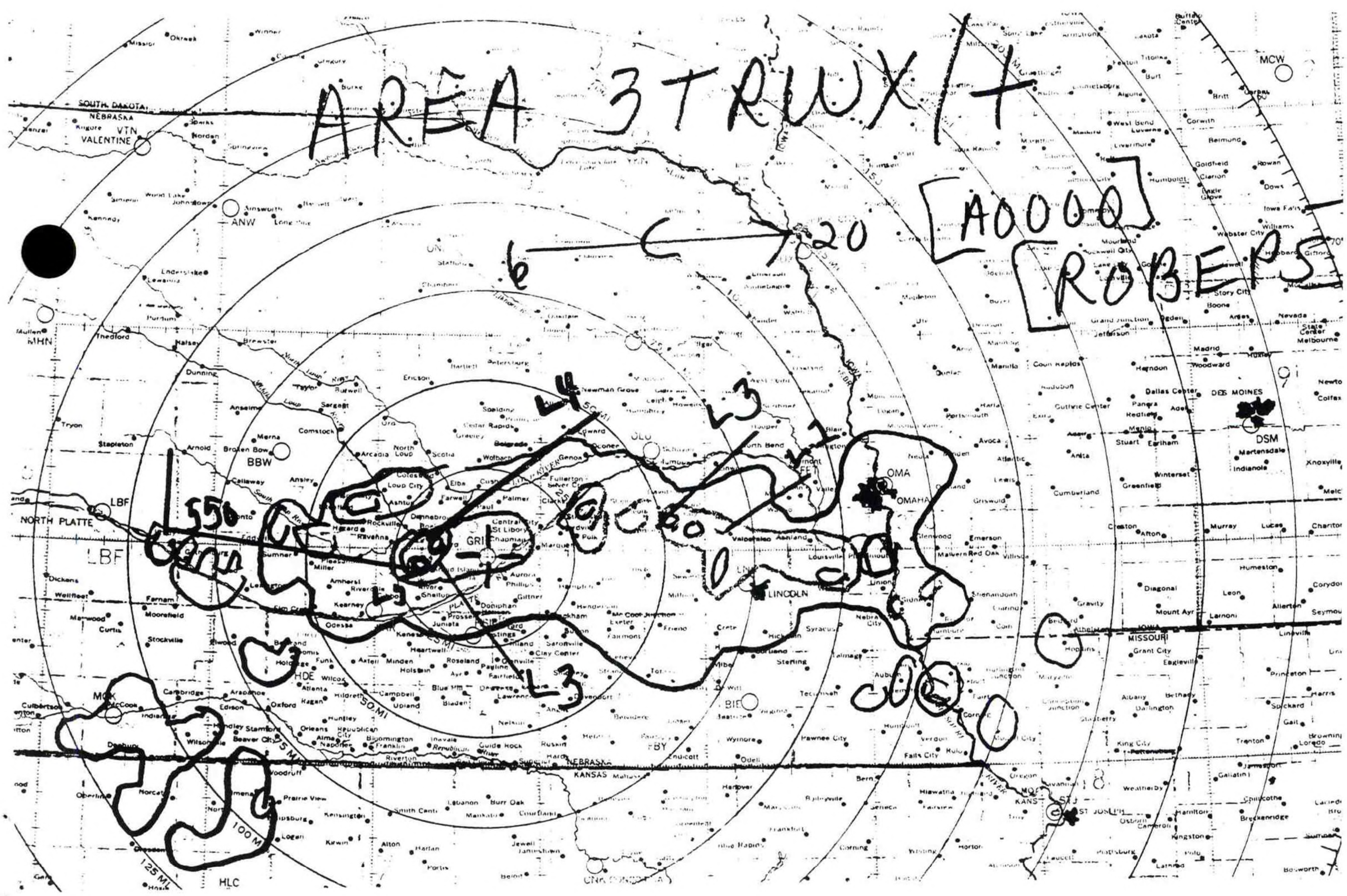

Figure 11. 0535Z July 9, 1991 Grand Island (GRI) Radar Overlay.

3. Conclusions

A. Meteorological Pattern

By studying the data above, the event could easily be categorized as a frontal forcing type pattern (Maddox et al 1979). Frontal forcing patterns are characterized by: a stationary frontal boundary (usually oriented west to east) with the storms occurring north of the boundary, upper level winds which flow parallel to the frontal boundary, an approaching short wave trough, vertical flow which veers sharply below 700 mb with little veering above 700 mb, and a strong nocturnal tendency (Chappel 1986). In some cases, there may also be a weak mesolow along the frontal boundary.

In the July 8-9, 1991 case, a west to east stationary frontal boundary was located to the south over Kansas. The upper level wind flow was parallel to the frontal boundary. An approaching short wave trough was over eastern Wyoming and eastern Montana. Vertical wind shear was weak outside of the frontal zone. A weak mesolow moved along the frontal boundary in central Kansas increasing convergence. The heavy rains occurred after midnight CDT, the time of characteristic diurnal convective maximum for eastern Nebraska. These factors set the stage for the quasi-stationary MCS to develop over south central Nebraska.

B. Storm Movement and Propagation

By using the radar data, the cell movement and the location of new cell development show why the MCS became quasi-stationary after initiation. Cells would form on the western flank of the MCS (about 25 to 50 miles west of GRI) and then would move east through the MCS. New cells would then develop and move east causing a train-echo effect over GRI. The continued new cell development on the storm flank opposite the direction of cell movement caused the quasi-stationary MCS to develop (Chappel 1986).

C. Thickness Pattern

The 850/500 mb thickness pattern also gave clues to a possible quasi-stationary MCS. The thickness pattern over southern Nebraska and northern Kansas had a relatively weak gradient and was diffluent over the eastern portions of the area. Barlow (1990) noted weak and diffluent thickness patterns to be associated with quasi-stationary or backwards propagating MCS due to stronger low-level convergence and new cell development on the rear flank.

4. Summary

A quasi-stationary MCS can produce very heavy rainfall and flash flooding making them a vital concern of the forecaster. When a forecaster suspects the possibility of MCS formation, a careful study of the upper-air and surface data should be made for the characteristics described in this case study. After the first storms develop, the forecaster should carefully monitor radar and satellite data to watch for repeat cells developing along the storm flank opposite of cell motion. By doing this, the forecaster can remain on top the situation as it develops and issue timely statements, forecasts, and warnings.

5. Acknowledgements

I would like to thank Steve Byrd and Jeff Johnson from WSFO Omaha, Rick Ewald from Central Region SSD, Jim Henderson from NSSFC, and the WSO Grand Island staff for helping me obtain the data for this report.

6. References

Barlow, W., 1990: Forecasting the Propagation of Kansas Mesoscale Convective Systems Using ADAP, Thickness, and Other Stability Fields. *Preprints, 16th Conference on Severe Local Storms*, Amer. Met. Soc., Boston, MA, 288-293.

Chappel, C. F., 1986: Quasi-Stationary Convective Events, *Mesoscale Meteorology and Forecasting*.

Maddox, R. A., C. F. Chappel, and L. R. Hoxit, 1979: Synoptic and Mesoscale Aspects of Flash Flood Events, *Bull. of the Amer. Met. Soc.*

Scofield, R. A., and J. Robinson, 1990: The "Water Vapor Imagery/Theta-E Connection" with Heavy Convective Rainfall, Satellite Applications Information Note 90/7, NOAA/NESDIS.

CENTRAL REGION APPLIED RESEARCH PAPER 9-2

A STUDY OF EXTENDED FORECAST VERIFICATION AT WSO PEORIA--SUMMER 1991

Christopher J. Miller
National Weather Service Office
Peoria, Illinois

1. Introduction

The National Weather Service Office (WSO) at Peoria, Illinois has been issuing extended forecasts for Peoria and vicinity since 1970, but no verification had ever been done. An extended forecast verification study was conducted at Peoria, from June 1 through August 31, 1991 to determine the skill of three to five day precipitation and temperature forecasts at the WSO level.

The hypothesis of the study was, at the WSO level, that precipitation forecasts could be equal or better in skill than guidance, and that three to five day temperature forecasts could show improvement over climatology. Recent extended forecast studies have been undertaken at Weather Service Forecast Offices (WSFOs) in Tennessee (Grant, 1990) and Indiana (De Lisi, 1991). These two studies illustrated diminishing forecast skill by day five. However, some skill over climatology was found in the Indiana study.

This study found that precipitation forecasting skill, at WSO Peoria, was either as good or better than guidance for all three days of the extended period. Temperature forecasts showed improvement over climatology on all three days. This improvement was found to be statistically significant for all high temperature forecasts and the Day Three low temperature forecast. Finally, this study supported the point implied by Livingston and Schaefer (1990), that excessive detail could not be forecast successfully in the extended period on a consistent basis.

2. Methodology

The summer months of 1991 (June, July, & August) were chosen for this study to provide the forecasters with the greatest challenge. According to Harnack (1986), three to five day forecasts for temperature and precipitation exhibited the lowest skill scores during the summer months, based on a study conducted by the National Meteorological Center (NMC) from 1970 through 1983.

The forecasters at Peoria had access to the same graphics used by most forecasters at WSFOs. The most commonly used AFOS graphics were the max/min temperature and probability of precipitation (PoP) charts (AFOS graphics 93P, 94P and 95P) and the surface pressure/frontal position charts (AFOS graphics 9JH, 9KH, and 9LH) valid for days three, four and five respectively. These six charts are produced daily by the Meteorological Operations Division (MOD) at NMC and are the most widely used pieces of guidance for extended forecasts. Some of the forecasters at Peoria also incorporated the guidance from the hemispheric (AFOS message PMDHMD) and extended forecast (PMDEPD) discussions into the decision making process.

After the available information was studied, the Peoria forecasters were asked to make both precipitation and temperature forecasts for the three to five day period. (This was done BEFORE the extended forecast for the state of Illinois was issued by WSFO Chicago.) The precipitation forecast was to be made for one of three categories: Dry (PoP of less than 30%), Chance (PoP of 30% to 50%), or Likely (PoP of 60% or greater). The actual word "likely" was not put into the public release, but rather was implied as a mention of precipitation without using the word "chance" (i.e., Showers each day).

The Peoria precipitation forecast verification was compared to the verification of the extended PoP guidance charts (93P, 94P, 95P). A forecast of "dry" was assumed for guidance when the PoPs were less than climatological normals (station circle open on the charts). The opposite was true for the chance forecasts. (This method is a "common practice" among forecasters). Since specific forecasts are not made for Peoria on the extended guidance chart, PoPs for surrounding locations were noted and a linear interpolation was done.

"Likely" forecasts were not made for guidance. During the verification process, "likely" did not hold any more weight than "chance". When precipitation occurred, either forecast was considered a "hit". The likely term was only introduced into the study to test for or against the use of detail in extended period precipitation forecasts.

The Peoria forecasters were also asked to make specific high and low temperature forecasts for days three, four and five. Specific values were not put into the public release, but rather were used to make verification easier and to test for or against the use of detail. (The public release, however, had to be consistent with the forecast values.) Temperature verification was done by comparing the Peoria forecasts to the actual highs and lows measured at the WSO in Peoria. The resultant verifica-

tion scores were then used to determine whether or not there was any improvement over climatology. A temperature comparison was done with climatology rather than guidance in this study for two reasons: (1) the available guidance charts did not provide specific temperature values for Peoria, and (2) to relate the results of this study with other recent extended forecast studies a temperature verification comparison with climatology was necessary.

3. Verification

A. Precipitation forecasts

Precipitation forecasting skill at Peoria was either as good or better than guidance for days three, four, and five of this three month study (Figures 1A and 1B). Precipitation was correctly forecast by Peoria about 55% of the time for all three days. Guidance, on the other hand, averaged about 40% accuracy for the same time period.

Figure 1B does indicate slightly better dry weather forecasting by guidance (an average of 77% versus 71%). These high percentages might be attributed to the fact that the summer of 1991 was the seventh driest summer in Peoria during the last 135 years.

Skill scores for both Peoria and guidance are shown in Figure 2. These skill scores take into account the success of forecasts, for both precipitation and dry weather, with respect to chance or randomness. The skill scores for Peoria show a consistently downward trend by day five. Guidance skill scores are quite erratic, with almost no skill for day four.

A study done by NMC from 1970 to 1983 indicated average skill scores for the nation of 17, 13, and 11, during the summer months, for days three through five respectively (Hughes, 1984). All of the Peoria forecasts illustrated improvement over this national average.

Note that in Figures 1A and 2, guidance percentages and skill scores with respect to precipitation forecasting for day four are significantly lower than days three and five. This may be the result of an inconsistency between successive model runs. Livingston and Schaefer (1990) alluded to such a result when they postulated that the Medium Range Forecast model (MRF) failed to foresee changes in the atmospheric flow when it developed large inconsistencies between consecutive runs.

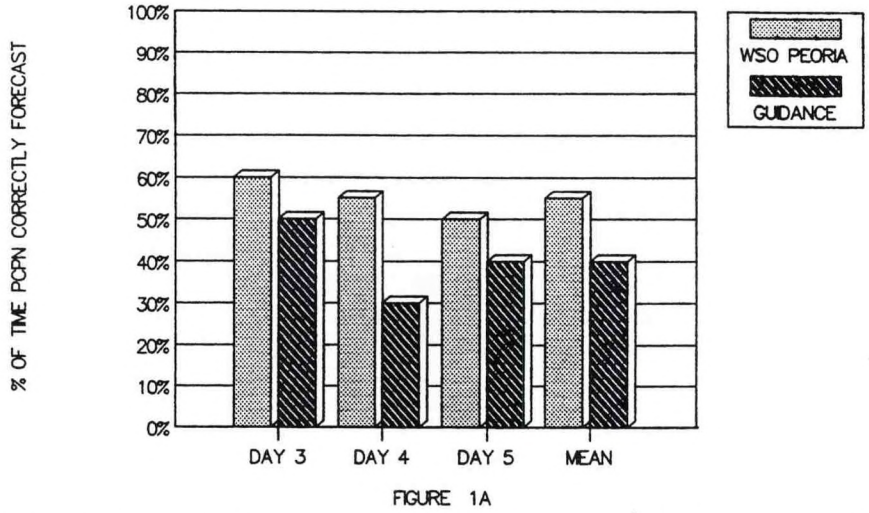

Figure 1A. Percentage of time precipitation was correctly forecast for Peoria, Illinois--Summer 1991.

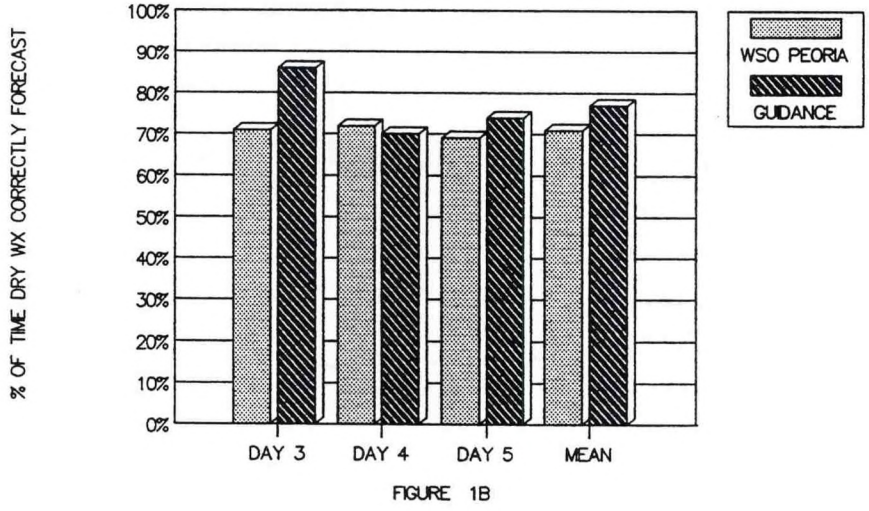

Figure 1B. Percentage of time dry weather was correctly forecast for Peoria, Illinois--Summer 1991.

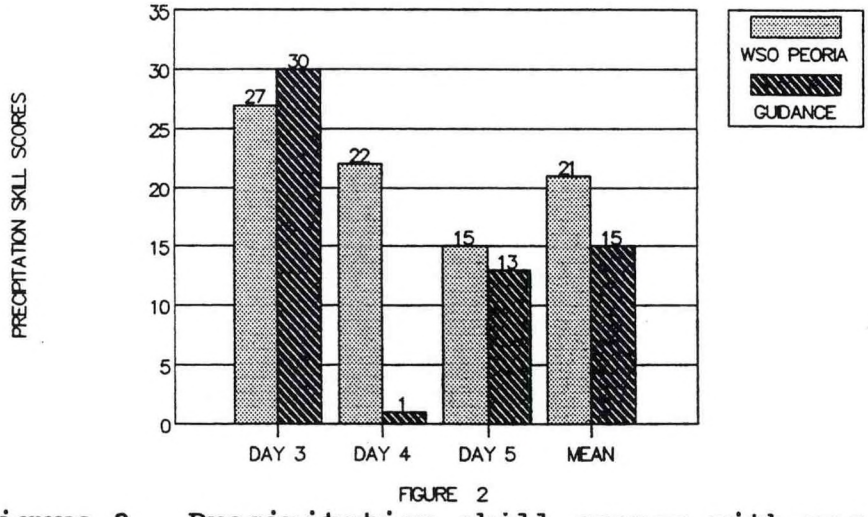

Figure 2. Precipitation skill scores with respect to randomness for Peoria, Illinois--Summer 1991.

Perfect skill = 100
No skill = 0 (success due only to randomness)
No value < 0 (randomness was a better forecast)

The test for detail in extended precipitation forecasting (use of the "likely" term) did show some promise for day three, but rapidly decreasing skill afterwards. The likely category was correctly forecast 67% of the time on day three, but dropped to only 14% by day five.

B. Temperature forecasts

Verification of the temperature forecasts (made by WSO Peoria) and climatology is given for days three, four, and five in Tables 1 through 3. Mean absolute errors (MAEs) for WSO Peoria were about 4.0° through the extended period. Improvement over climatological MAEs occurred for both highs and lows all three days. The percentage of improvement ranged from about 20 to 35% for high temperature forecasts, and from about 5 to 30% for low temperature forecasts. As a comparison, the Hughes study at NMC indicated improvement over climatological high temperature MAEs of roughly 5 to 20% (as a national average) for the summers of 1971 through 1983.

Student's t-test indicated that the improvement over climatology for day three high and low temperature MAEs was significant at the .99 confidence level. (This means that chance can be excluded as an explanation for success 99% of the time with a set of data like the one in this study.) Improvement over climatological MAEs was significant at the .95 and .90 confidence levels for day four and day five high temperature forecasts, respectively. No statistical significance was found in the improvement over climatological MAEs for day four and five low temperature forecasts.

The three to five day MAEs (made by WSO Peoria) were about twice as great as the MAEs for first period local forecast verification at Peoria during the same time period (2.1° from June 1 through August 31, 1991).

Temperatures at Peoria, from June 1 through August 31, averaged about 2.1° above normal. Note that the WSO Peoria bias is nearly positive 2°. This means that the Peoria forecasters overcompensated for the above normal temperatures and had about a 2° warm bias.

Two simple tests were done with respect to temperature detail in extended forecasts. First, a comparison was made between perfect forecasts (error of 0°) and forecasts where the error was outside the largest forecast range (error of 10° or greater) by WSO Peoria. There were twice as many perfect forecasts on day three as there were large error forecasts (22 versus 11).

TEMPERATURE ERRORS	PEORIA		CLIMATOLOGY	
	HIGH	LOW	HIGH	LOW
# OF FCSTS	92	92	92	92
BIAS	0.8	2.0	-2.1	-1.4
MAE	3.6	3.4	5.3	4.8
SD OF MAE	3.5	2.4	3.9	3.3
RMSE	5.0	4.2	XXXXXXXXXXXXXXX	

TABLE 1. Temperature statistics for WSO Peoria and climatology for Day 3 -- Summer 1991.

TEMPERATURE ERRORS	PEORIA		CLIMATOLOGY	
	HIGH	LOW	HIGH	LOW
# OF FCSTS	91	91	91	91
BIAS	1.3	2.3	-2.0	-1.3
MAE	4.0	4.1	5.2	4.7
SD OF MAE	3.7	2.7	3.8	3.3
RMSE	5.5	4.9	XXXXXXXXXXXXXXX	

TABLE 2. Temperature statistics for WSO Peoria and climatology for Day 4 -- Summer 1991.

TEMPERATURE ERRORS	PEORIA		CLIMATOLOGY	
	HIGH	LOW	HIGH	LOW
# OF FCSTS	90	90	90	90
BIAS	1.5	2.7	-1.9	-1.1
MAE	4.1	4.4	5.1	4.6
SD OF MAE	3.4	3.0	3.8	3.1
RMSE	5.3	5.3	XXXXXXXXXXXXXXX	

TABLE 3. Temperature statistics for WSO Peoria and climatology for Day 5 -- Summer 1991.

BIAS (MEAN)= AVERAGE OF THE ERRORS. A NEGATIVE BIAS MEANS THE FORECAST WAS COOLER THAN THE OBSERVED TEMPERATURES.

MAE= MEAN ABSOULUTE ERROR--A DIRECT INDICATION OF FORECAST ACCURACY.

SD= STANDARD DEVIATION OF THE MAE's. THIS MEANS THAT APPROXIMATELY 68% OF THE TEMPERATURE FORECASTS HAVE AN ABSOLUTE ERROR WITHIN +/- ONE SD VALUE OF THE MAE. APPROXIMATELY 95% OF THE FORECASTS HAVE AN ABSOLUTE ERROR WITHIN +/- TWO SD VALUES OF THE MAE.

RMSE= ROOT MEAN SQUARE ERROR--THIS IS A +/- MEASURE OF THE SPREAD OR RANGE OF THE ERROR BETWEEN FORECASTS AND OBSERVATIONS.

However, on day four the two were equal (17 versus 17), and by day five the trend completely reversed (10 versus 21).

Finally, Tables 1 through 3 exhibit root mean square errors (RMSEs) in the range of 8.4° to 11.0°. This means that for all of the extended forecasts made in this study, an average temperature forecast range of at least 10° (i.e., 50 to 59 or just 50s) would have been necessary to cover most of the error.

4. Conclusion and Summary

Medium range extended forecasting has been, and always will be, a challenge to weather forecasters due to the limited accuracy of hemispheric models. This study attempted to illustrate that at the WSO level extended forecasts with reasonable results could be made for areas smaller than whole states in spite of the limitations of medium range models. The reader is reminded however, that this does not mean more detail should be put into an extended forecast covering a smaller area. It has been illustrated here, and in other recent studies (DeLisi, 1991 & Livingston and Schaefer, 1990) that no scientific evidence supports the introduction of detail into extended forecasts.

Precipitation forecasts in this extended forecast study were better than guidance all three days even though actual rainfall was well below seasonal normals. Precipitation skill scores with respect to randomness were as good or slightly better than guidance for days three and five, and were much better for day four. The Peoria forecasters seemed to notice the trend of inconsistent model forecasts between successive runs, which may explain the significant improvement over guidance on day four.

Mean absolute errors for temperature forecasts demonstrated improvement over climatology. In addition, Student's t-test indicated that statistical significance was achieved for all high temperature forecasts and day three low temperature forecasts. Throughout the study, though, the Peoria forecasters had about a 2° warm bias.

Finally, the tests for detail in extended forecasts reiterated the notion that specific information could not be forecast on a consistent basis. With respect to precipitation forecasting, the use of the term "likely" in the extended range showed reasonable results for day three. However, the accuracy was significantly worse for days four and five. Even though this was only a three month study, the results support the usage of only a "yes" or "no" precipitation forecast.

One of the tests for specific detail in temperature forecasting also indicated significantly worse errors by day five. A look at the RMSEs for all three days supported the case against specificity by indicating that a temperature range of 8° to 11° was needed just to cover most of the errors on a daily basis.

5. Acknowledgements

I would like to thank the entire staff at WSO Peoria, Illinois for their co-operation, input into the data gathering, and ideas for this study. I would also like to thank Mr. Bob Somrek of WSFO Chicago, Illinois for his very insightful comments and critiques.

6. References

De Lisi, M. P., 1991: Verification of the Extended Forecast at WSFO Indianapolis, NWS Central Region Technical Attachment 91-10.

Grant, B. A., 1990: Verification of the Three to Five Day Extended Forecasts, NWS Southern Region Technical Attachment 90-38.

Harnack, R. P., 1986: Principles and Methods of Extended Period Forecasting in the United States, *NWA Meteor. Monogr.*, **1**, 86.

Hughes, F. D., 1984: Skill of Medium Range Forecast Group, National Meteorological Center Office Note 284, 115 pp.

Livingston, R. L. and J. T. Schaefer, 1990: Medium Range Model Guidance in the Three to Five Day Extended Forecast, *Wea. & For.*, **5**, 361-376.

Panofsky, H. A. and G. W. Brier, 1958: Some Applications of Statistics to Meteorology, Pennsylvania State University, University Park, PA.

Sprinthall, R. C., 1987: Basic Statistical Analysis, 2nd Edition, Prentice-Hall, Inc., Englewood Cliffs, NJ.

CENTRAL REGION APPLIED RESEARCH PAPER 9-3

AN INVESTIGATION OF THE RELATIONSHIP BETWEEN TERRAIN RELIEF AND TORNADO ACTIVITY ON THE MISSOURI OZARK PLATEAU

Michael D. McCoy
National Weather Service Meteorological Observatory
Marseilles, Illinois

1. Introduction

One of the greatest challenges in meteorology is to enhance our understanding of the impact of relatively minor topographic variations on mesoscale and microscale meteorological phenomena. Current data collection networks are not dense enough to detect certain meso-meteorological events, the most important of which includes many tornadoes.

Previous studies have noted certain areas of low tornado incidence within broad regions of relatively high tornado frequency (Safford 1970, Stolle 1971, Grazulis and Abbey, 1983). One such area is the Ozark Plateau, which has been of special interest to many scientists, because it is located within a region of the United States where synoptic and dynamic parameters favorable for tornadogenesis typically occur many times in a given year.

Terrain relief is relatively minor over much of the Ozark Plateau, particularly in the northern part of the region in Missouri. Therefore, some researchers believe the apparent diminished tornado incidence on the Ozark Plateau is associated primarily with elevation (Fawbush, et al., 1951). A question which has not been thoroughly investigated is whether the apparent modification of severe convective weather over the Ozark Plateau is solely a large-scale phenomenon, or whether a variable pattern of tornado activity associated with local terrain relief is also evident within the region.

2. The Study Area

The Ozark Plateau encompasses approximately 60,000 square miles of the southcentral United States, covering most of the southern one-half of Missouri, parts of northern Arkansas, the southeast corner of Kansas, and extreme northeastern Oklahoma (Figure 1). This research was confined to 51 counties in the Missouri portion of the Ozark Plateau (Figure 2).

Elevation on the Missouri Ozark Plateau ranges from approximately 400 to 1700 feet above mean sea level. The highest elevations are in the central and eastern parts of the region,

OZARK PLATEAU AND SURROUNDING PHYSIOGRAPHIC REGIONS

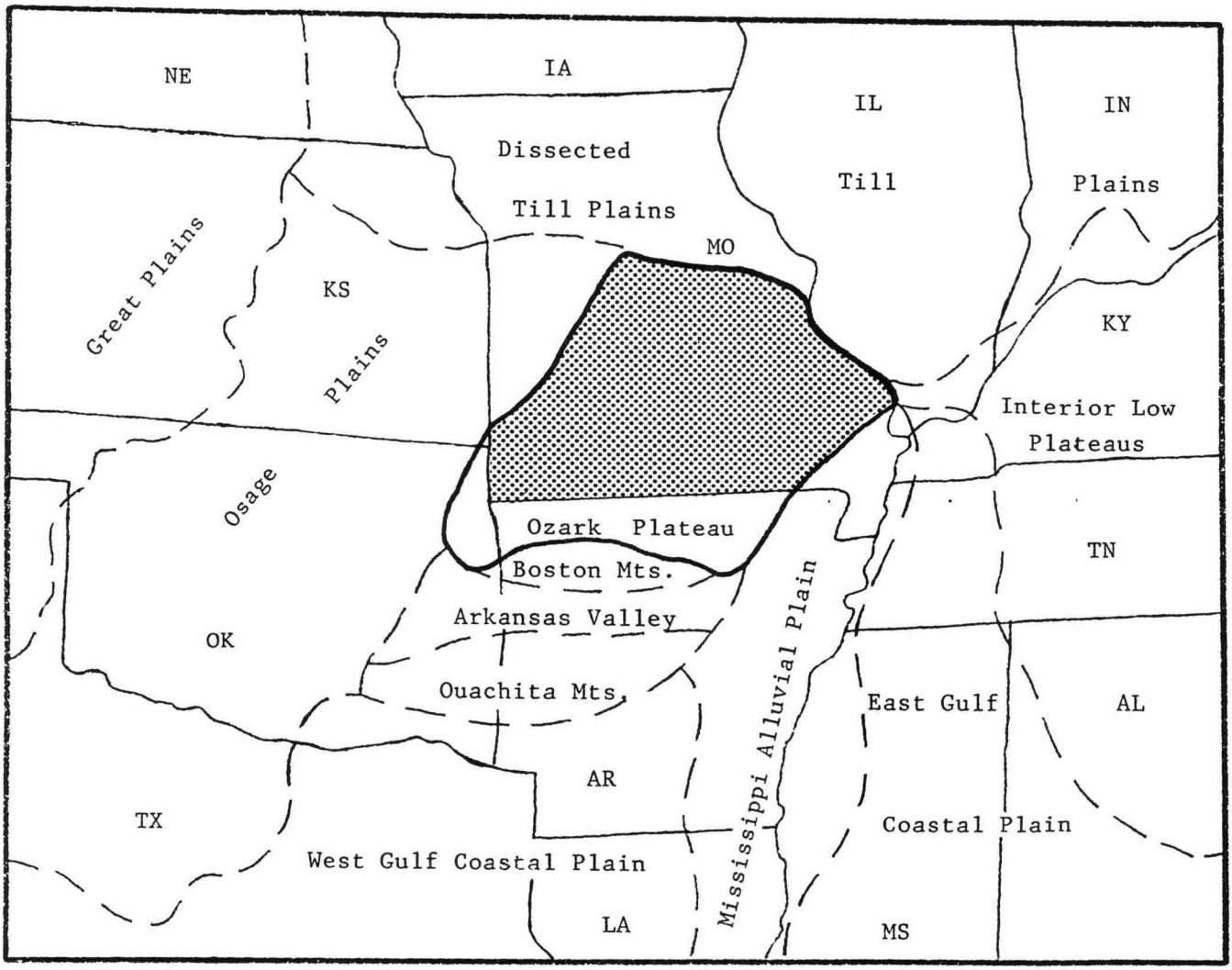

FIGURE 1

Adapted from: Milton D. Rafferty, The Ozarks Land and Life. Norman, Oklahoma: University of Oklahoma Press, 1982.

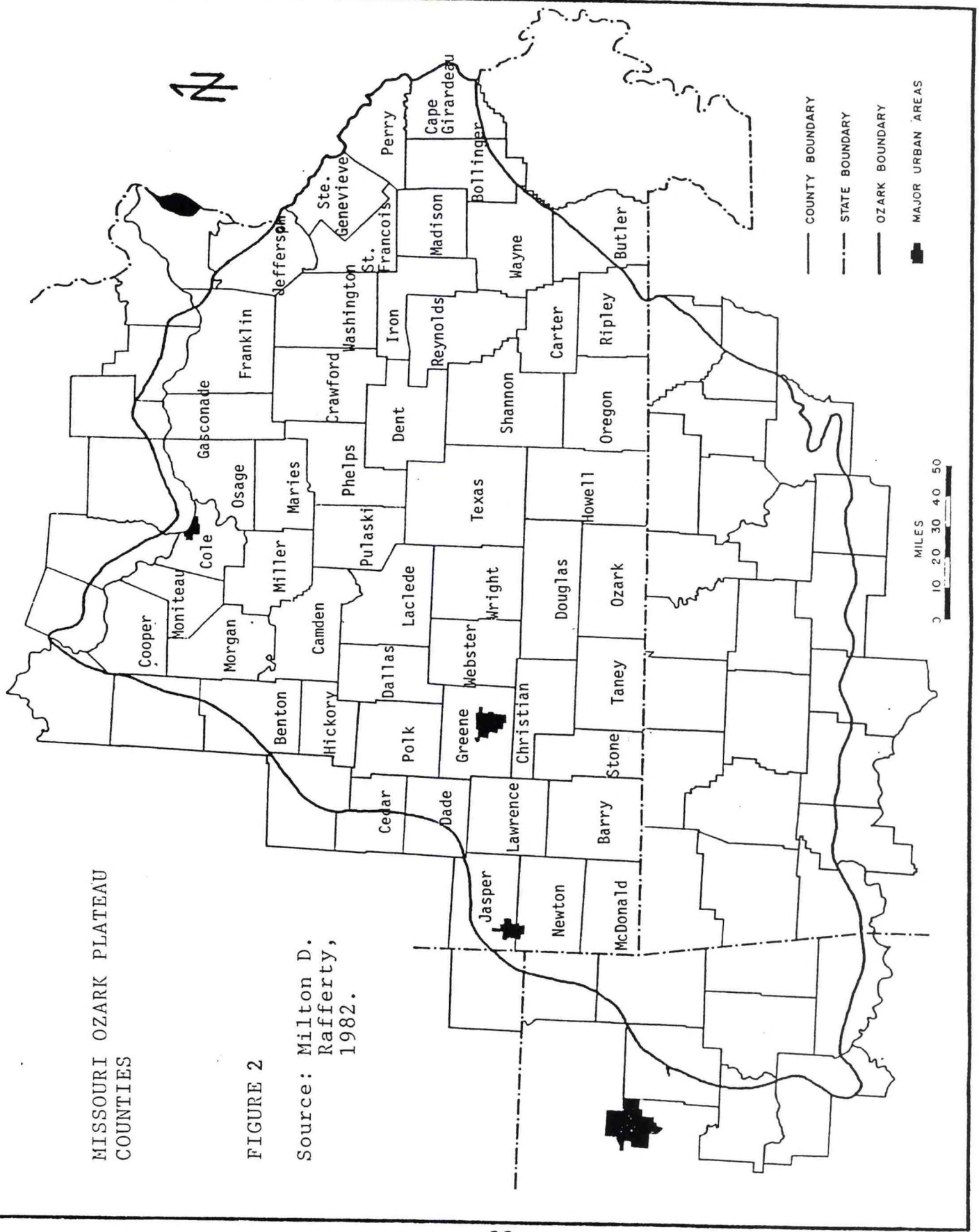

MISSOURI OZARK PLATEAU COUNTIES

FIGURE 2

Source: Milton D. Rafferty, 1982.

over the Central Plateau and Courtois Hills (Figure 3). Relief generally increases from west to east, with the greatest relief in the southern and eastcentral areas. The extreme western part of the area is relatively level.

3. Data Collection

A. The Nature of the Data

Although the data in this study represent phenomena which are continuous in nature, analytical research methodology and the unavoidable limitations of sampling techniques required all data to be represented in discrete units. The political unit of the county was used as the level of aggregation for the data. Data collected for each county in the study area represented the following variables: terrain relief, tornado incidence and tornado intensity. Data bases for each variable were organized as ordinal and interval data for testing and analysis (Yeattes, 1974).

B. Terrain Relief

A topographic base map was used to derive relief data in the study area. A grid consisting of equally spaced points was overlayed on the base map to obtain a sample of elevation data points (Brier and Panofsky, 1958). This provided a sample of elevation over intervals of five statute miles throughout the study area. This systematic sampling technique was employed to reduce distortion of data resulting from the varying sizes of counties. Elevation was recorded to the nearest 10 feet for each data point. The difference between each successive elevation data point was added and divided by the total number of data points to yield a mean relief index for each county (Figure 4). This technique for the representation of relief is similar to those employed in previous studies (Tecson, et al., 1983). The mean relief index is probably slightly more accurate in counties with relatively level and gently sloping terrain than in those counties of greater relief, because a lower range of elevation is sampled in more level areas.

C. Tornado Incidence

The ephemeral nature of tornadoes and the imperfection of detection capabilities prohibit a complete account of tornado activity. Differences in the geographic distribution of tornado incidence can be established only by examining data over a period of several decades. The tornado data for this study span the 70-year period from 1916 through 1985, and were compiled primarily from the research publications of Dr. G. L. Darkow of the

PHYSIOGRAPHIC REGIONS OF THE OZARK PLATEAU

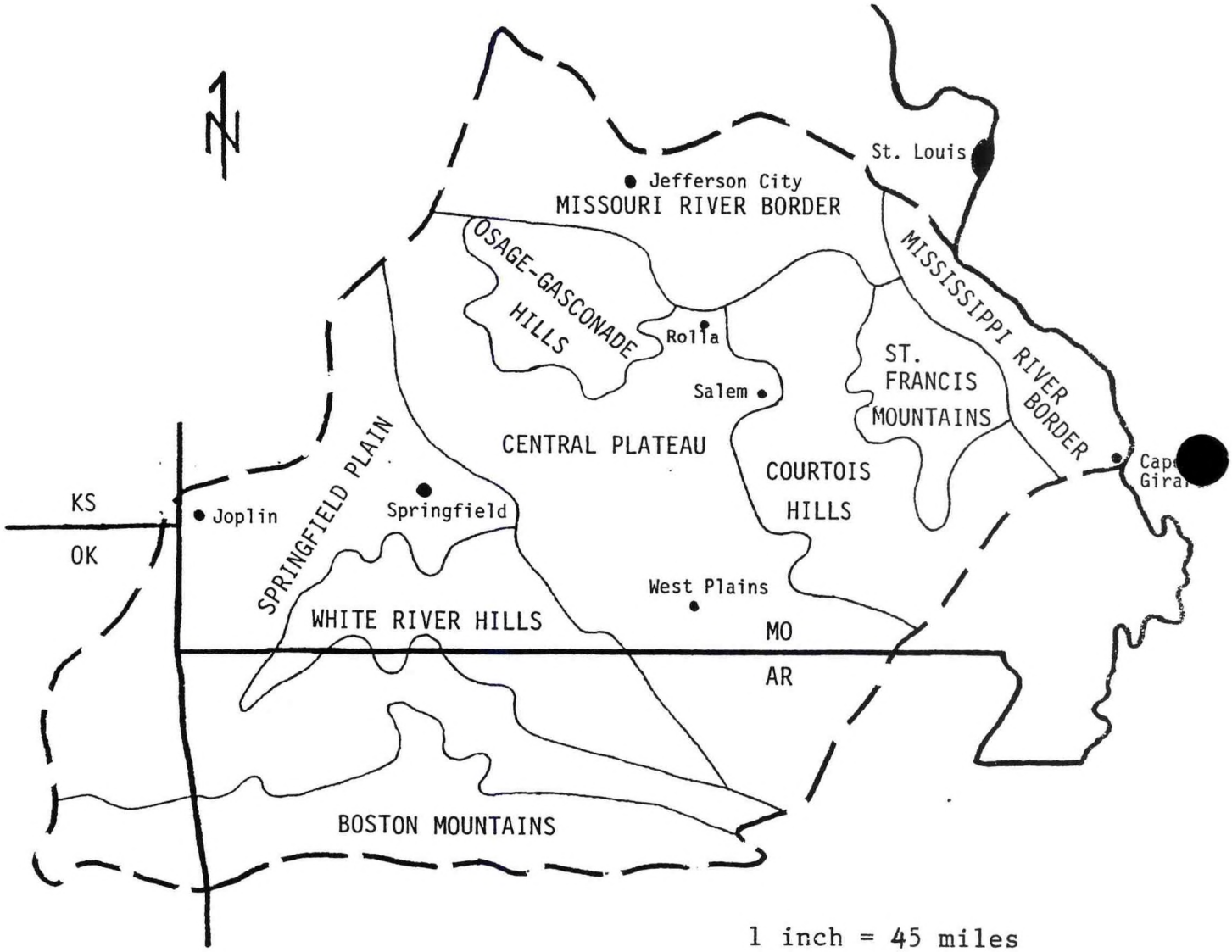

FIGURE 3

Adapted From: Milton D. Rafferty, The Ozarks Land and Life. Norman, Oklahoma: University of Oklahoma Press, 1982.

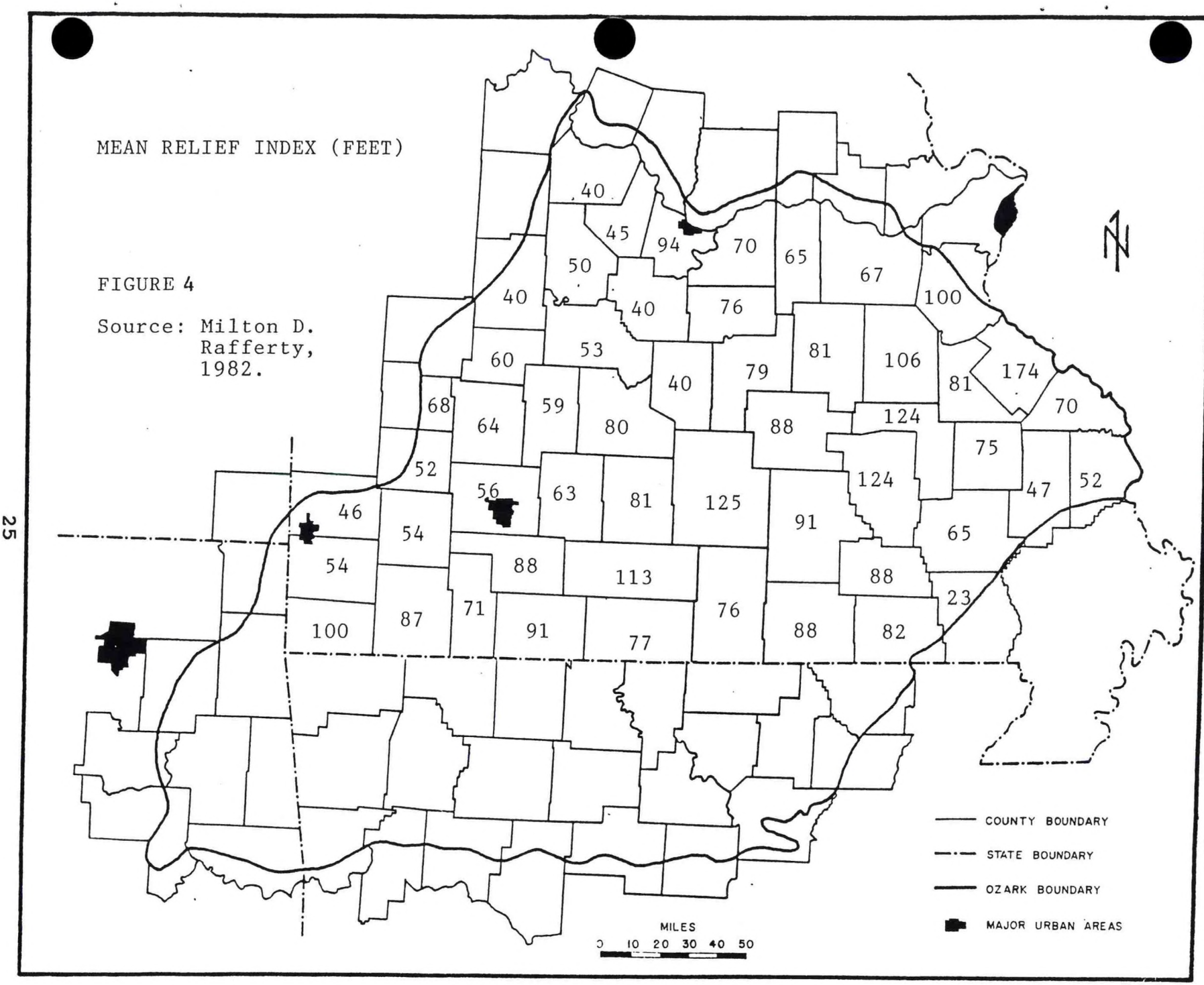

FIGURE 4

Source: Milton D. Rafferty, 1982.

University of Missouri (Darkow, 1968) and Dr. T. Theodore Fujita of the University of Chicago (Fujita, 1987). Supplementary data were collected from the publication Storm Data (National Oceanic and Atmospheric Administration, 1980-1986).

Although statistics may reveal specific geographic tornado distributions, an accurate interpretation of the meaning of these patterns is complicated by the nature and variety of factors which influence both actual tornado occurrences and the number of reported tornadoes. The number of reported tornadoes is consistently higher in and near large population centers, and until recent decades, many of these reports were not verified.

To reduce the impact of human population distribution on the data, tornado incidence was compiled as a ratio of the number of tornadoes per 1000 persons over the 70-year period in each county. Although the population of the study area increased greatly between 1916 and 1985, the relative differences between county populations did not appreciably change between 1950 and 1985. Also, aggregate tornado statistics are skewed toward occurrences in recent decades, due to vastly improved documentation of tornado activity. Since 1950, there has been a significant increase in the number of reported tornadoes, and improvements in the quality of tornado data (Tecson, et al., 1983).

Therefore, 1980 census data were used to calculate tornado incidence per 1000 persons (Figure 5). The 1980 census also gave a greater account of the impact of large cities on the data, congruent with improvements in reporting networks and procedures.

Similarly, tornado incidence statistics may reflect the impact of the relative sizes of counties as much as the possible effects of terrain relief on tornado occurrence. Therefore, a second measure of tornado incidence was determined for each county: the total number of tornadoes from 1916 through 1985 per 100 square miles (Figure 6).

D. Tornado Intensity

Most tornadoes are small and short-lived, and many of these are never detected or reported. However, large tornadoes seldom go undetected, and incidence statistics for more intense tornadoes should not be greatly affected by human population distribution. Tornadoes of the most intense category are rare in the Ozark region, and did not provide an adequate data base for an analysis of a possible relationship between tornado intensity and terrain relief. The data used in this analysis included the incidence of tornadoes in intensity categories F2 through F5, or "strong" and "violent" tornadoes (Appendix A). Intensity data

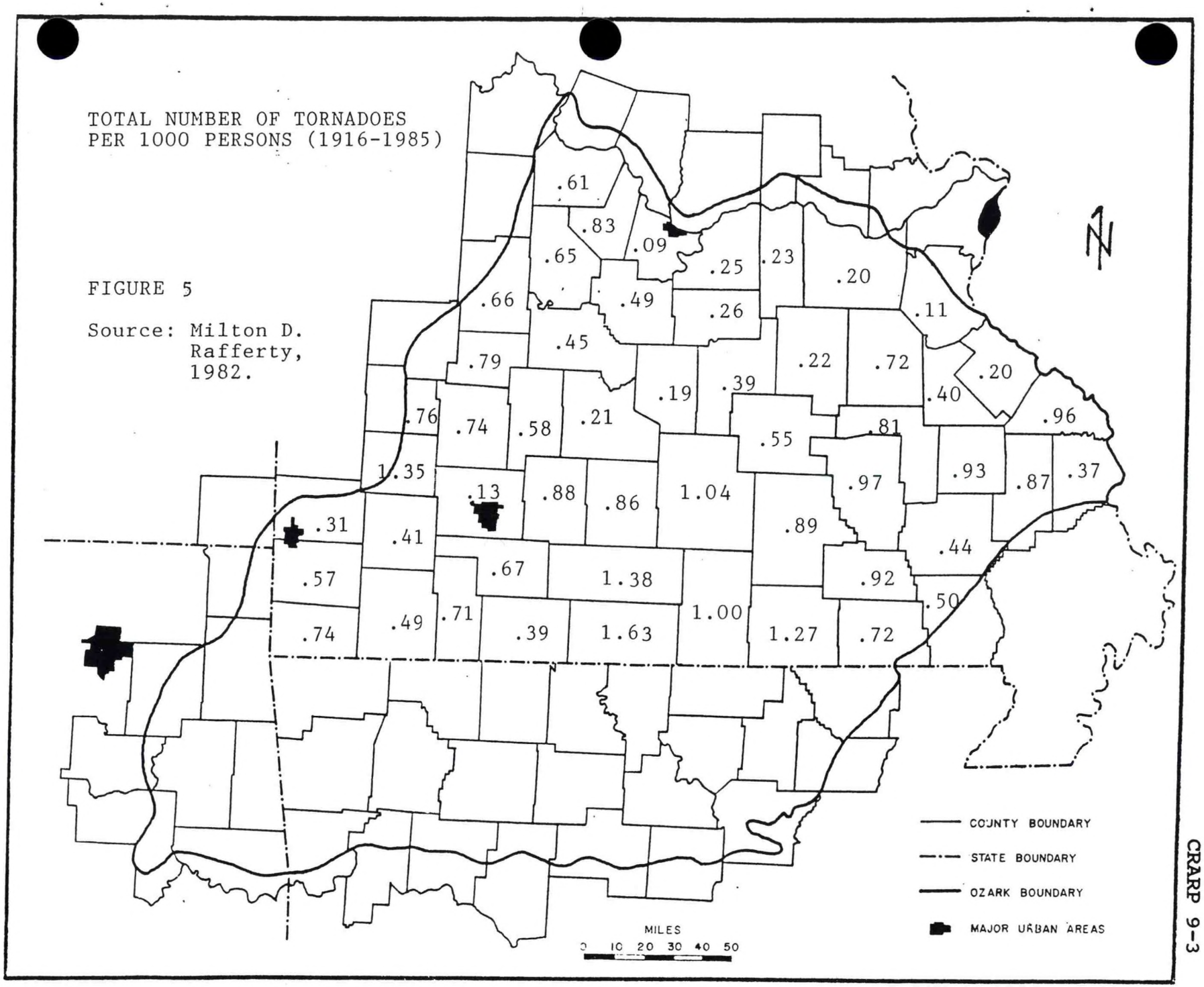

FIGURE 5

Source: Milton D. Rafferty, 1982.

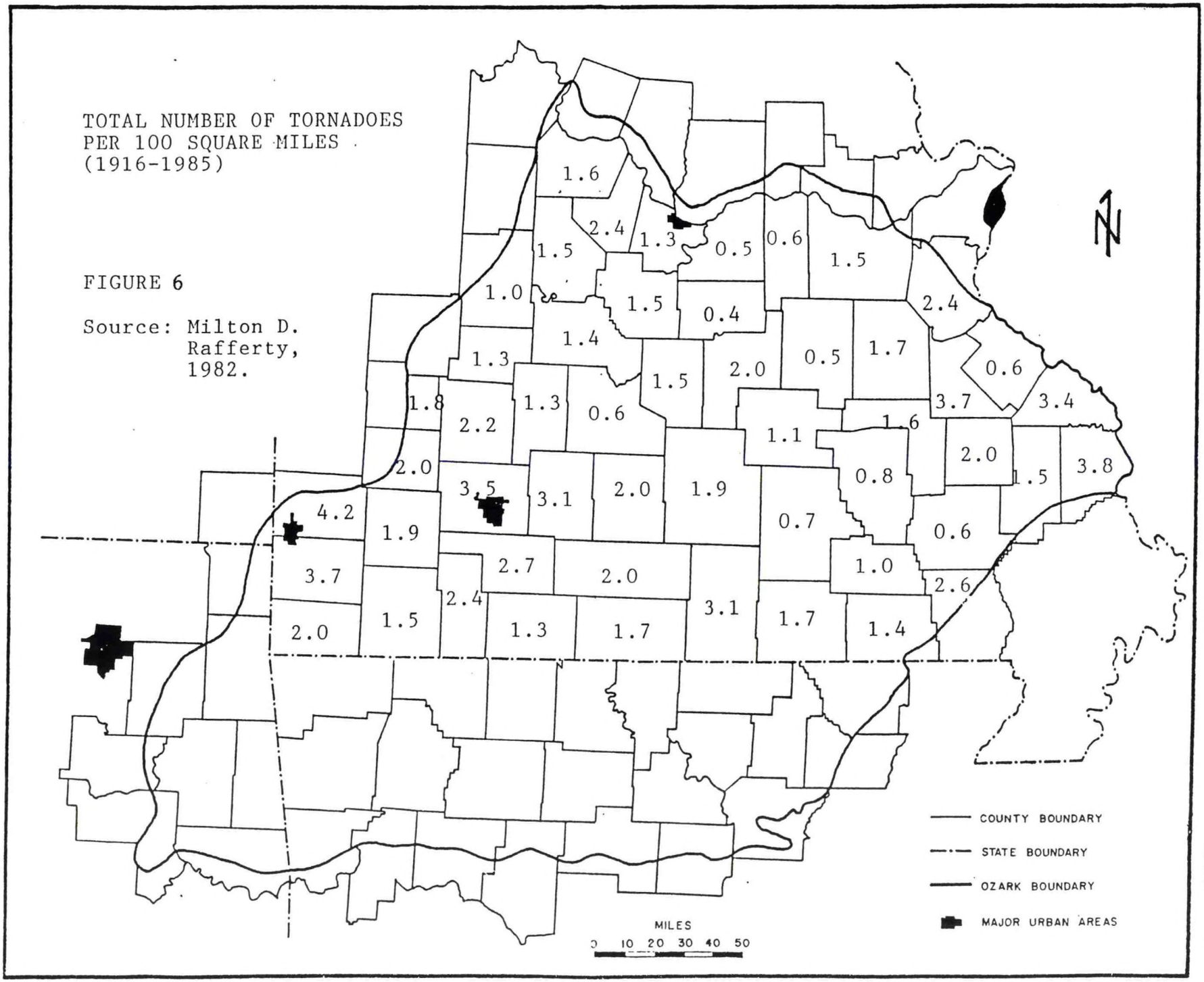

FIGURE 6

Source: Milton D. Rafferty, 1982.

for each county is represented by the total number of F2 through F5 category tornadoes per 100 square miles from 1916 through 1985 (Figure 7).

4. Data Analysis

A. Preliminary Results

The total number of tornadoes for the 70-year period ranges from 0.40/100 square miles in Maries County to 4.21/100 square miles in Jasper County (Figure 6). Maries County is located in the northern Ozarks in the Missouri River Border Region near the Osage-Gasconade Hills, and Jasper County is in extreme southwestern Missouri at the edge of the Ozark Plateau (Figures 2 and 3). Jasper County also displays one of the lowest mean relief indices on the plateau (Figure 4).

Several of the counties with the lowest mean relief indices show a high number of tornadoes per 100 square miles and a low number of tornadoes per 1000 persons (Figures 4, 5 and 6). A measure of tornado incidence as a function of population produces some intriguing results when compared to the data for relief and tornado incidence per 100 square miles. Cole County, at the northern edge of the region along the Missouri River, has the lowest incidence of tornadoes, at 0.08/1000 persons, and one of the highest mean relief indices (Figures 2, 3 and 5). Cole County also shows one of the lower values of tornado incidence per 100 square miles (Figure 6). Ozark County has a tornado incidence of 1.63/1000 persons, the highest in the study area (Figure 5). The mean relief index and tornadoes per 100 square miles rank Ozark County near the middle of the respective values for each data category (Figures 4 and 6).

Data for tornado intensity was based on the total number of F2 through F5 category tornadoes from 1916 through 1985. This data shows a low of 0.13/100 square miles in Douglas County, and a high of 1.20/100 square miles in both Lawrence and Dade Counties (Figure 7). The most striking characteristic of the areal distribution of strong and violent (F2 - F5) tornadoes is its concentration along the western and eastern peripheries of the Missouri Ozark Plateau (Figure 7). Both of these regions have generally lower mean relief indices than the interior of the study area.

B. Quantitative Analysis

Each of the three data sets was tested for correlation using the Pearson Product-Moment Coefficient of Correlation (r). The .05 level of significance was used to determine the significant

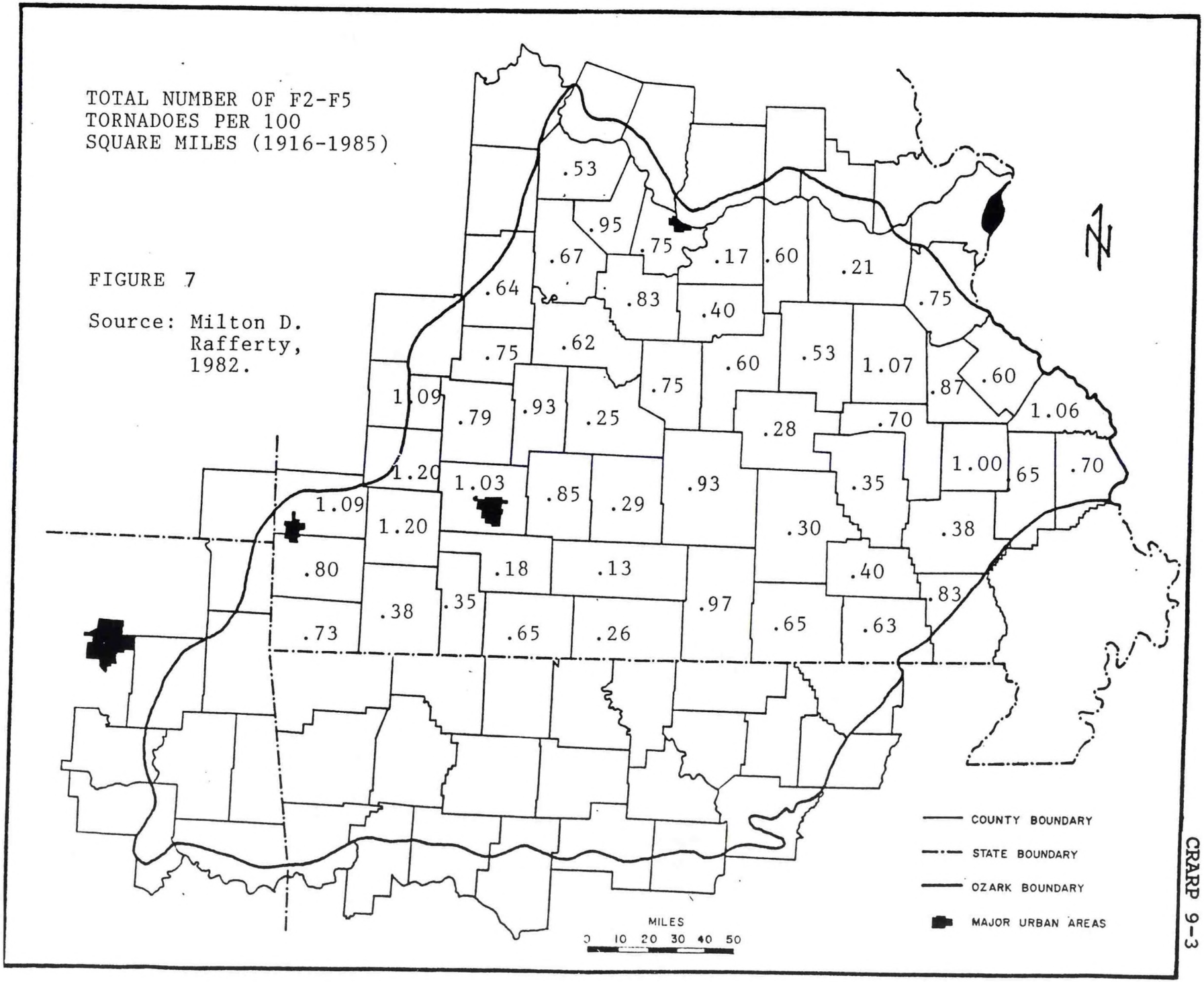

FIGURE 7

Source: Milton D. Rafferty, 1982.

values of (r). Coefficients of Determination (r^2) provided a measure of the association between the independent and dependent variables (Appendix B). An estimation of the true variability of the dependent variables was given by the Standard Error of the Estimate (S.E.).

The test of a significant relationship between terrain relief and tornado incidence specifies the dependent variable as tornado incidence and the terrain relief index as the independent variable. The dependent variable was tested for tornado incidence measured as the total number of tornadoes per 100 square miles.

A linear regression analysis of the mean relief index and tornado incidence per 100 square miles is shown in Figure 8. Numbers greater than one indicate more than one county has the same value for the independent and/or dependent variable. The regression line for this data set shows a slight negative relationship between the variables.

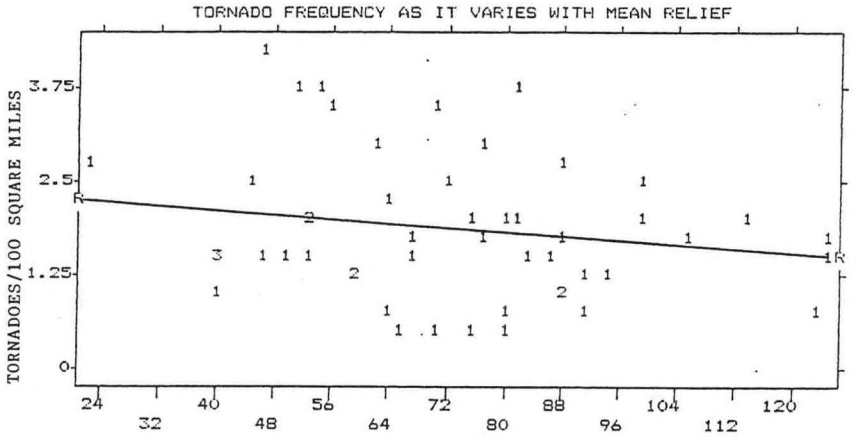

FIGURE 8

A test with the Pearsonian Product-Moment Correlation Technique yielded a correlation coefficient (r) of -0.214, which implies a small inverse relationship exists between the amount of terrain relief and tornado frequency. However, the coefficient is not within the .05 significance level for this sample size (0.273) (Haring and Loundsbury, 1975). The Coefficient of Determination (r^2) indicates only 0.046 of the variation in the total number of tornadoes is attributable to variation in the mean relief index.

The amount of terrain relief exhibits a slight negative relationship with the number of strong or violent (F2 - F5) tornadoes (Figure 9). A concentration of these tornadoes is evident in counties with lower mean relief indices, while those counties with greater relief show very few strong or violent tornadoes (Figures 4 and 7). A correlation coefficient (r) of -0.297, shows a small but statistically significant relationship at the 0.037 significance level. However, the determination coefficient (r^2) indicates only 8.8 percent of the variation in the number of strong and violent tornadoes is explained by variation in the mean relief index.

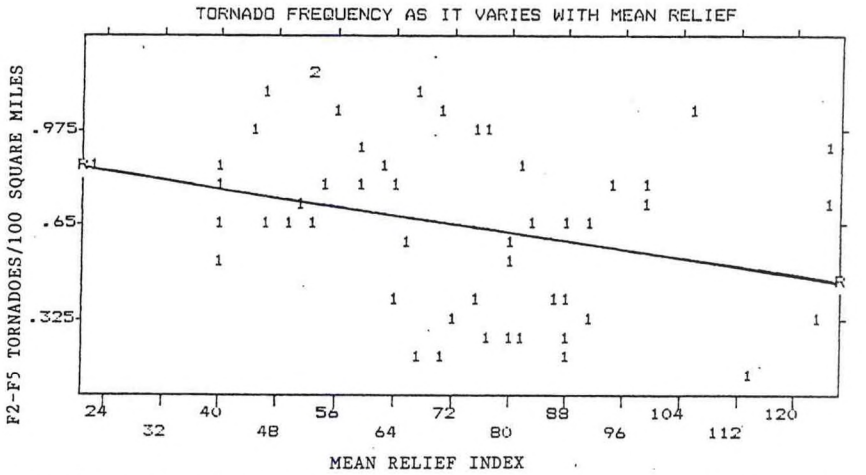

FIGURE 9

5. Conclusions

The results of this study indicate that tornado incidence and intensity patterns across the Missouri Ozark Plateau appear to be at best only marginally related to the amount of terrain relief. Less than 10 percent of the variation in the number and intensity of tornadoes is related to variations in the relief index used in this study. Tornado incidence is generally lower over the interior of the region, but this occurs within an area of relatively wide ranges in relief. Therefore, the apparent decrease in tornado activity on the Missouri Ozark Plateau seems to be primarily a large-scale phenomenon which does not vary significantly within the region. Nevertheless, a complete survey of the data indicates strong and violent tornadoes in the study area have occurred most frequently in areas with less relief, particularly along the western and eastern peripheries of the region.

These results generally support the research results of Grazulis and Abbey (1983), who studied 31,000 tornado events in the central United States, covering the period from 1880 through 1982. Their study revealed an apparent minimum of violent tornadoes in a band from northeast Texas to Wisconsin, including the central part of the Missouri Ozark Plateau. Abbey and Grazulis also noted the relative increase in tornado incidence over southeast Missouri, along the eastern periphery of the Ozark Plateau.

The conclusions of this study must be accompanied by a reminder of the methodological difficulties inherent in such research. The collection and analysis of data involving topographic characteristics and tornado activity necessarily results in the loss of some potentially meaningful aspects of these phenomena. Sampling techniques employed to minimize distortion of data may introduce statistical bias into the study. The nature of research in tornado climatology necessitates a subordination of detail to the temporal aspects of data. Although such studies require data spanning at least several decades, changes in reporting techniques and improvements in detection capabilities have affected aggregate tornado statistics. Improved understanding of the nature and extent of the relationship between topography and severe convective storms requires a continuous refinement of data and elaboration of the results of research. New systems for meteorological data acquisition and analysis will enhance our knowledge of these complex interactions.

6. References

Brier, Glenn W. and Hans A. Panofsky, 1958: *Some Applications of Statistics to Meteorology*. Pennsylvania State University, University Park, Pennsylvania, 170-171.

Darkow, G. L., 1968: Tornado Climatology of Missouri, 1916-1968. Columbia, Missouri, Department of Atmospheric Sciences, University of Missouri, 1-14.

Fawbush, E. J., R. C. Miller, and L. G. Starrett, 1951: An Empirical Method of Forecasting Tornado Development. *Bull. Amer. Meteor. Soc.*, **32**, 1-9.

Fujita, T. Theodore, 1987: U. S. Tornadoes Part One: 70-Year Statistics. Satellite and Mesometeorology Research Paper No. 218, Chicago: Satellite and Meteorology Research Project Group, University of Chicago, 13-16.

Grazulis, T. P. and R. F. Abbey, Jr., 1983: 103 Years of Violent Tornadoes... Patterns of Serendipity, Population, and Mesoscale Topography. *Preprints, 13th conference on Severe Local Storms*. Amer. Meteor. Soc., Boston, Massachusetts, 124-127.

Haring, L. Lloyd, and John F. Loundsbury, 1975: *Introduction to Scientific Geographic Research*. Dubuque, Iowa, William C. Brown Company Publishers, 120.

Lapin, Lawrence, 1975: Statistics: Meaning and Method. New York: Harcourt Brace Jovanovich, Inc., NOAA, 1980-1986: Storm Data. Vol. 22-28.

Rafferty, Milton D., 1980: *The Ozarks Land and Life*. Norman, Oklahoma, University of Oklahoma Press, 3-11.

Safford, A. T., 1970: The Influence of Terrain Frequency Distribution on Tornado and Hail Occurrence in the Central Midwest. Master's thesis, St. Louis, Saint Louis University, 40.

Stolle, Hans A., 1971: A Geographic Analysis of Selected Causes and Effects of Michigan Tornado Patterns, 1930-1969. Master's thesis, Western Michigan University, 38-56.

Tecson, J. J., T. T. Fujita, and R. F. Abbey, Jr., 1983: Statistical Analyses of U.S. Tornadoes Based on the Geographic Distribution of Popluation, Community, and Other Parameters. *Preprints, 13th Conference on Severe Local Storms*, Amer. Meteor. Soc., Boston, Massachusetts, 120-123.

Yeattes, Maurice, 1974: *An Introduction to Quantitative Analysis in Human Geography*. New York, McGraw-Hill, Inc., **7-8**, 48-50, 84-89.

APPENDIX A

FUJITA TORNADO INTENSITY SCALE (F0-F5)

F0 - LIGHT DAMAGE (40-72 MPH): Some damage to chimneys; break twigs and branches off trees; push over shallow-rooted trees; damage signboards; some windows broken.

F1 - MODERATE DAMAGE (73-112 MPH): Peel surface off roofs; mobile homes pushed off foundations or overturned; outbuildings demolished; moving autos pushed off the road; trees snapped or broken.

F2 - CONSIDERABLE DAMAGE (113-157 MPH): Roofs torn off frame houses; mobile homes demolished; frame houses with weak foundations lifted and moved; large trees snapped or uprooted; light-object missiles generated.

F3 - SEVERE DAMAGE (158-206 MPH): Roofs and some walls torn off well-constructed houses; most trees in forest uprooted; heavy cars lifted off the ground and thrown; weak pavement blown off the roads.

F4 - DEVASTATING DAMAGE (207-260 MPH): Well-constructed houses leveled; structures with weak foundations blown off some distance; cars thrown and disintegrated; trees in forest uprooted and carried some distance.

F5 - INCREDIBLE DAMAGE (261-318 MPH): Strong frame houses lifted off foundations and carried considerable distance to disintegrate; automobile-sized missiles fly through the air in excess of 300 ft.; trees debarked; incredible phenomena occur.

Source: T. Theodore Fujita, U. S. Tornadoes. Part One: 70-Year Statistics. Chicago: Satellite and Meteorology Research Project Group, University of Chicago, 1987.

APPENDIX B

DATA ANALYSIS TECHNIQUES

PEARSONIAN PRODUCT-MOMENT COEFFICIENT OF CORRELATION

The first step in this technique is to determine the value by which each of the two variables (dependent and independent) differs from the mean of the variables and then to total the product of the difference. The correlation coefficient is calculated from the following formula:

$$r = \frac{\frac{1}{n\Sigma(a-\bar{a})^2(b-\bar{b})^2}}{\sigma a \cdot \sigma b}$$

This formula finds the sum of the product of the total variations in the two variables (a and b) and divides this value by the number of pairs (n). From this co-variance ratio, a correlation coefficient (r) is derived by dividing the ratio by the product of the two standard deviations.

r = 1.0 (perfect positive correlation)

r = -1.0 (perfect negative correlation)

COEFFICIENT OF DETERMINATION (r^2)

This coefficient measures the amount of variation in the dependent variable resulting from variation in the independent variable.

Source: Maurice Yeattes: *An Introduction to Quantitative Analysis in Human Geography*. New York: McGraw-Hill, Inc., 1974.

CENTRAL REGION APPLIED RESEARCH PAPER 9-4

THE RECORD SNOW EVENT OF OCTOBER 18TH-20TH 1989 IN THE LOWER OHIO VALLEY

Tim Troutman
National Weather Service Office
Evansville, Indiana

1. Introduction

The snow event of October 18 through 20, 1989 was the earliest measured snowfall on record for much of Indiana and Illinois. This rare occurrence of snow was forecast for most of the Ohio Valley by forecasters in Illinois, Indiana and Kentucky.

On October 18, winter storm watches were issued by National Weather Service Offices in Illinois and Indiana for heavy, wet snow over southern Illinois and all of central and southwest Indiana. The Indianapolis, Indiana area received 9.3 inches of snowfall compared to 0.9 inches of snow in the Evansville, Indiana area from October 18-20. This paper will explore the model forecasts, what occurred, and why dynamically this abnormal weather occurrence resulted in the Indianapolis, Indiana area receiving so much more snow than the Evansville, Indiana area.

The initial questions about heavy snow over the Lower Ohio Valley region were justified as a 500 millibar upper level low pressure area developed in Eastern Kansas by 0000Z, October 19. This system was advecting colder than normal air into the Lower Midwest and Ohio Valley.

Another factor in producing the possibility of heavy snow over the region was the fact that both the LFM and NGM models were retrograding a surface low pressure area from central North Carolina on 1200Z, October 19 to the eastern Great Lakes area by 1200Z, October 20. There were differences, however, between the two models involving the strength of the surface low pressure area. The NGM developed the surface low more than the LFM, as evidenced by the 1008 millibar center compared to the 1011 millibar center of the low pressure area by the LFM. The NGM also took more into consideration moisture that would be advected northwest toward the area from the Atlantic Coast as the low pressure area moved closer to the Lower Ohio Valley.

The movement of the 500 millibar upper low toward the Lower Ohio Valley would be important for the forecast of heavy snow. A problem was the forecast movement of the upper level low. The LFM and NGM models differed with the movement of the system after it moved out of eastern Kansas.

The LFM pushed the upper low southeast from eastern Kansas on 0000Z October 19 to south central Kentucky by 0000Z, October 20. The NGM model moved the upper low to southeast Missouri by 0000Z, October 20.

There was also speculation by area forecasters whether temperatures through the layers of the atmosphere would be cold enough to support a snowstorm. The temperature forecasts at 850 millibars for the LFM and NGM were in the -5°C range throughout the period from 0000Z, October 19 to 1200Z, October 20.

Both models verified closely with their 500 millibar vorticity forecast. The NGM brought slightly more positive vorticity advection (pva) up through central Tennessee into central Kentucky with lesser positive vorticity forecast for central Indiana on 0000Z October 19. By 1200Z, October 19, a vorticity maximum was forecast to be centered over east central Arkansas, rotating around the base of the upper level low over Southern Missouri.

The axis of pva on 1200Z, October 19 (Figure 1) was north of a line from central Arkansas to just south of the Ohio River in northwest Kentucky then into central Indiana. The areas through central Illinois and central Indiana were forecast to receive more positive vorticity, further suggesting that heavy snow was possible in the Indianapolis, Indiana area.

Both the LFM and NGM vorticity charts continued to show pva over central Indiana with lesser energy to support precipitation over southwest Indiana by 0000Z, October 20. Based on the 1200Z, October 19 forecast position of the upper level low and progged forecast of high levels of instability and positive vorticity advection across the lower Ohio Valley, forecasters at the National Meteorological Center (NMC) forecasted 4-8" of snow across southern Illinois, northwest Kentucky and most of Indiana for the time period running from 1900Z, October 18, 0000Z, October 20 (Figure 2).

Another important factor for the potential of a snowstorm occurring would be the amount of moisture available. Both the LFM and NGM models initiated a 90 percent mean relative humidity area across most of Kentucky by 0000Z, October 19. An upper air analysis of Paducah, Kentucky's 0000Z, October 19 upper air sounding also showed relative humidities from 1000 millibars to 500 millibars greater than 80 percent with greater than 90 percent relative humidities existing from 1000 millibars to 650 mill-ibars, supporting both models forecast of abundant moisture flow into the region.

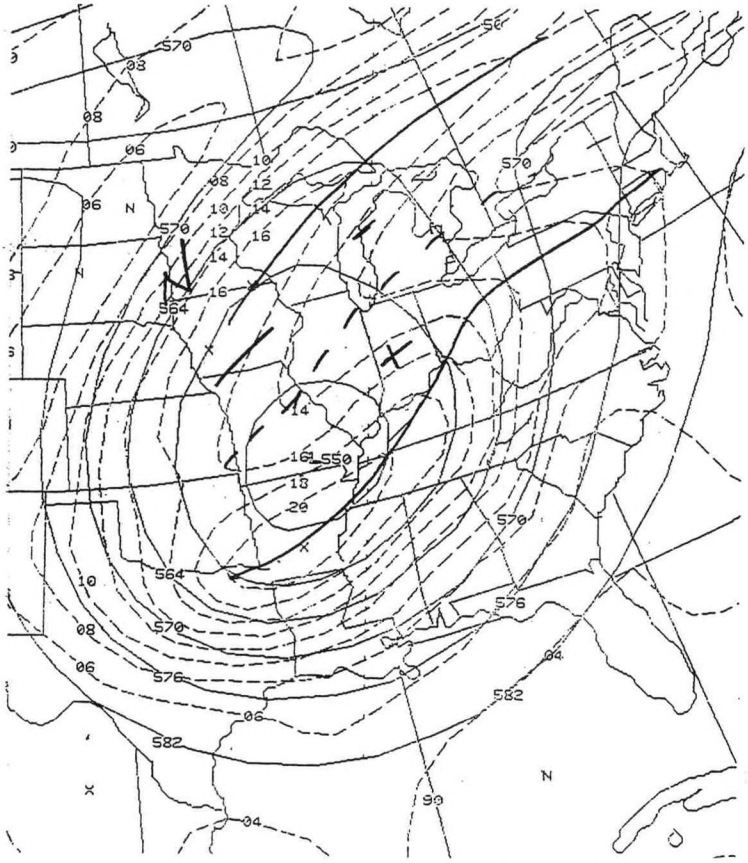

Figure 1. LFM 12 hr 500 mb heights and vorticity 1200Z, October 19, 1989.

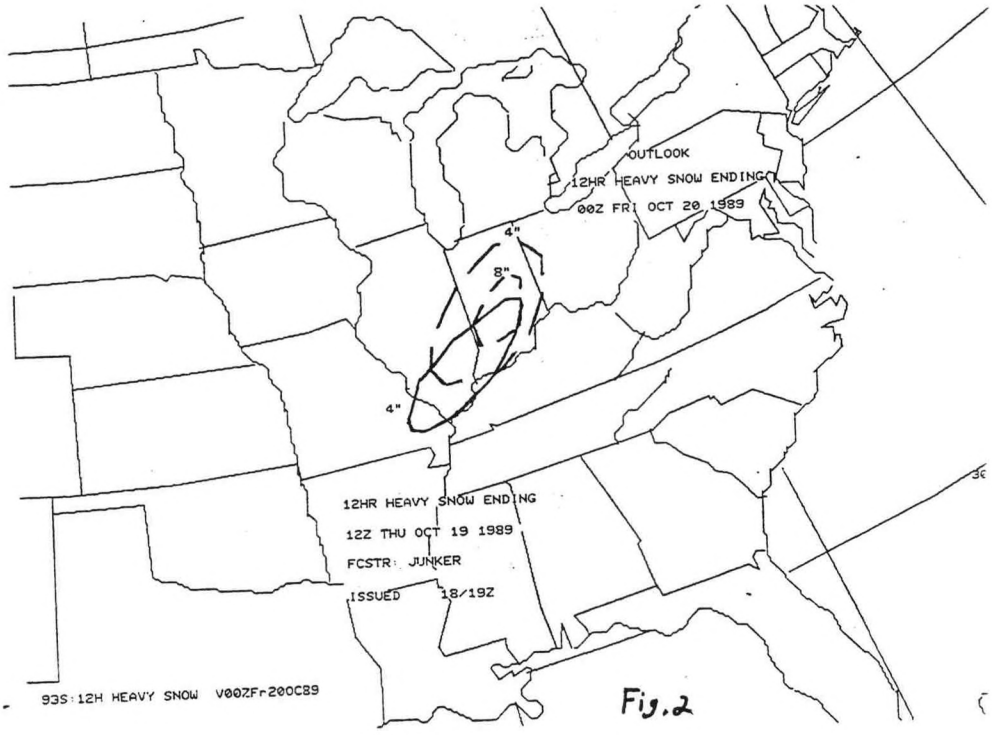

Figure 2 NMC 12 hr Heavy Snow Outlook for 1900Z, October 18 to 0000Z, October 20 1989.

2. Event Progression and Occurrence of Snow

Both the LFM and NGM models were close with the development of an upper level low pressure area in eastern Kansas by 0000Z, October 19. However, both models were way off track on the further movement of the upper level low, as it moved from east central Missouri on 1100Z, October 19 to southeast Missouri by 1700Z, October 19 to northern Illinois by 0000Z, October 20 based on information provided by the Satellite Services Branch (Figure 3). The movement of the upper level low pressure area and the proximity of the axis of vorticity that was evident across central Illinois and central Indiana, showed that more pva and instability was over the Indianapolis area than the Evansville area.

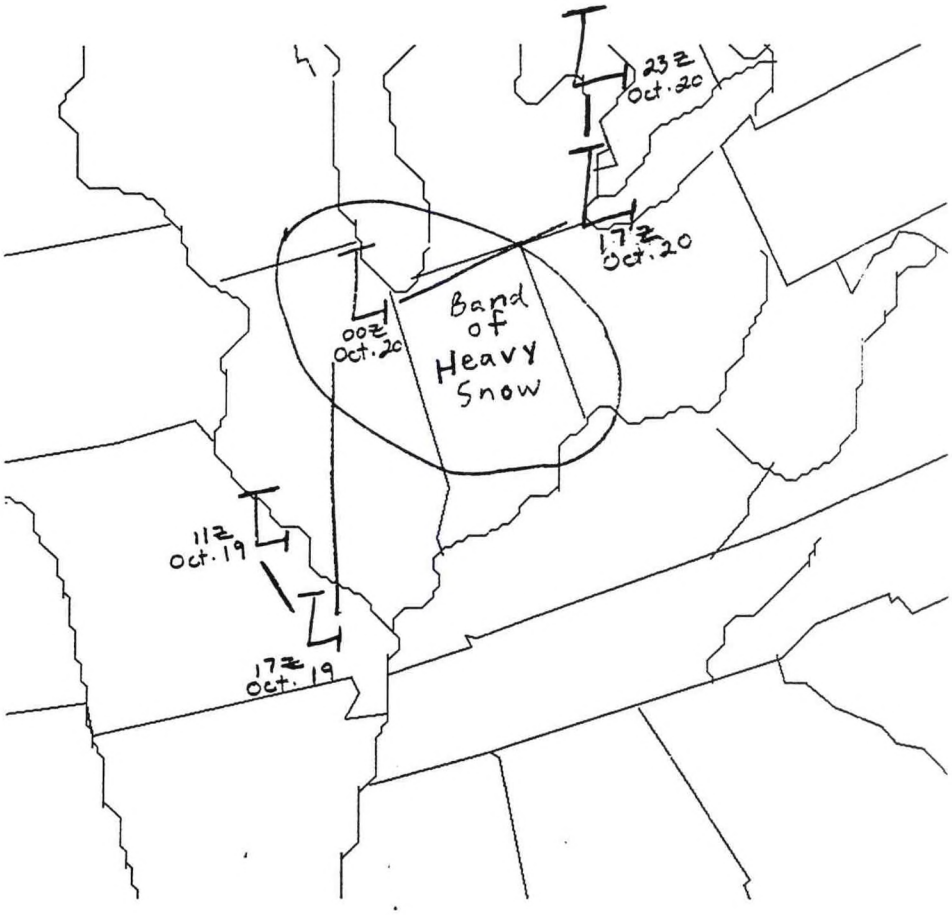

Figure 3 500 millibar low track 1100Z, October 19 to 2300Z, October 20 1989.

The Vertical Total Index (VT), (Table 1), (850 millibar temperature - 500 millibar temperature), which is a measure of stability without regard to moisture, was figured for both Peoria, Illinois and Paducah, Kentucky soundings. Calculated values ranged from 16.1°C for Peoria, Illinois and 17.1°C for Paducah, Kentucky at 0000Z, October 19. The Vertical Totals for Paducah at 1200Z, October 19 was 23.3°C compared with 17.1°C for Peoria, Illinois. These figures were high, further pointing to a large temperature lapse rate with warm air advection occurring across southwest Kentucky into southwest Indiana.

TABLE 1
Vertical Totals Index for Paducah, KY and Peoria, IL from 1200Z, OCTOBER 18 1989 to 0000Z, OCTOBER 20 1989.

VERTICAL TOTALS INDEX = 850 MB TEMP - 500 MB TEMP

PAH KY	1200Z OCT. 18TH=	12.2 DEGREES CELSIUS
	0000Z OCT. 19TH=	17.1 DEGREES CELSIUS
	1200Z OCT. 19TH=	23.3 DEGREES CELSIUS
	0000Z OCT. 20TH=	20.9 DEGREES CELSIUS
PIA IL	1200Z OCT. 18TH=	16.1 DEGREES CELSIUS
	0000Z OCT. 19TH=	16.1 DEGREES CELSIUS
	1200Z OCT. 19TH=	17.1 DEGREES CELSIUS
	0000Z OCT. 20TH=	17.6 DEGREES CELSIUS

1000-500 millibar thickness calculated on 1200Z, October 19 gave a 5,280 meter thickness for Paducah. With this value 60 meters lower than the 5,340 meter thickness value used by Goree and Younkin (1966) to determine the possibility for heavy snow, a heavy snow event also seemed evident for the Evansville area, which is about 90 miles northeast of Paducah. Even with Paducah's 5,280 meter thickness value and their 1200Z, October 19 850 millibar temperature less than 0°C at -7.7°C, Evansville was receiving a rain and snow mixture. Between 0000Z, and 1200Z, October 19, the Indianapolis area was receiving 7.7 inches of heavy, wet snow. The rain/snow mixture in Evansville changed to snow during the late morning hours on October 19, but changed back to rain before ending late in the evening on October 19.

3. Why Heavy Snow Didn't Occur In Southwest Indiana

There were a few factors why heavy snow occurred in northern and central Illinois and Indiana and not in southwest Indiana. The 700 millibar low track (Figure 4) showed that the heavy snow line was 60 to 80 miles to the northwest of the low as it moved from northwest Kentucky on 1200Z, October 19 to southwest Michigan by 1200Z, October 20. The proximity of the 700 millibar low

to southwest Indiana verified the heavy, wet snow across parts of central Illinois and central Indiana during the 24 hour period. The movement of the 700 millibar low center in reference to the Evansville area allowed an intrusion of warm air into the area. Paducah's 0000Z, October 19 upper air sounding (Figure 5) showed winds from 1000 millibars to 950 millibars turning anticyclonically and veering with warm advection occurring in advance of the precipitation to allow for enough warming in the bottom 50 millibars for the precipitation to start as a rain/snow mixture as this air was advected northeast into the Evansville area.

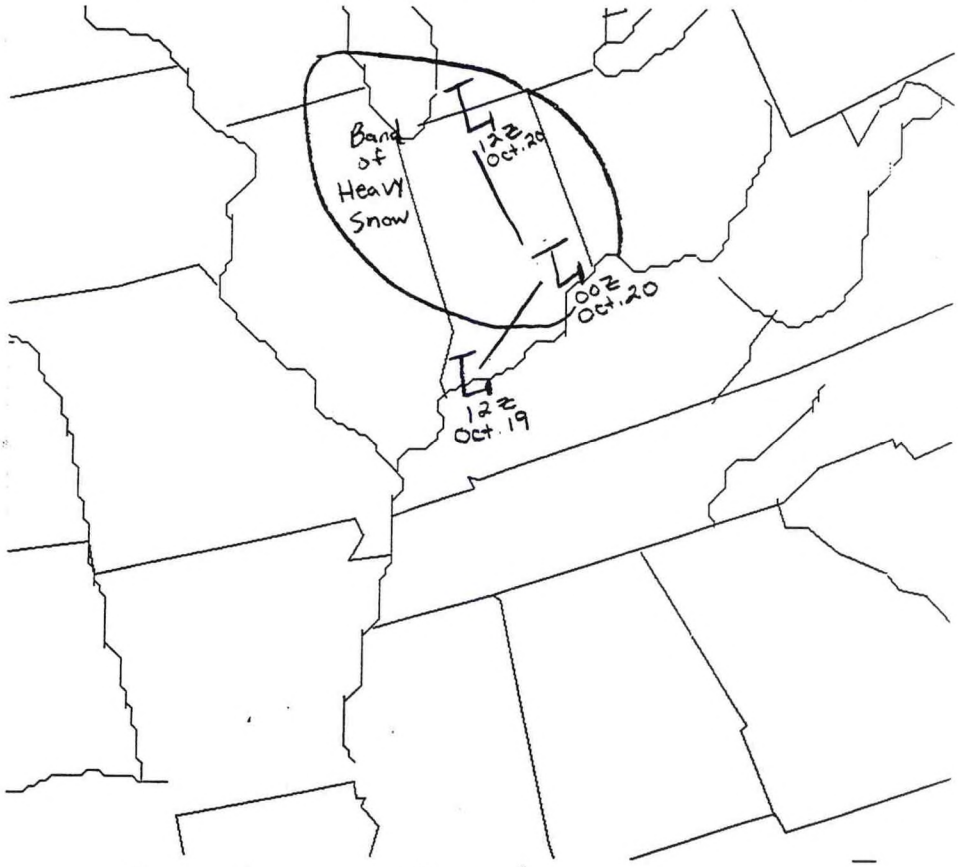

Figure 4 700 millibar low track 1200Z, October 19; 1200Z, October 20 1989.

Due to the critical movement of the 700 millibar low, calculated thickness values showed rises of 50 meters from 5,280 meters on 1200Z, October 19 to 5,330 meters on 0000Z, October 20 in northwest Kentucky and southwest Indiana, further pointing to a warmer stratum of air over the area.

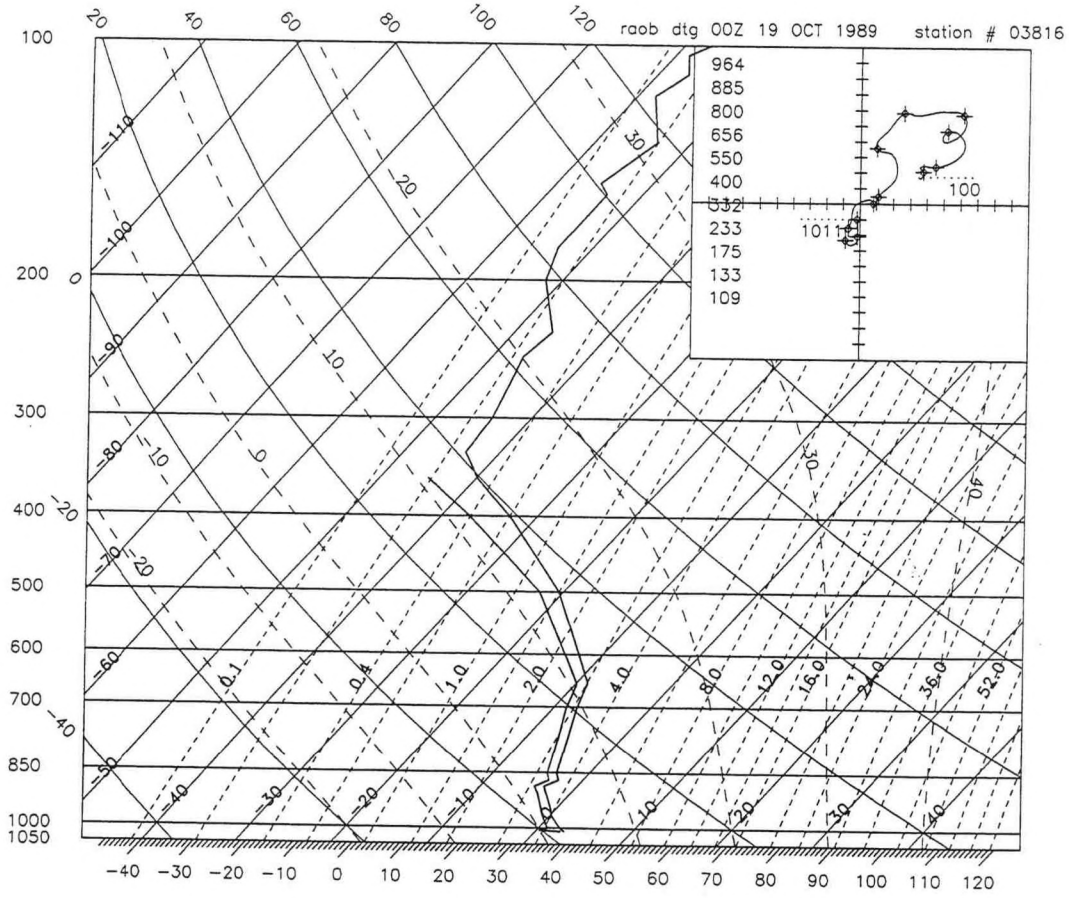

Figure 5 Paducah, KY 0000Z, OCTOBER 19, 1989 upper air sounding.

A 1000-850 millibar thickness calculation of the thickness across the region also showed a correlation that indicated that heavy snow fell over parts of central Illinois and central Indiana where the calculated thickness was between 1286 to 1291 geopotential meters through the period of 1200Z, October 19 to 1200Z, October 20. The band of heavy snow seemed to precisely follow a 1288 geopotential meter path with the mean virtual temperature around 2.5°C being the dividing line between heavy snow and a rain/snow mixture.

Then calculating the thickness between 850-700 millibars and doing an iso-thickness analysis for six stations in the South and Midwest on 1200Z, October 19 also showed another trend. For this snow storm, the calculated thickness value of 3950 geopotential meters was the thickness that the heavy snow band followed.

Paducah's 1200Z, October 19 upper air sounding also showed a conditionally unstable layer of air from 1000 to 950 millibars, indicating that some low level warm advection was spreading into Paducah and areas northeast of Paducah. Advecting this layer of air with the movement of the 700 millibar low evidently brought this warmer stratum of air into the Evansville area and south and southeast of the Indianapolis area. Therefore, enough cold air advection existed in the lower layers in the Indianapolis area to support heavy snow. Indianapolis remained north of the 700 millibar lows path, as was evident of the cold air advection moving into the area by Peoria, Illinois' 1200Z, October 19 upper air sounding. An analysis of this sounding showed wind fields from 1000-800 millibars veering with the cyclonic flow further induced by the position of the 700 millibar low over northwest Kentucky.

Peoria, Illinois' 1200Z, October 19 upper air sounding also had conditionally unstable air from 1000-850 millibars. But, a much larger subsidence inversion in the vicinity of 790 millibars gave indications also that there would be enough cold air advection from 800-500 millibars if advected northeast along the 700 millibar low track to support heavy snow in the Indianapolis area.

850 Millibar temperatures advected into the Evansville area from Paducah brought around a -6°C temperature in the area. However, a cross sectional analysis of Peoria and Paducah (Figures 6a and 6b) also verified a warm stratum of air from 1000-950 millibars that probably kept heavy snow from occurring in southwest Indiana and northwest Kentucky, compared to the heavy snow that occurred in parts of central Indiana.

McNulty (1988) stated, "The freezing level must be at least 1200 feet above the surface to insure that the snow will melt to rain." McNulty (1988) also added, "The rate of heat transfer is proportional to the temperature difference between the melting snowflake (at 0°C) and the surrounding air."

Further analysis of Paducah, Kentucky's 0000Z-1200Z, October 19 and Peoria, Illinois' 1200Z, October 19 soundings (Figures 5, 7-8) all generally indicated heating above the 0°C mark beginning around 940-960 millibars. This was a non-adiabatic effect that occurred with the eventual melting of snow to rain. "Snow extracts heat from the surrounding environment when it melts." In this situation, this cooling effect was not large enough over a period of time to offset warming due to the low level warm air advection that occurred. These soundings also showed a (Hess, 1959) variation of precipitation type with a change in temperature lapse rate, y= -dT/dz, due to the fact that even though temperatures at 850 millibars were in the -8°C range, the warmer air from 940-960 millibars to the surface changed the precipitation type from snow to a rain/snow mixture during the majority of the snow event.

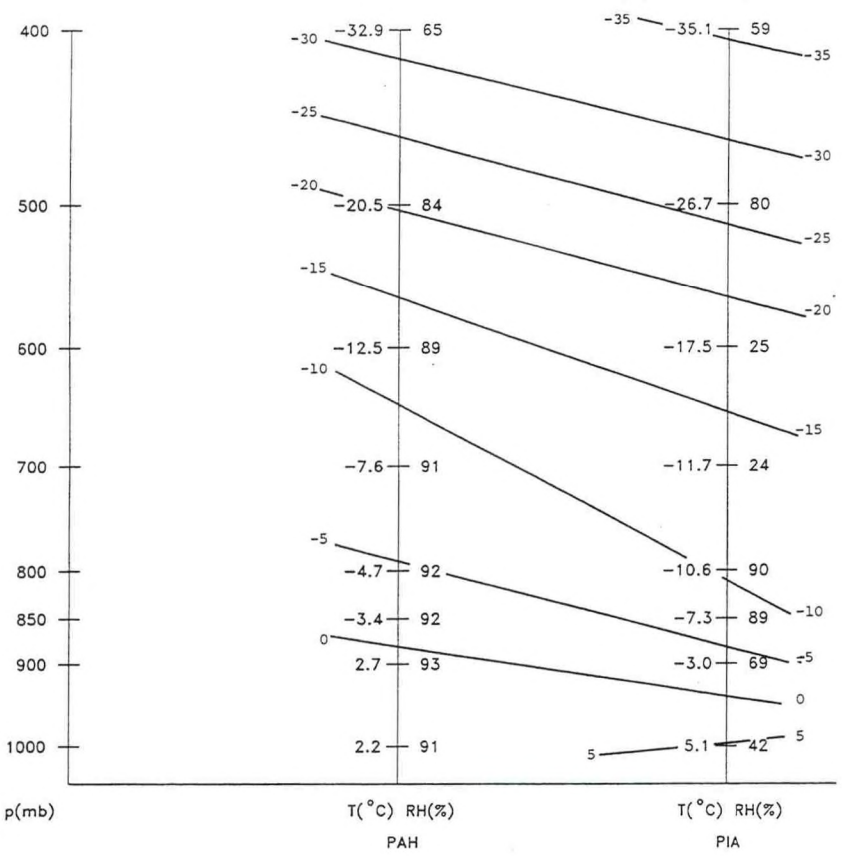

6a.

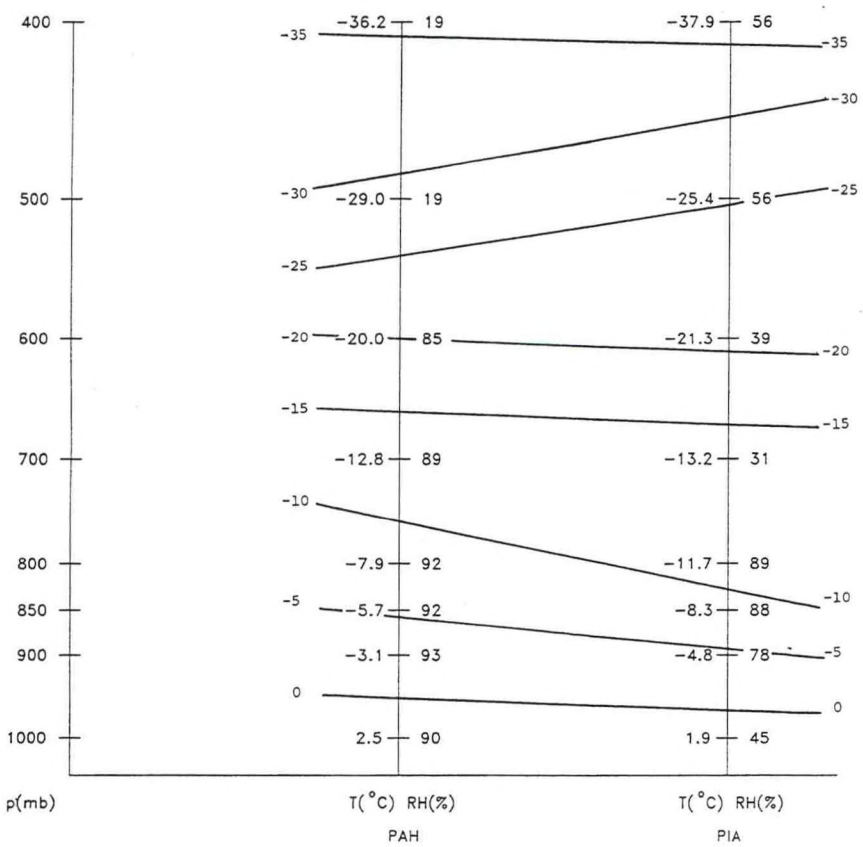

6b.

Figure 6 (a) 0000Z and (b) 1200Z, October 19, 1989 Cross Sectional Analyses; Paducah, KY (PAH) to Peoria, IL (PIA).

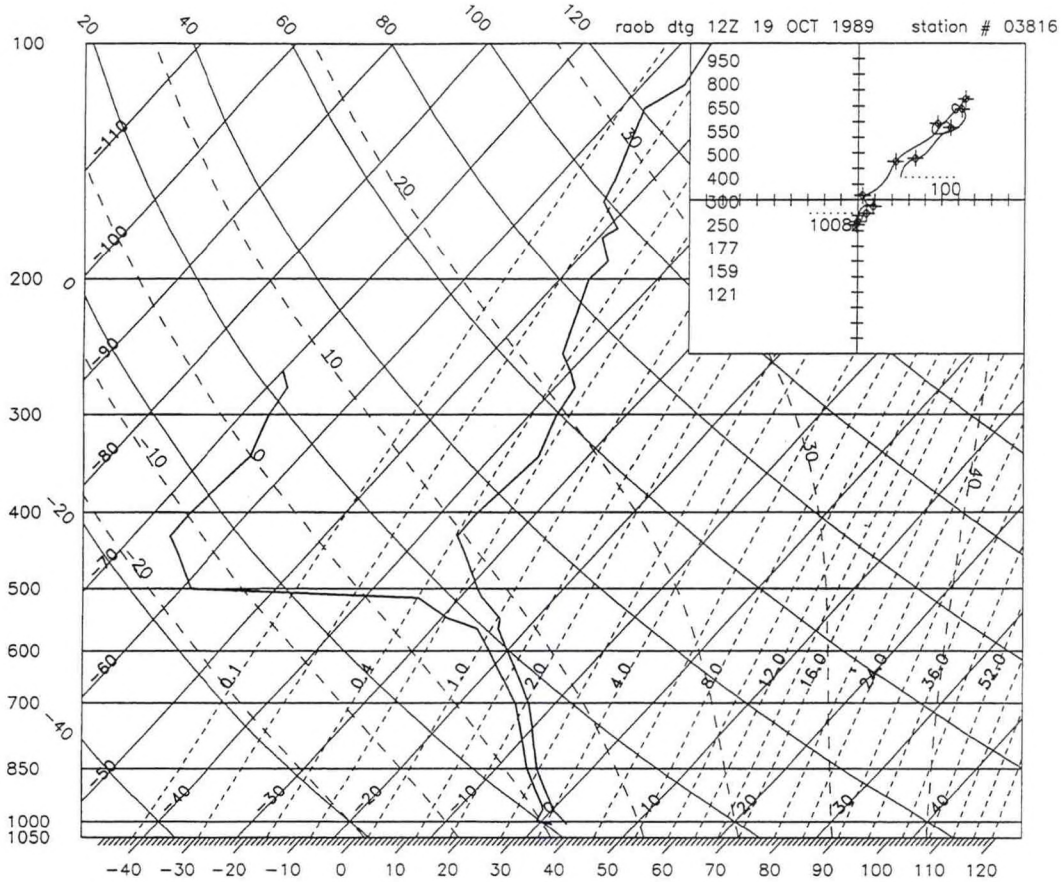

Figure 7 1200Z, October 19, 1989 Paducah, KY upper air sounding.

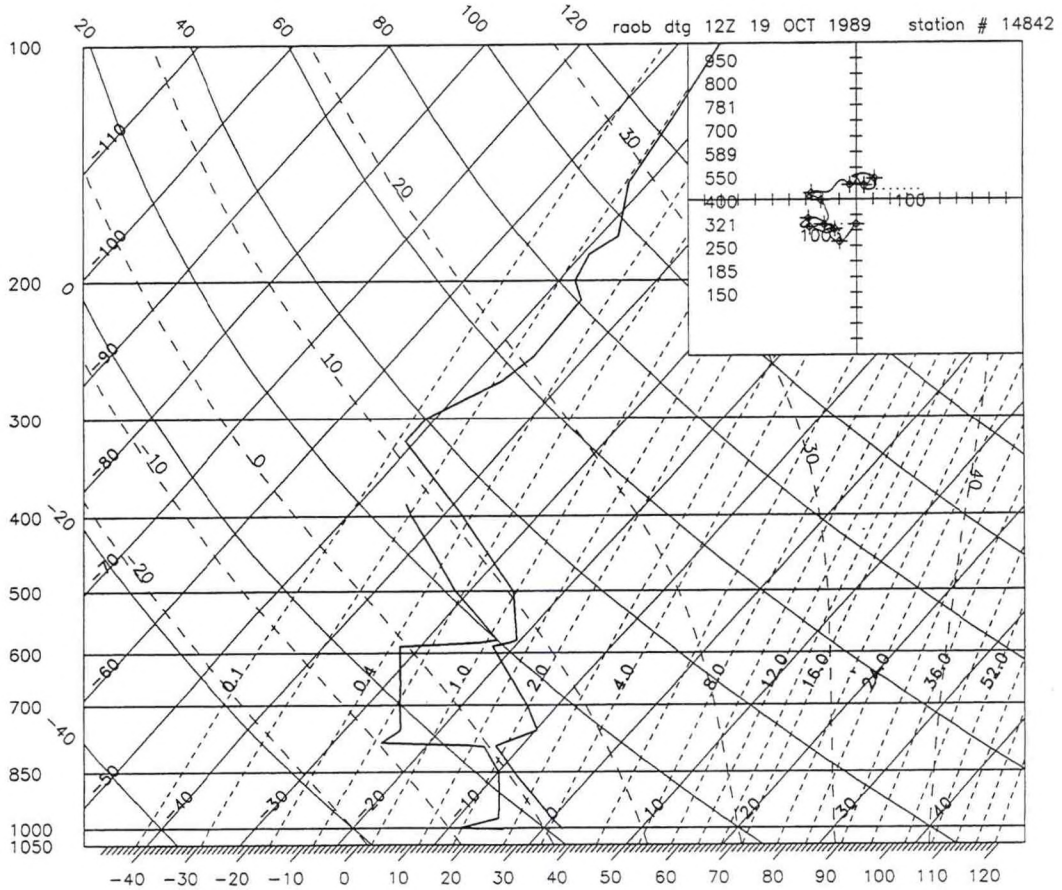

Figure 8 1200Z, October 19, 1989 Peoria, IL upper air sounding.

4. Summary

Snow forecasting is a tough problem that continues for weather forecasters. The snowstorm of October 18-20, 1989 was another rare event that showed that even though temperatures and thickness levels were cold and low enough to support snow in the Evansville area, other factors were needed. The primary reason that heavy snow missed the Evansville, Indiana area was the fact that the 700 millibar low moved too far south, through southwest Indiana on 1200Z, October 19 to southeast Indiana by 0000Z, October 20. This movement of the 700 millibar low as the system moved through the area, allowed for the intrusion of enough warmer air from the southwest of the Evansville, Indiana area that was the end result of the light amounts of snowfall in the Evansville area compared to the heavy snow that fell across the Indianapolis, Indiana area.

5. References

Goree, P. A. and R. J. Younkin, 1966: Synoptic Climatology of Heavy Snowfall Over the Central and Eastern United States. *Mon, Wea, Rev.*, 666.

Hess, S. L., 1979: Introduction To Theoretical Meteorology, 81.

McNulty, R. P., 1988: Winter Precipitation Type, Central Region Technical Attachment 88-4.

CENTRAL REGION APPLIED RESEARCH PAPER 9-5

A CORRELATION OF THETA-E AND Q VECTORS WITH A SEVERE WEATHER EVENT ACROSS SOUTH DAKOTA

Scott A. Mentzer and Cliff Millsapps
National Weather Service Forecast Office
Sioux Falls, South Dakota

1. Introduction

In recent years, a number of derived meteorological parameters have been made available to the National Weather Service field forecaster via various computer programs. Two such fields, the theta-e analysis and the Q vector analysis, can be important in determining where adequate Convective Available Potential Energy (CAPE) and ample quasi-geostrophic vertical lift are located. Programs are now available which will analyze these fields for the operational field forecaster: theta-e is obtained from the PC-THETAE program (Last, 1991) while Q vectors are obtained from the Upper Air Diagnostic Program (Foster, 1988).

Recent literature describes these two specific parameters in detail, and only a few basic points will be reviewed.

Areas with large values of theta-e are relatively high in CAPE, and therefore areas are prone to upward parcel acceleration. These high theta-e areas are often indicative of deep warm, humid air which occasionally nose north over the Great Plain states. Theta-e ridges usually move or change little over 12 hours, and are relatively easy to track on the upper air analysis (Campbell 1991). Often the small changes that do occur can be inferred by monitoring a correlated moisture plume in the water vapor imagery (Scofield and Robinson 1990). Further applications of theta-e are discussed by Campbell (1991).

Q vectors (or, more specifically, divergence of Q) imply vertical motion based on absolute vorticity advection and temperature advection. This parameter neglects friction and diabatic influences, but requires much less computational power then omega which it approximates. Areas with low divergence of Q (DIVQ) can be very transitory, as was the case in this study; thus, it can be tricky to predict changes between the upper air runs. Negative DIVQ implies upward motion and positive DIVQ implies downward motion. For a detailed explanation of Q vectors, see Durran and Snellman (1987) or Barnes (1985).

From the evening of June 18, 1991, to the morning June 21, 1991, severe weather occurred over eastern South Dakota. Three

tornadoes, moderate flooding, and numerous severe thunderstorms all occurred during this time. Figure 1 shows the locations of the severe weather events, while Figure 2 is an isohyet map showing rainfall for the three-day period.

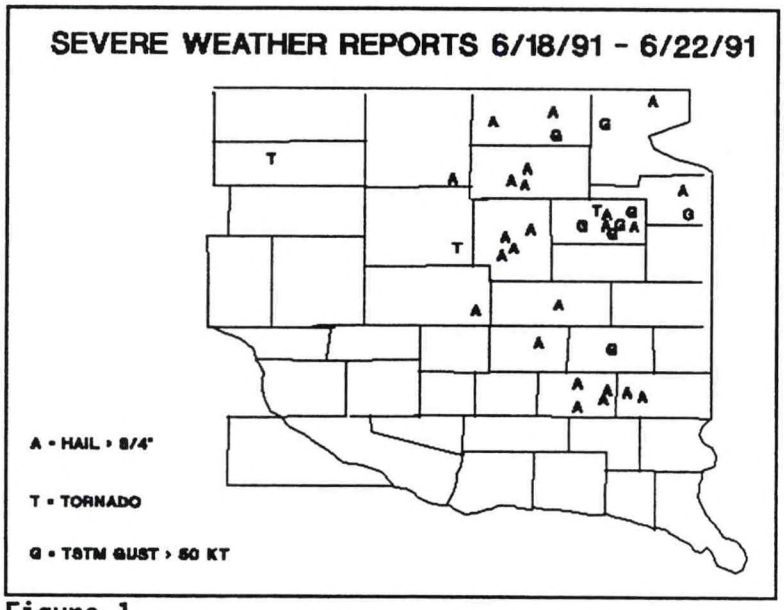

Figure 1

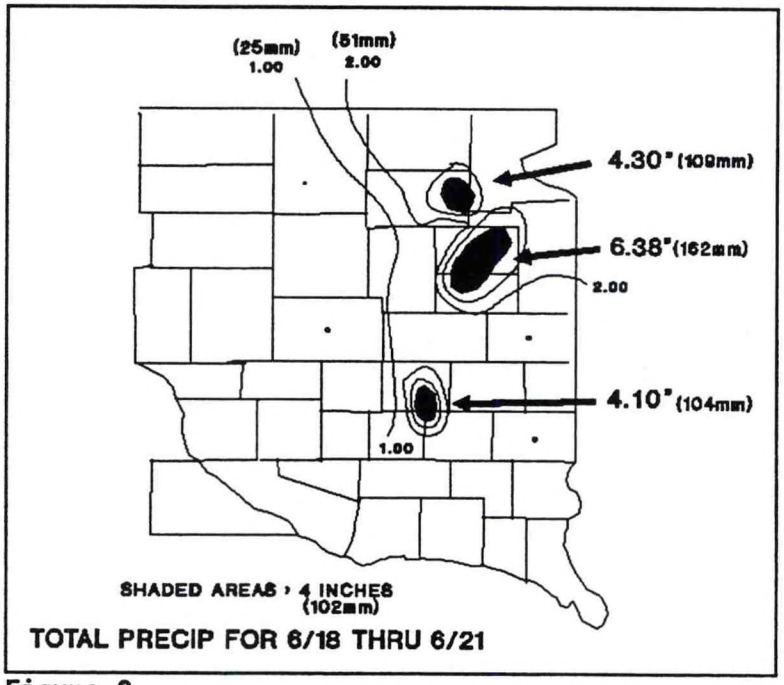

Figure 2

The authors wished to examine the performance of theta-e and the Q vectors during this event primarily for three reasons: 1) to spawn interest in these parameters at a local level, 2) to examine the performance of these fields in relation to one another over the span of the event, and 3) to take a specific look at the "Watertown Flood", which was one of the most damaging weather events in South Dakota during 1991.

The northeastern South Dakota area is where most of the notable weather occurred. This area is generally flat with a line of 300 foot (100 meter) hills extending northwest to southeast (Figure 11). The Big Sioux River Basin sits on a slightly raised plateau of glacial debris. Therefore, when lower layer air-flow is from the south or southwest it climbs a gradual grade onto the plateau; then it climbs along the east side of the Big Sioux Basin over

some low but steep hills. Watertown is located between the Big Sioux River and these hills.

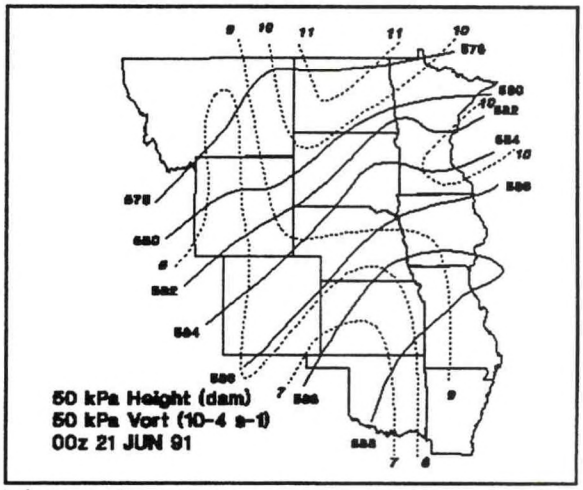

Figure 3

2. General Synoptic Pattern

Figures 3 through 5 show an upper air analysis at various levels on 0000 UTC 21 June 1991. This particular analysis was chosen since it was representative of the entire event. However, there were synoptic differences on the various days, and these will be discussed later.

At 50 kPa, a broad trough remained stationary over the western United States. This produced a general southwest flow across the Dakotas. Various minor vorticity maxima or lobes rotated across the Dakotas approximately every 12 hours.

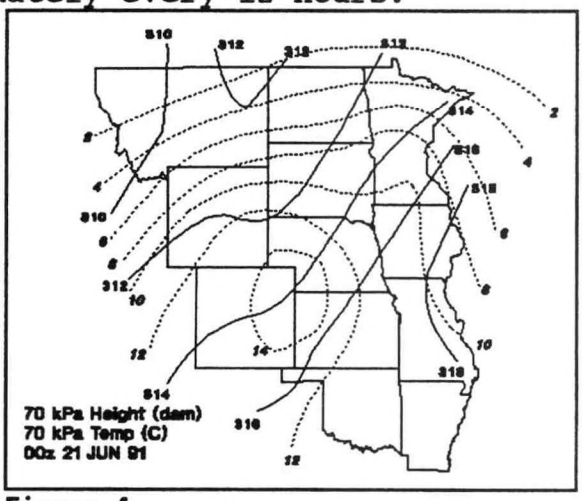

Figure 4

Similarly, southwest flow was present at 70 kPa. The 70 kPa analysis also indicated significant warm advection from Nebraska to northern Minnesota.

The lower levels (85 kPa) were relatively moist through the entire event. Dew points at 85 kPa were generally between 10°C and 12°C across eastern South Dakota. The trajectories at the 85 kPa level continued to show an influx of moisture from the Gulf of Mexico. There were many factors favorable for thunderstorm development: strong warm advection in the lower levels, a good supply of low level moisture, and adequate mid-level dynamics. Also, a surface stationary front focused an area of low level convergence over eastern South Dakota for much of the event.

3. Daily Divergence of Q and Theta-E Analysis

Recent work by Robinson and others (Robinson and Scofield, 1990) has shown the relationship between the position of theta-e ridges and theta-e maxima with the potential location of severe

weather, the potential location of flooding, and the prediction of a storm's movement. Therefore, it is valuable to determine where theta-e ridges are located, especially when the forecaster already has other indications of potential severe weather development.

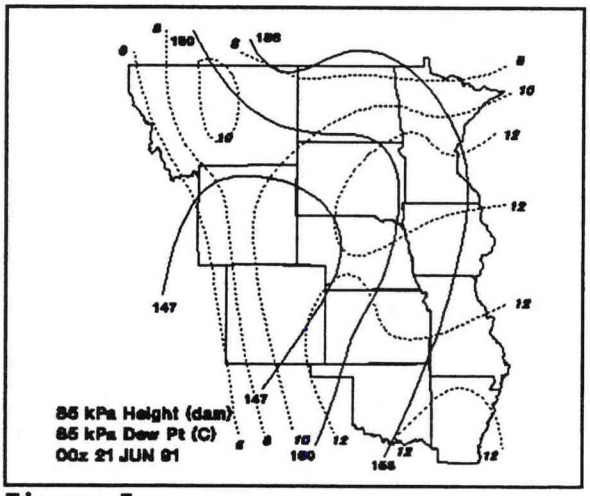

Figure 5

The problem of determining the location of upward vertical motion from "standard" synoptic charts has been well documented (Trenberth, 1978). The Q vector analysis partially solves this problem by using quasi-geostrophic theory. By examining the DIVQ, a forecaster can determine where prime synoptic scale vertical lift is located. The application of Q vector analyses in an operational forecast situation has been documented by Barnes (1985).

Figures 6 through 9 show the evolving theta-e and DIVQ patterns from 1200 UTC on 19 June 1991 to 0000 UTC on 21 June 1991. The figures also contain reports of severe weather which occurred during the succeeding 12 hours. The 12-hour precipitation amounts at Watertown (ATY) South Dakota are also included. Remember that negative values of DIVQ imply forcing for upward vertical motion.

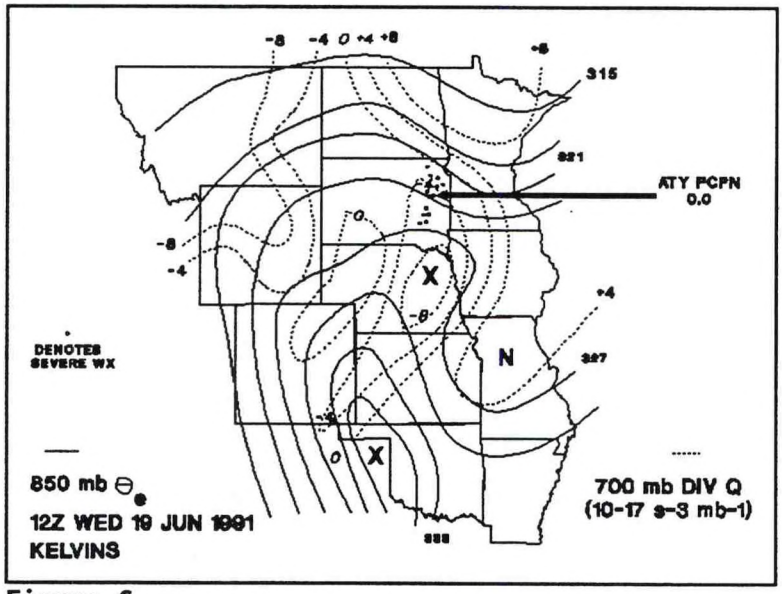

Figure 6

A. 1200 UTC 19 June 1991

A theta-e ridge axis extended from the panhandle of Oklahoma to the western Dakotas. A theta-e maximum was centered over northeast Nebraska. The DIVQ chart indicated moderate upward

forcing across eastern Nebraska and eastern South Dakota. Basic synoptic features included a weak short wave trough passing over central North Dakota and strong warm air advection over the Central Plain States.

The moderate upward forcing, indicated by DIVQ, was most likely the result of strong warm advection. Warm advection of 5°C from southwest South Dakota to northeast South Dakota was noted. The theta-e ridge axis, although not well defined over South Dakota, still indicated enough CAPE for strong convection to be produced.

Severe thunderstorms did occur during the afternoon across the entire eastern plains of South Dakota, primarily where the theta-e axis and the DIVQ trough intersected. These storms occurred approximately 8 hours <u>after</u> the 1200 UTC analysis. A tornado (F0 on the Fujita scale) was produced about 10 miles northwest of Watertown, South Dakota during the afternoon. Hail in excess of 1 inch (2.5 cm) in diameter was common with thunderstorms, and one storm over extreme north central South Dakota produced hail 2.75 inches (7.0 cm) in diameter.

B. 0000 UTC 20 June 1991

The weak short wave trough that moved across central North Dakota during the day was exiting the Dakotas. However, pronounced warm advection continued over South Dakota. Additionally, low level dew point temperatures were increasing over the state, especially over areas where rain had already fallen.

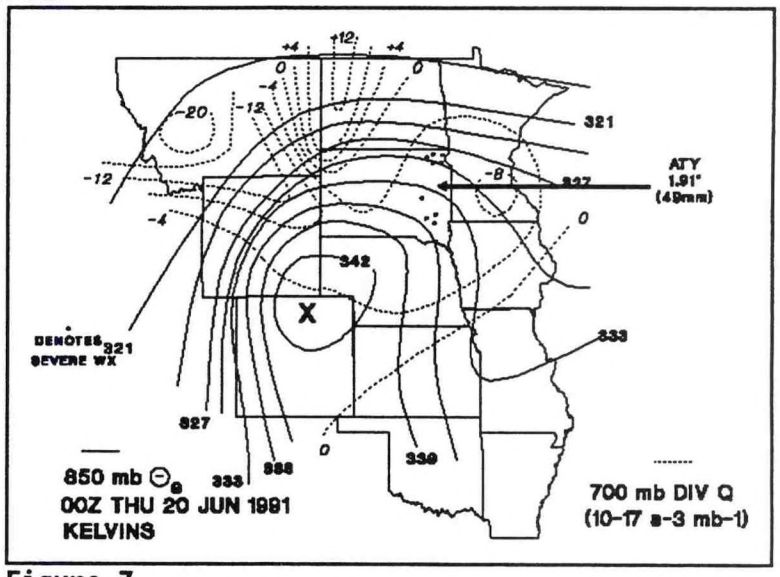

Figure 7

The theta-e ridge had now shifted slightly west and extended across eastern Wyoming and eastern Montana. A secondary ridge axis extended from the Nebraska panhandle to central Minnesota. Forcing for upward vertical motion was again implied across the eastern half of South Dakota. Strong downward vertical motion was indicated over North Dakota even though weak warm advection at 70 kPa continued.

Although some severe thunderstorms again occurred over eastern South Dakota, much of that evening's weather focused on heavy rain and flooding. Nearly 5 inches (127 mm) of rain fell about 40 km west of Sioux Falls. This excessive rain produced minor flooding in the town of Salem, South Dakota. The Watertown area also received abundant amount of rain. The rain was centered along the secondary theta-e ridge axis.

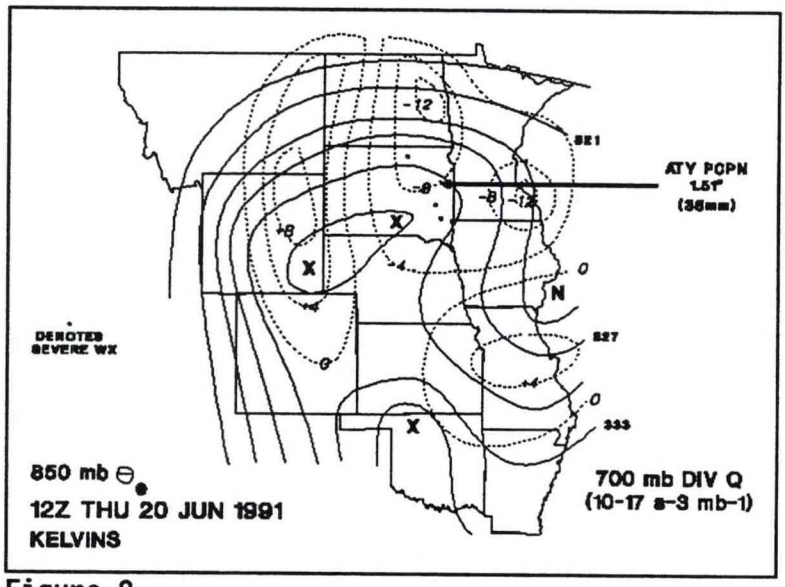

Figure 8

C. 1200 UTC 20 June 1991

Strong 70 kPa warm advection continued over the north central United States. Also, another short wave trough was approaching western South Dakota. Consequently, DIVQ charts showed massive forcing for upward vertical motion across the eastern Dakotas where an area of cyclonic vorticity advection was located. The theta-e ridge was now a broad feature across the north central United States. A theta-e maximum was located across the Nebraska panhandle to south central South Dakota. A theta-e ridge axis extended from southeast Wyoming to central Minnesota.

Severe thunderstorms again occurred across the eastern section of South Dakota. Most of the storms occurred where the DIVQ chart indicated the greatest upward vertical motion and intersected on the west side of the theta-e ridge axis. A late afternoon tornado (F0) occurred over north central South Dakota. Watertown again received excessive rainfall and reported flooding.

D. 0000 UTC 21 June 1991

Another short wave trough was about to enter western South Dakota, although cyclonic vorticity advection was limited at the 50 kPa level. Warm advection remained over the entire area. The DIVQ chart showed strong upward vertical motion over eastern South Dakota due to this warm advection. Although 50 kPa vorticity was weak, differential vorticity advection through the

atmosphere was pronounced due to the approaching trough. This also contributed to strong upward vertical motion. A well defined theta-e ridge extended from western Kansas to northeast South Dakota.

A tornado (F0) formed over northeast South Dakota where large negative DIVQ values intersected with the western edge of the theta-e ridge. Severe thunderstorms also occurred over northeast South Dakota. Flooding was compounded in and near Watertown where heavy rains occurred again.

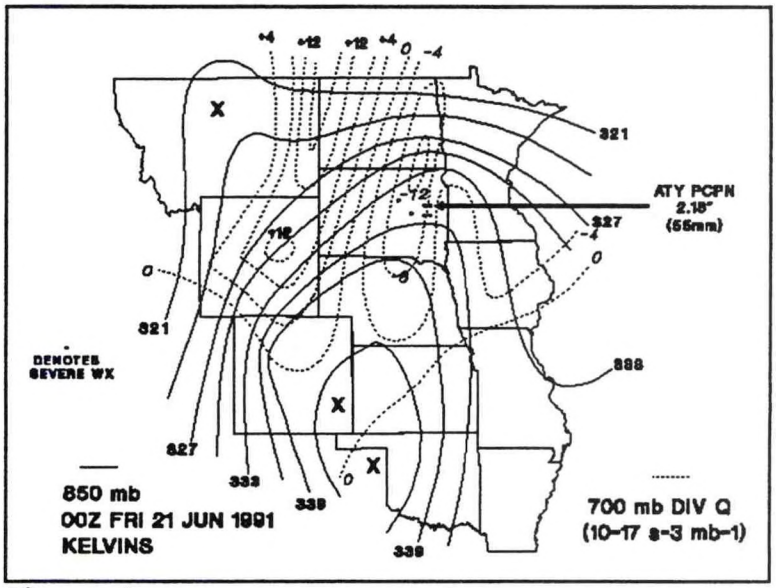

Figure 9

E. Analysis

The intersection of DIVQ with various locations along the theta-e ridge axis provided a good estimate of where possible severe weather and flooding would occur during this event.

4. Mesoscale Features and the Watertown Flood

During this particular event, minor flooding was scattered across eastern South Dakota while moderate flooding occurred across the northeast portion of the state. Watertown is believed to have been close to the core of the greatest rain accumulations and, being the urban center of the area, suffered the greatest damage. Watertown received over six inches (over 150 mm) of rain during the event. The water level at Lake Kampeska, located a few miles northwest of Watertown, rose 11 inches (about 28 cm) during one 12-hour span. Heavy rains produced much culvert, road, and urban flood damage along with lowland flooding along the Big Sioux River in the Watertown area. Due to the damage caused and data available, the authors took a closer look at this event.

Mesoscale features served to focus thunderstorm development, although we have emphasized synoptic scale contributions to lift and available energy. As Doswell has discussed (Doswell, 1987), it is impossible to discuss the initiation of severe thunderstorms without analyzing features in the mesoscale. In the case

of the Watertown flood, we examined two such features: low level moisture convergence and orography.

Figure 10 shows a surface map for 1200 UTC 20 June 1991. Two features are especially worth noting. The first is the influx of low level moisture over eastern South Dakota from the Southern Plains. The second is a stationary front that focused an area of convergence over eastern South Dakota. Since a good supply of low level moisture was already in place and theta-e charts indicated an abundant amount of CAPE, surface wind convergence produced upward vertical motion in the moist air, and convection across South Dakota was initiated.

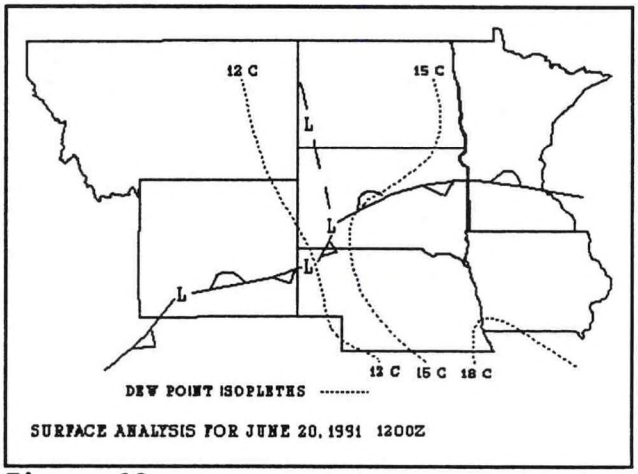

Figure 10

However, a more subtle and, perhaps, more important source of lift was due to the orographic effects acting upon moist air in the area (Huston, 1990). Figure 11 is a southwest perspective of the major relief features in northeast South Dakota. With surface through 85 kPa trajectories from the south (preceding the stationary front) moist air was forced to move from relatively flat land across the Lakota Hills. This orographic lift was likely the trigger for thunderstorm initiation.

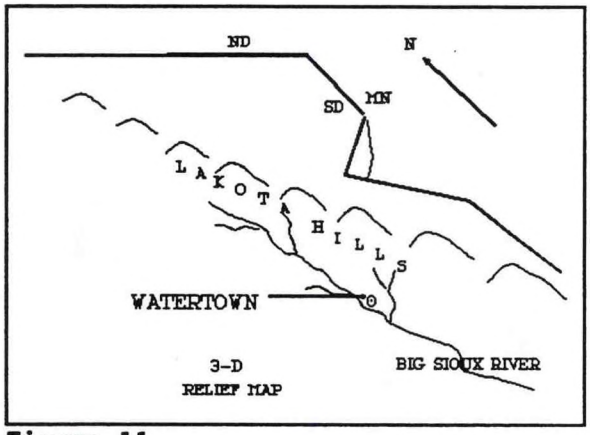

Figure 11

5. Theta-E, Q Vectors, and the Watertown Flood

Once convection was initiated by (primarily) mesoscale forcing, convection continued and intensified due to synoptic scale lift. Q vectors indicated upward vertical motion through the entire event. Not surprisingly, the greatest amount of precipitation Watertown received (55 mm) through any 12 hour period occurred when the DIVQ implied the greatest forcing of upward vertical motion at 0000 UTC on 21 June 1991 (Figure 9).

However, lift by itself does not guarantee strong/severe thunderstorm development. By using the theta-e analysis with the DIVQ chart, a forecaster can see where the greatest upward vertical motion will coincide with greatest CAPE. Figure 9, in particular, shows the intersection of these fields. The intersection correlates well with the "Watertown Flood" (and also with the corresponding severe weather north of Watertown).

Finally, theta-e also gives a clue on how storms may propagate. Figure 12 is a satellite photo at 1031 UTC. Note the developing mesoscale convective system (MCS) across northeast South Dakota which has a clear western border along the Lakota Hills. Though 70 kPa through 50 kPa flow was from the southwest, note in Figure 13 that there is significant development of convective cells to the southwest of the main MCS just 30 minutes later. This seems to indicate a backward propagating system toward higher theta-e values (Robinson and Scofield, 1990).

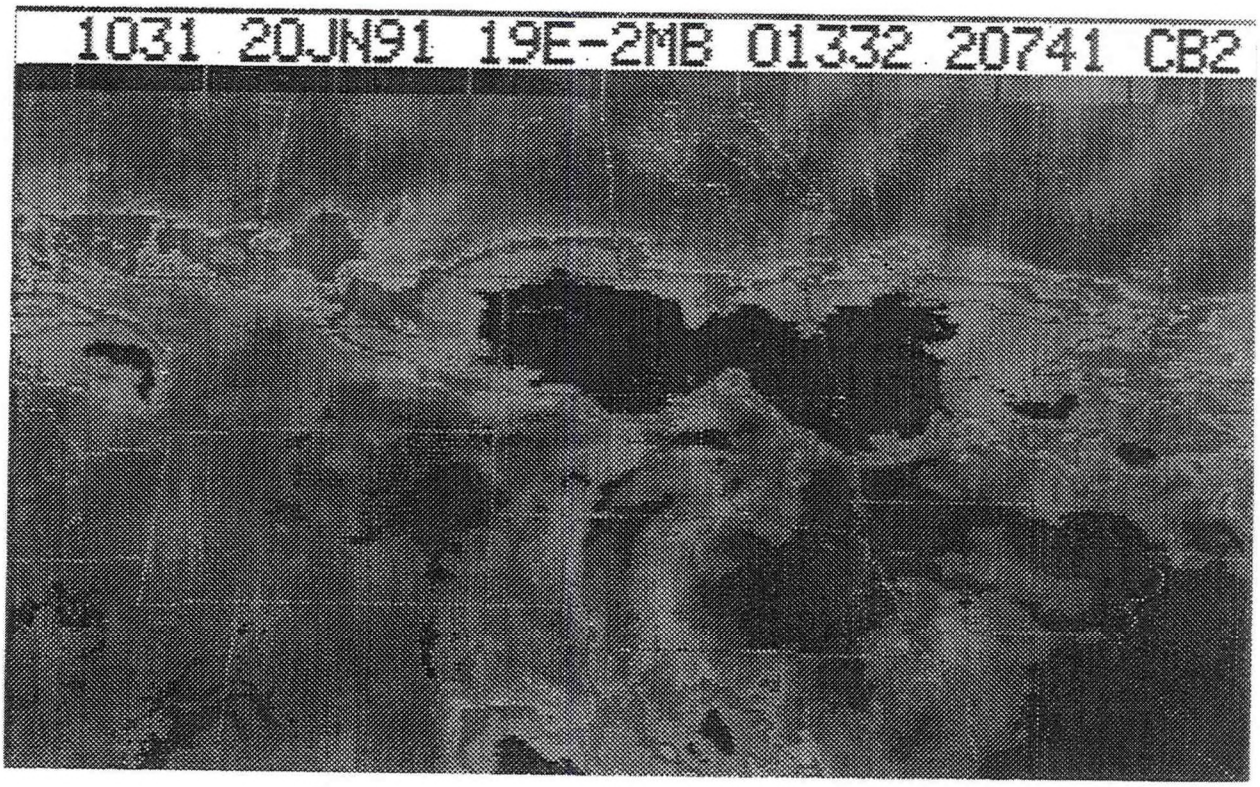

Figure 12. Infra-red (IR) satellite imagery for 1031 UTC, 20 June 1991.

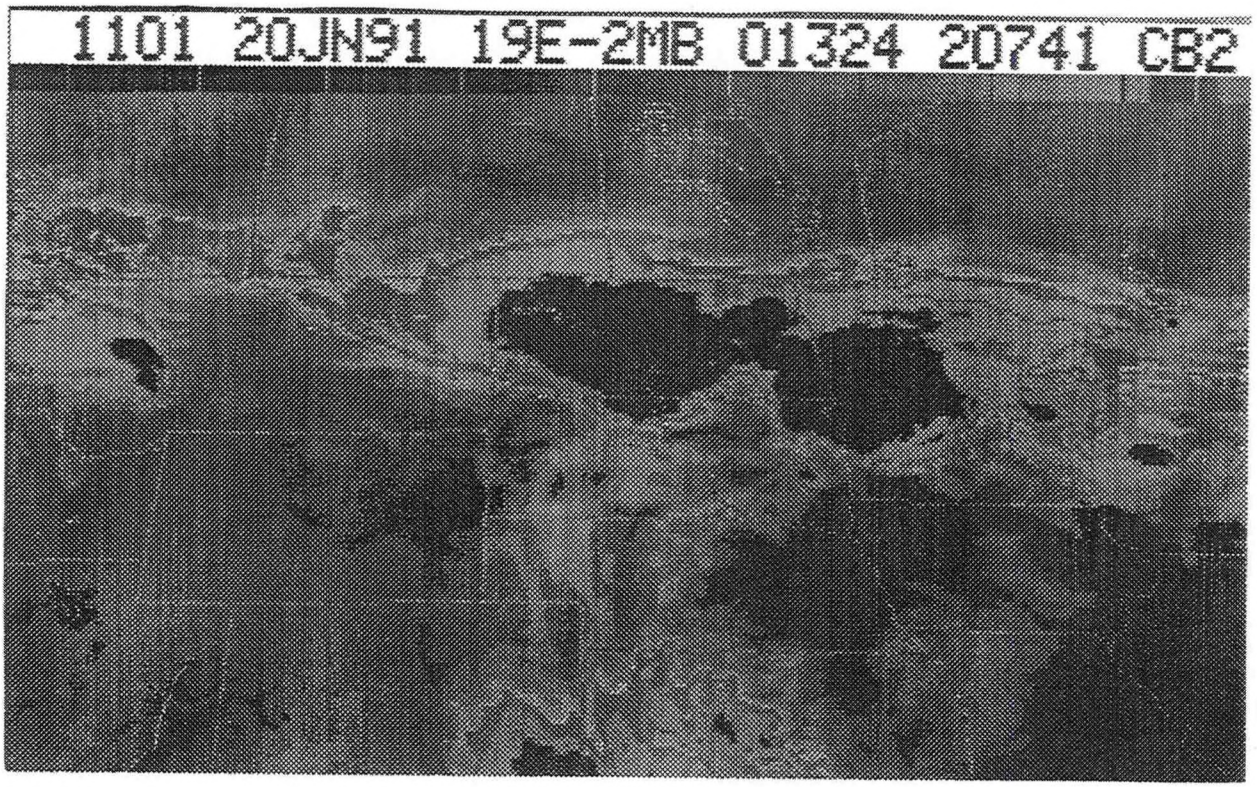

Figure 13. Infra-red (IR) satellite imagery for 1101 UTC, 20 June 1991

Putting all features together: mesoscale features like orography and low level moisture convergence initiated convection over northeast South Dakota. Theta-e maps indicated that the air mass contained large CAPE for the potential of flooding and severe thunderstorm development. DIVQ charts showed moderate to strong synoptic scale vertical lift which aided in convective development. Finally, once an MCS formed, the new cells appeared to regenerate toward the area of higher theta-e values.

6. Conclusion

This study was done primarily to promote an interest in two relatively new tools available to the operational forecaster. The interplay between Q vectors and theta-e looks to be promising in determining where severe weather or flooding events may occur. However, more importantly, this study wishes to underscore to the field forecaster the interaction between mesoscale and synoptic scale features in convective development. It can become very easy to rely on numerical guidance, upper air analysis using questionable assumptions (for example, using only the 50 kPa chart to determine vertical motions based on cyclonic vorticity advection alone), and model generated products to issue a convec-

tive forecast. By understanding how the mesoscale interacts with the synoptic scale, the forecaster gains a deeper insight into convective processes and, hopefully, in determining where the most significant weather will be. Evolving technology, such as the theta-e analysis and the Q vector charts, can bring useful information into the meteorological mosaic.

7. Acknowledgements

The authors wish to thank Mr. Richard Pritchard from NESDIS for providing the satellite data. Mr. Mike Buss also helped with some graphic creations.

8. References

Barnes, S. L., 1985: Omega Diagnostics as a Supplement to LFM/MOS Guidance in Weakly Forced Convective Situations. *Mon. Wea. Rev.*, **113**, 2122-2141.

Campbell, M., 1991: Equivalent Potential Temperature (Theta-E) Applications. Western Region Technical Attachment 91-37, NWS Western Region, Scientific Services Division, Salt Lake City, Utah.

Doswell, C. A., 1987: The Distinction between Large-Scale and Mesoscale Contribution to Severe Convection: A Case Study Example. *Wea. and For.*, **2**, 3-16.

Durran, D. R. and L. W. Snellman: The Diagnosis of Synoptic-Scale Vertical Motion in an Operational Environment. *Wea. and For.*, **2**, 17-31.

Gilbertson, J. P., 1989: Quaternary Geology of Northeastern South Dakota. University of South Dakota.

Huston, D. D., 1990: Orographic Lift in a Seemingly Flat Envi ronment. Central Region Technical Attachment 90-16, NWS Central Region, Scientific Services Division, Kansas City, Missouri.

Foster, M. P., 1988: Upper Air Analyses and Quasi-Geostrophic Diagnostics for Personal Computers. NWS Southern Region, Scientific Services Division, Ft. Worth, Texas.

Last, J. K., 1991: PC-Thetae, Central Region Computer Program No. 9MC. NWS Central Region, Scientific Services Division, Kansas City, Missouri.

Robinson, J. and R. Scofield, 1990: Backward Propagating Mesoscale Convective Systems and Flash Floods. Satellite Applications Information Note 90/6, NESDIS, Washington DC.

Scofield, R. A. and J. Robinson, 1990: The "Water Vapor Imagery/Theta-e Connection" with Heavy Convective Rainfall. Satellite Applications Information Note 90/7, NESDIS, Washington DC.

Trenberth, K. E., 1978: On the Interpretation of the Diagnostic Quasi-geostrophic Omega Equation. *Mon. Wea. Rev.*, **106**, 131-137.

Weldon, R. B. and Holmes S. J., 1991: Water Vapor Imagery; Interpretation and Applications to Weather Analysis and Forecasting. NOAA Technical Report NESDIS 57, Washington DC.

CENTRAL REGION APPLIED RESEARCH PAPER 9-6

ANALYZING CASE STUDIES AND FORECASTING LEE-ENHANCED CLOUDS ALONG THE COLORADO FRONT RANGE

Michael K. Holzinger
National Weather Service Forecast Office
Denver, Colorado

1. Introduction

Lee-enhanced clouds (mountain wave clouds) can have a significant impact on weather along the Front Range of Colorado. When lee-clouds develop, cloud cover, and possibly other weather parameters, such as temperature and wind may also be affected. Lee-enhanced clouds are clouds that are produced or enhanced as a result of the vertical deformation of the wind pattern by a mountain barrier or other high terrain feature.

The focus of this paper is to begin looking for some concrete means of forecasting lee-clouds along the Front Range. Five cases were studied. Specific data for two of the cases are included here. Data in Figures 2 through 10 are from the DARRRE II (Denver AWIPS Risk Reduction and Requirements Evaluation) workstation.

To understand the topography upwind (during lee-enhancement) from Denver (Figure 1), which is a cross-section of terrain extending 75 miles westward from Denver. Lee-enhanced clouds in the neighborhood of Denver can occur at any level from mountain top level, or about 13,000 feet, on up.

2. Case of 31 January - 1 February 1991

This was the longest-lasting of the five cases. A cirriform ceiling was reported at Denver continuously from 1500 UTC, 31 January until 2100 UTC, 1 February. IR satellite pictures showed the cloud cover trends. Figure 2 at 1400 UTC, 1 February was taken near the peak of the lee-enhancement.

Winds aloft at 1500 UTC, 31 January were northwesterly, but backed to a more westerly direction by 0600 UTC, 1 February. Winds from the demonstration network profiler at Platteville (PLT in Figure 2) in Figure 3 show westerly winds through the middle and latter part of the event decreasing but remaining westerly. Lee-enhanced clouds decreased as the winds decreased but did not disappear completely.

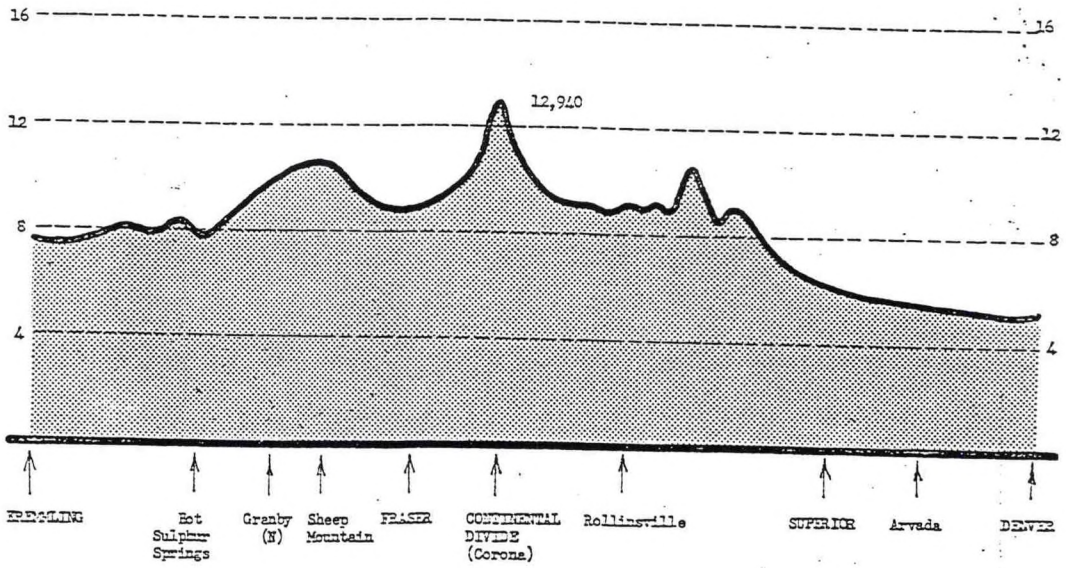

Figure 1. Upwind (during lee-enhancement) topography from Denver, Colorado.

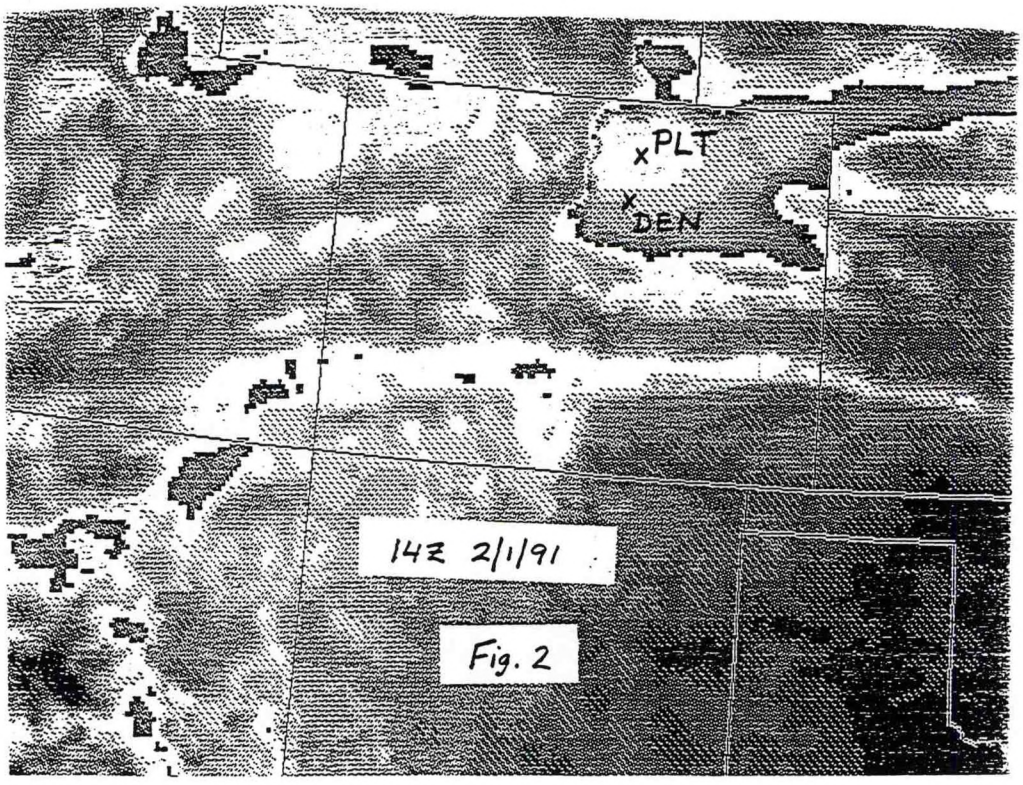

Figure 2. IR satellite imagery of lee-enhanced clouds at 1400 UTC, 1 February 1991.

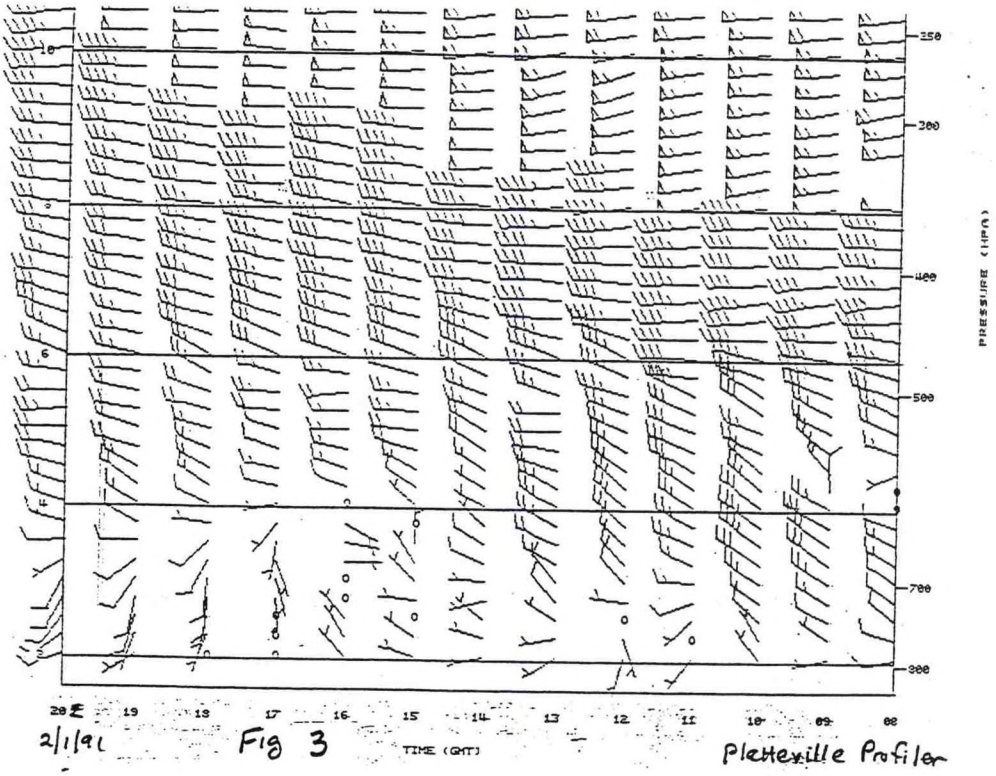

Figure 3. Time section of winds from Platteville, Colorado, wind profiler from 0800 UTC to 2000 UTC on 1 February 1991.

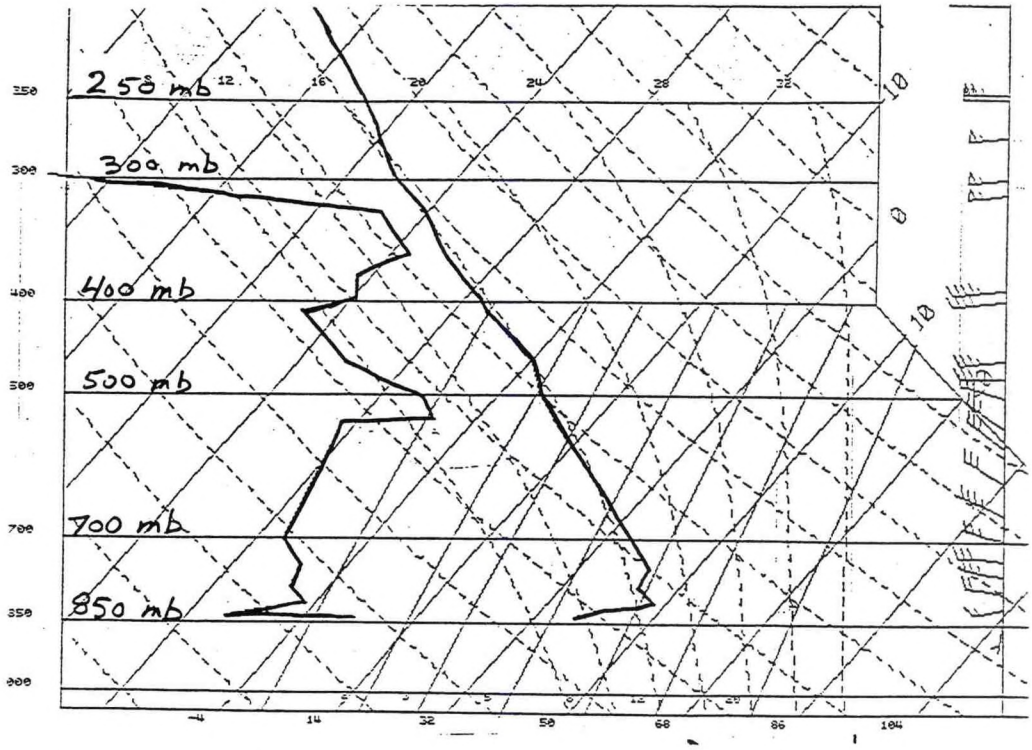

Figure 4. 1200 UTC, 1 February 1991 sounding from Denver, Colorado.

The 1200 UTC, 1 February Denver radiosonde (Figure 4) shows the main moist layer between 400 mb and 300 mb with another layer of moisture hinted at near 500 mb. Examination of moisture at 400 mb and 300 mb could have been misleading since it was nearly dry at those levels. Analysis of tropopause winds and isotachs near the maximum lee-enhancement at 1500 UTC, 1 February (Figure 5) shows that the Front Range was in the right-rear quadrant of a jet maximum--an area usually associated with upward vertical motion (McNulty, 1978, NWS, 1991). Cross-sections (time versus height) of NGM analyses and forecasts of vorticity advection (not shown) showed weak NVA and weak PVA at various times and at differing levels of the atmosphere without having any obvious relationship to lee-cloud development.

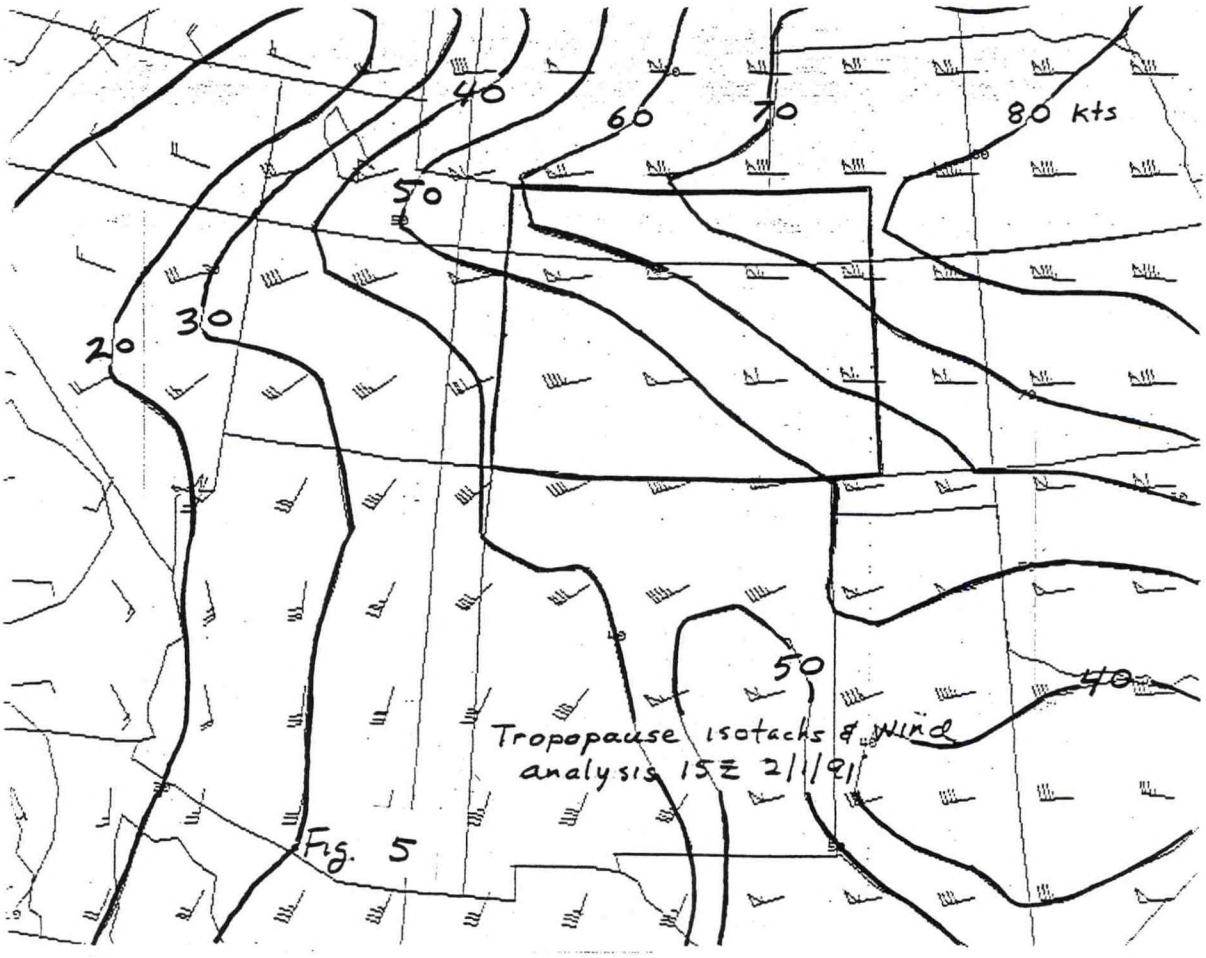

Figure 5. Isotachs and winds at tropopause level at 1500 UTC, 1 Feburary 1991.

3. Case of 18 October 1990

The 1200 UTC, 18 October 1990 Denver (DEN) raob (Figure 6) showed a layer of moisture just above 500 mb with northwesterly flow at that level. There was a stable layer just above the moist layer. An upstream raob, Ely, Nevada (ELY, Figure 7), showed much more high level moisture. The Platteville profiler (Figure 8) showed winds backing with time as the ridge axis went by and a short wave trough approached.

Lee clouds developed at Denver, increased, and became broken to overcast about 1700 UTC, 18 October. Clouds did not begin to decrease until after 0000 UTC, 19 October. An IR satellite picture (Figure 9), taken during the afternoon, revealed extensive lee enhanced clouds extending from southeastern Wyoming southward to New Mexico.

A cross section, using data from the Mesoscale Analysis and Prediction System (MAPS) (Benjamin et al., 1991) is shown in Figure 10. The height versus distance cross section is a six hour forecast valid at 1800 UTC, 18 October 1990 showing winds and isopleths of vorticity advection. Note the strong NVA centered at 250 mb just exiting the Front Range with PVA centered at the same level approaching. It appears that the PVA in Figure 10 coincided well with the lee enhanced clouds.

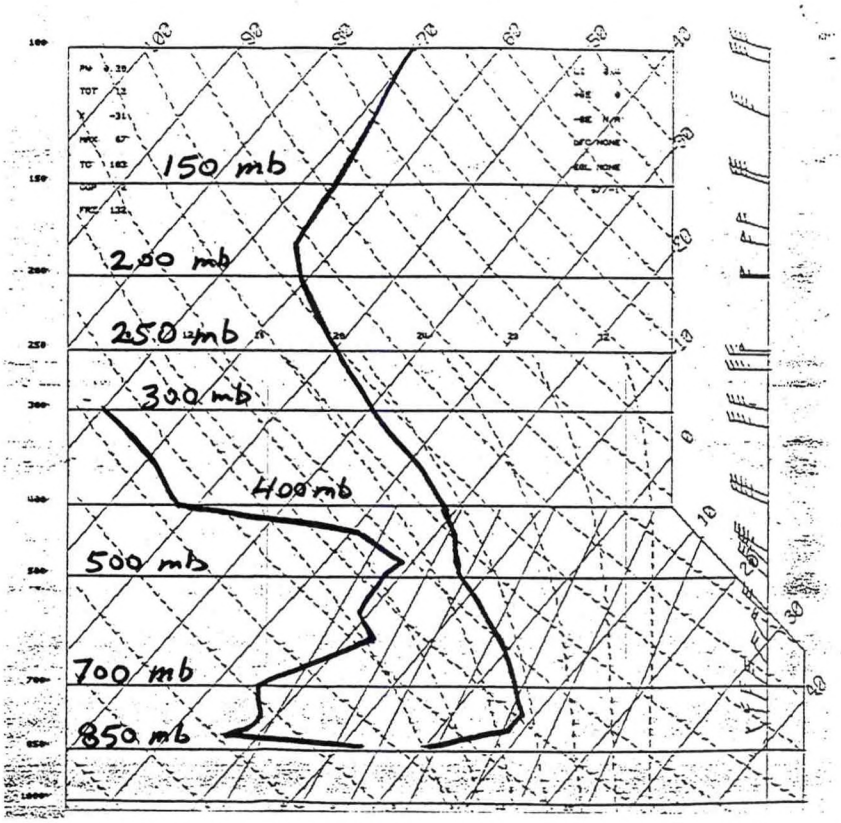

Figure 6. 1200 UTC, 18 October 1990 sounding from Denver, Colorado (DEN).

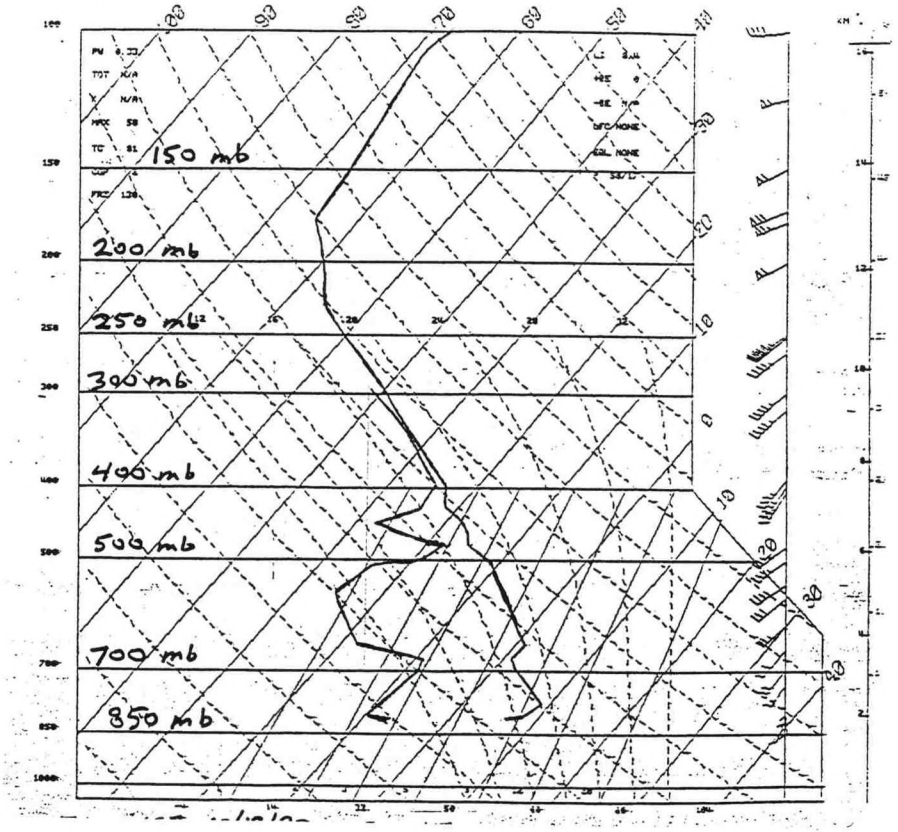

Figure 7. 1200 UTC, 18 October 1990 sounding from Ely, Nevada (ELY).

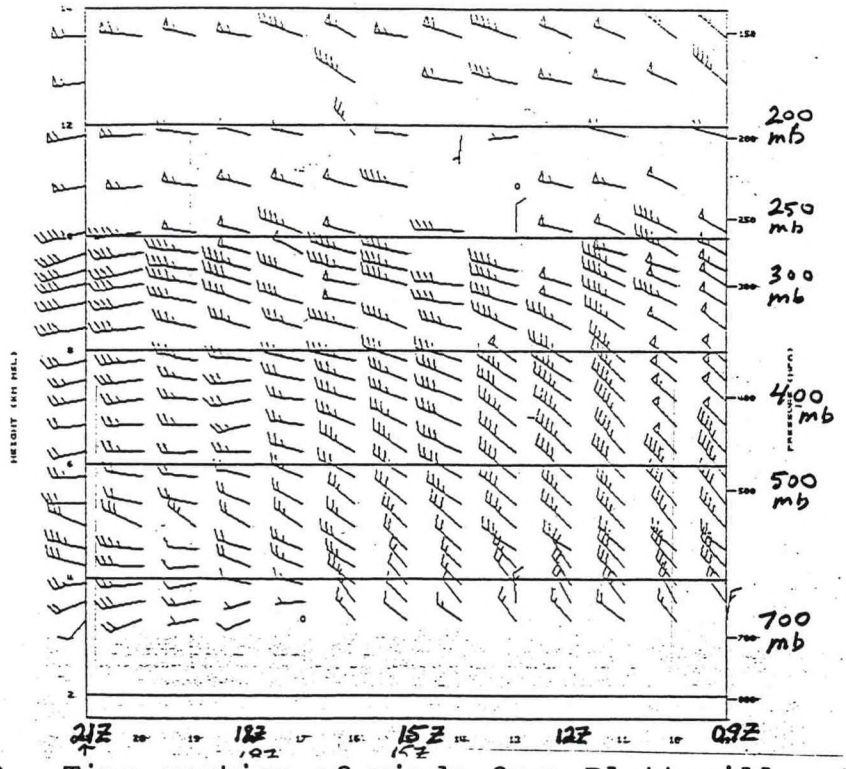

Figure 8. Time section of winds from Platteville, Colorado wind profiler from 0900 UTC to 2100 UTC, 18 October 1990.

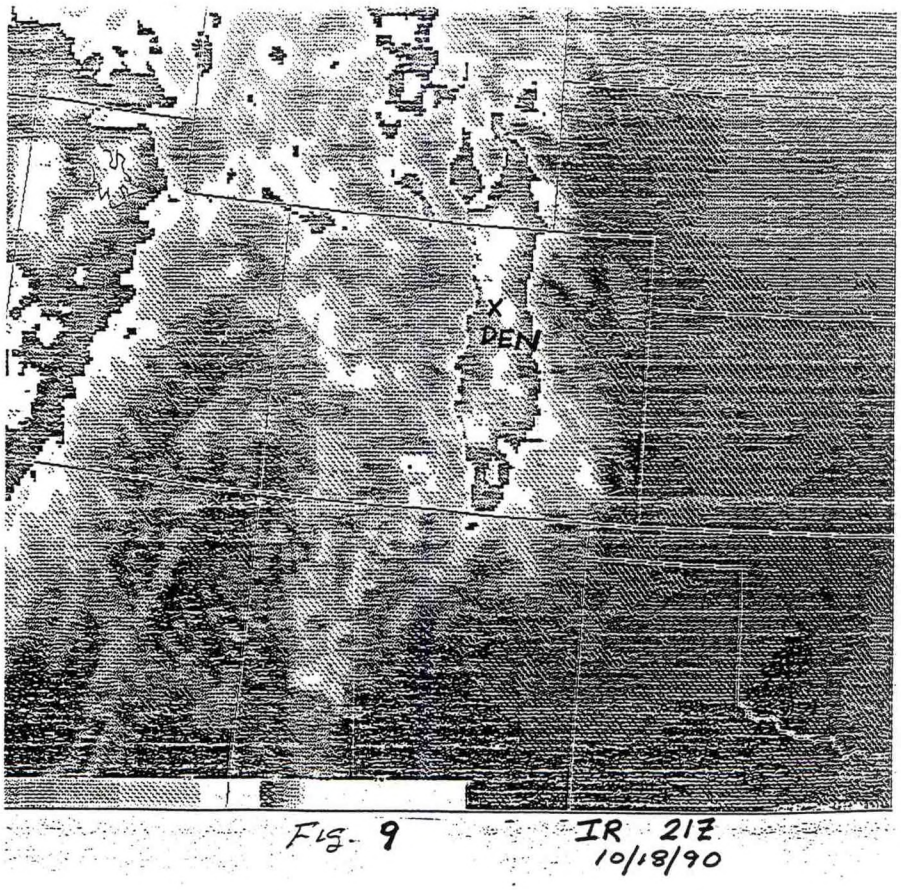

Figure 9. IR satellite imagery of lee-enhanced clouds at 2100 UTC, 18 October 1990.

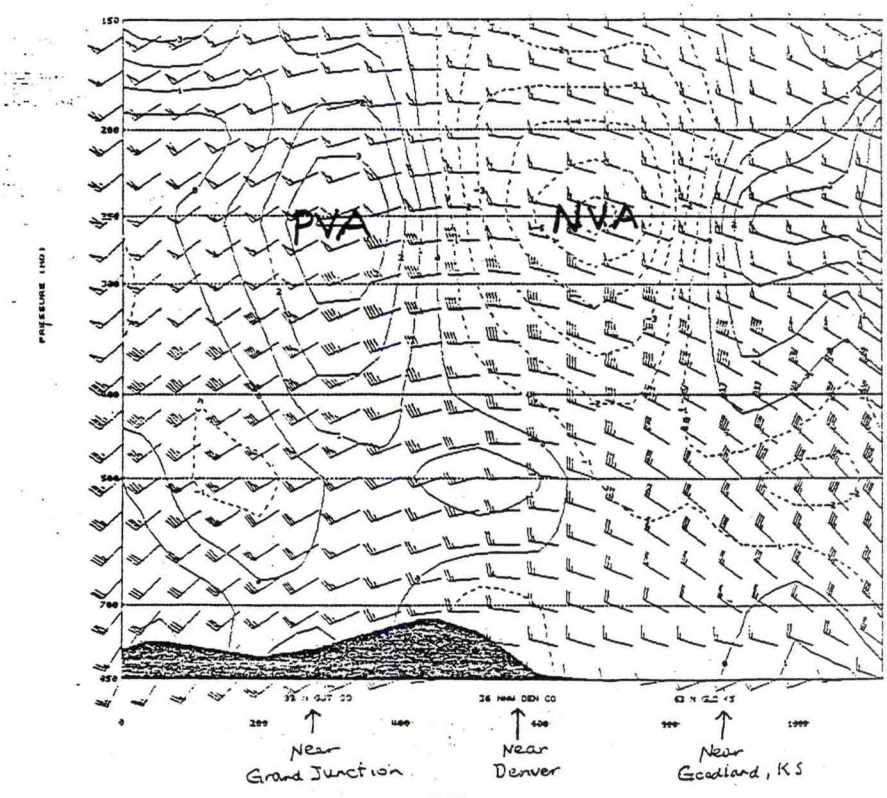

Figure 10. Six-hour forecast cross section from MAPS valid at 1800 UTC, 18 October 1990.

4. Summary of Cases

Wind direction and speed appear to be critical to the formation of lee-enhanced clouds. Raob data suggests that in lee-cloud situations along the Front Range 400 mb is the best single level to look at for moisture. However, as case two suggests, it is best to look at several levels or preferably layers from mountain top level (about 600 mb) to 300 mb.

In the five cases examined, during periods of lee-enhanced clouds wind direction at 400 mb ranged from 250 to 330 degrees (Table 1). This tendency, to favor a west northwest direction rather than due west, is most likely due to the fact that the Continental Divide, west of Denver, is oriented from north northeast to south southwest.

Wind speeds at 400 mb ranged from 25 knots to near 60 knots (Table 1). The lower threshold wind speed at mountain top level in the Sierra Nevada Mountains of California was found to be 25 knots (Jenkins, 1952), the same as it was for these five cases.

In four of the five cases, there was an approaching short wave trough as lee clouds developed, and lee clouds decreased after the short wave moved by. Similarly in the Sierras, the most favorable conditions for wave formation were found ahead of an approaching trough aloft or cold front (Jenkins, 1952). In the one case of the five which didn't exhibit an obvious trough (Case 2), the Front Range was in the right-rear quadrant of a jet maximum.

TABLE 1

Wind Speeds and Directions at 400 Millibars
During Periods of Lee-enhancement

Case	Direction (degrees)	Speed (knots)
10/06/90	250	40
10/18/90*	250-290	25-30
11/22/90	290-330	35-60
11/29/90	310	35
01/31-02/01-91*	260-310	35-55

* The two cases presented in this study.

The Denver raob may not be a good indicator for moisture because many times the balloon has been carried a considerable distance downstream by the time it reaches the moist layer, and moisture may not be as great downstream as it is over Denver. Consequently, it makes sense to look at upstream raobs if you are trying to predict what will happen at Denver.

From raob data, there were stable layers present in each case to a greater or lesser degree at or above the moist layer.

5. Conclusions

When considering the possibility of opaque lee-cloud development, forecasters should:

A. Look at present and forecast wind speed and direction. Winds are likely to be similar to the winds in the five cases presented.

B. Look for increasing moisture from upstream. The Denver raob, especially ahead of or near the beginning of the event may not show much moisture. Examine upstream raobs and humidity progs.

C. Examine satellite pictures and upper air analyses for an approaching short wave trough, although this ingredient is not absolutely necessary. If there is an approaching short wave trough, more than likely clouds will significantly decrease once the trough has passed.

D. Examine the current and progged location of the jet stream and jet maxima. If the Front Range will be in the right rear quadrant of a jet and other factors are favorable, the likelihood may be increased that lee-enhanced clouds will develop.

E. Even if temperature forecasts are right on target, lee-cloud development is important to the forecast, if only to avoid the need to update a forecast and say "mostly cloudy", instead of "mostly sunny" or "mostly clear".

Although the five cases studied give some clues, more case studies are needed to find:

A. The extreme ranges of wind speed and direction.

B. How important an approaching short wave trough really is.

C. How important is the location of the jet stream.

D. The impact of lee-cloud development on temperatures and surface winds. It would be necessary to find a means to separate the affect of cloud cover versus the affect of other weather parameters that determine temperatures and surface winds.

E. Whether or not there is a diurnal trend.

F. Objective relationships for wind shear and stability as they relate to lee-cloud development. Wind profiles and stability are important in lee-cloud development (Queney et al., 1960, Labas, 1988). The DARRRE II workstation provides the forecaster with the potential to study wind shear and stability as they relate to lee-enhanced cloud development.

6. References

Benjamin, S.C., Brewster, K.A., Brummer, R., Jewett, B.F., Schlatter, T. W., Smith, T. L., Stamus, P.A., 1991: An Isentropic Three-hourly Data Assimilation System Using ACARS Aircraft Observation. *Mon. Wea. Rev.*, **119**, 888-906.

Harrison, H.T., 1957: Mountain Wave Zones in the U.S. United Airlines Meteorology Circular #43.

Jenkins, C.F., 1952: Forecasting the Mountain Wave. Air Force Surveys in Geophysics, No. 15.

Labas, K., 1988: Wave Clouds--Shear vs. Stability. Western Region Technical Attachment 88-22.

McNulty, R.P., 1978: On Upper Tropospheric Kinematics and Severe Weather Occurrance. *Mon. Wea. Rev.*, **106**, 662-672.

National Weather Service, 1991: Jets and Severe Convection in the West. Western Region Technical Attachment 91-19.

Queney, P., Corby, G. A., Gerbier, N., Koschmieder, H., Zierep, J., 1960: The Airflow Over Mountains. World Meteorological Organization Technical Note #34.

CENTRAL REGION APPLIED RESEARCH PAPER 9-7

TORNADIC THUNDERSTORMS ASSOCIATED WITH A STRONG WINTER STORM

Matthew L. Gerard
National Weather Service Office
Grand Island, Nebraska

1. Introduction

Late afternoon January 7, 1992, two tornado producing thunderstorms developed over southcentral Nebraska. The storms occurred ahead of an intense, nearly vertically stacked low pressure system that was moving out of eastern Colorado. Figure 1 shows a composite of the two tornado producing thunderstorms and their movement.

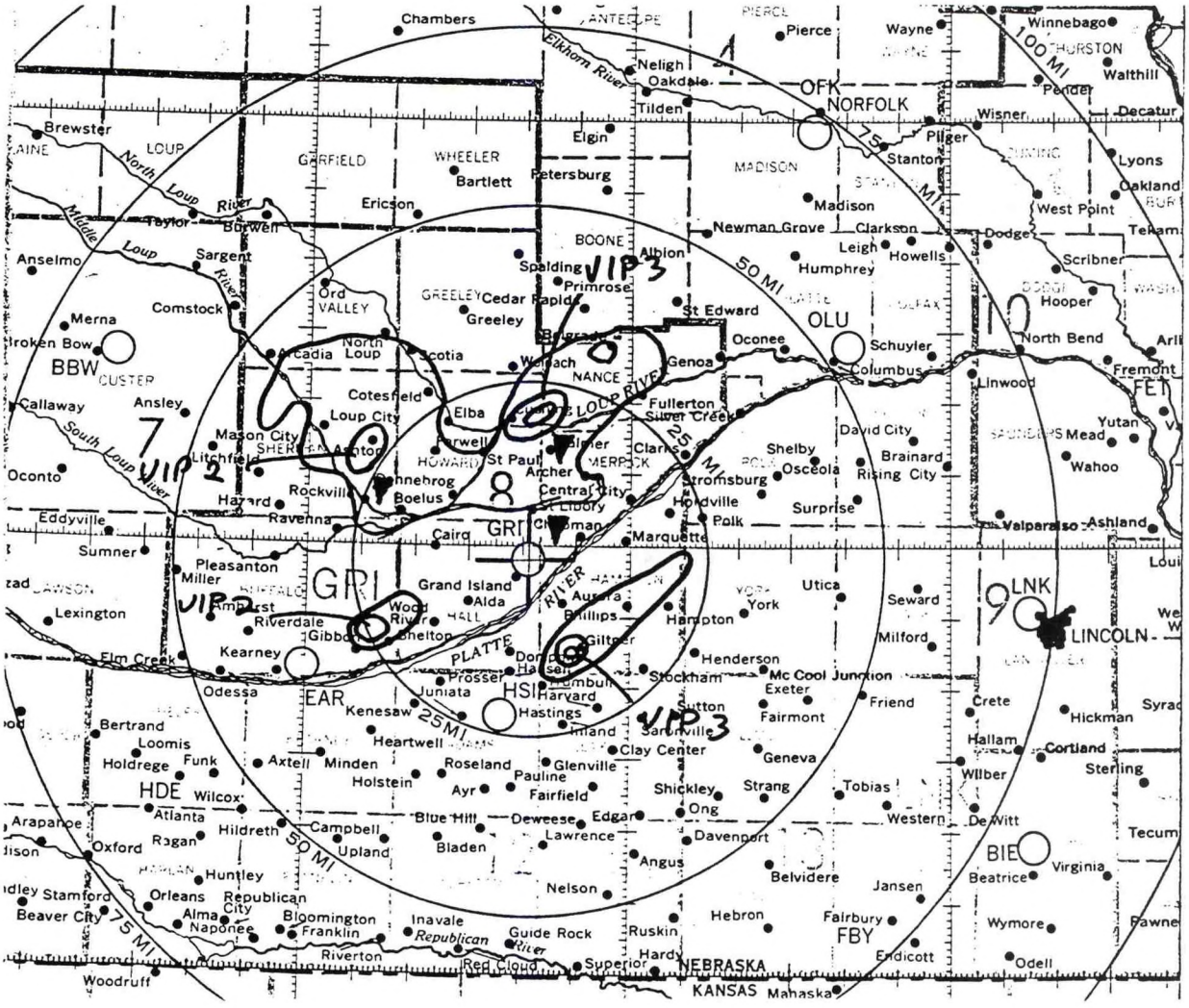

Figure 1. Composite of the two thunderstorms between 2225 and 2337 UTC, January 7,1992. Storm movement was from 170°. Triangles indicate locations where tornadoes struck.

The first thunderstorm moved north from northeast of Hastings, near Giltner, Nebraska; passing about six miles east of Grand Island. Funnel clouds and a striated base to the thunderstorm were observed by Weather Service personnel at the Grand Island airport. Figure 2a shows a picture of the tornado near the time it damaged a farm (Figure 2b) seven miles northeast of the airport. This storm later produced a tornado that damaged trees and scattered irrigation pipe on a farm near Palmer, 16 miles northeast of Grand Island.

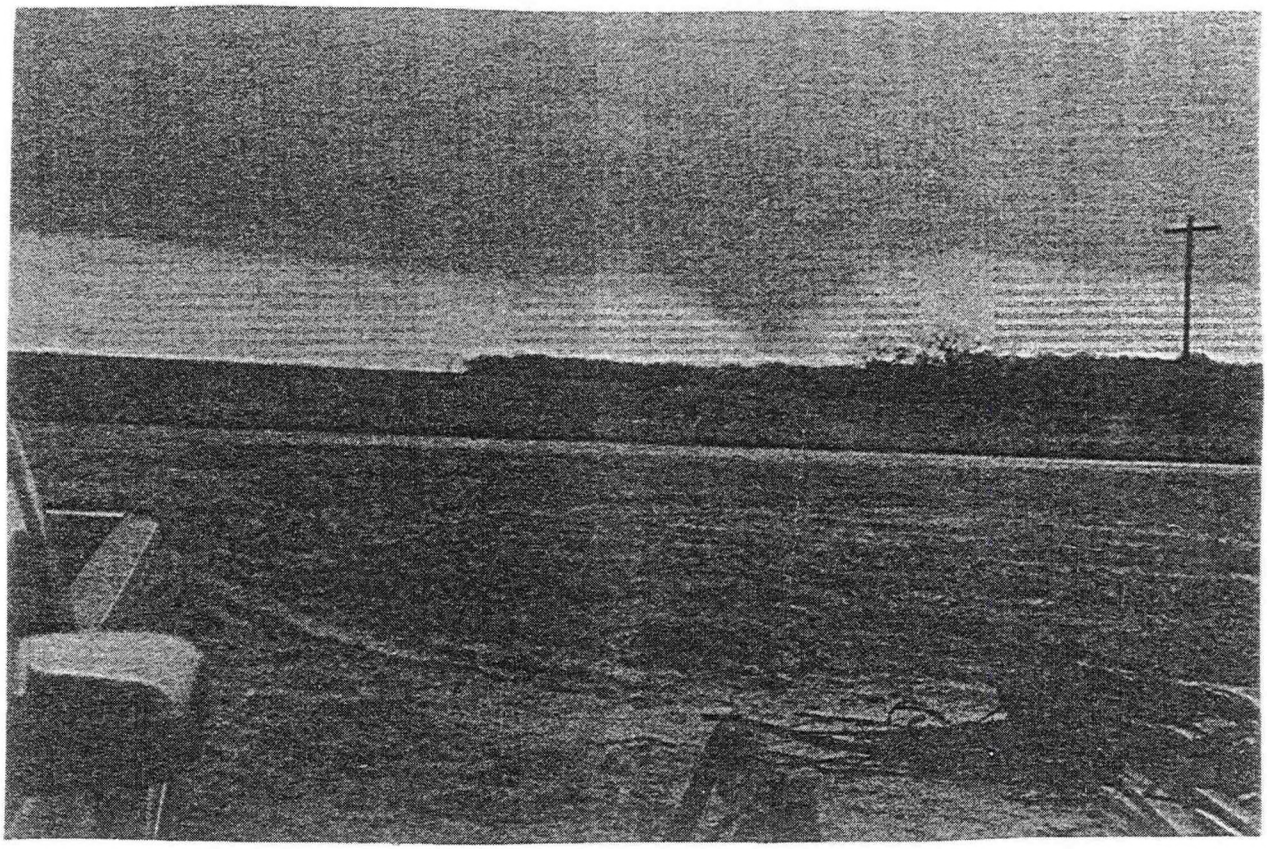

Figure 2a. Photograph was taken about the time the tornado did damage to the farm seven miles northeast of Grand Island.

The second storm moved north from east of Kearney, near Gibbon Nebraska, passing near the town of Rockville. There were several reports of funnel clouds from this storm, and a tornado did damage to a farmhouse three miles east of Rockville, or 26 miles northwest of Grand Island.

The storm to the east of Grand Island maintained VIP 3 intensity, while the storm to the west was VIP 2. Storm tops were not high, ranging from 25 to 28 thousand feet.

Figure 2b. Photograph is of the resulting damage. (Photos courtesy of Grand Island Daily Independent.)

2. Synoptic Conditions

Strong dynamic forcing was evident at all levels of the atmosphere at the time the tornadoes occurred. Southcentral Nebraska was under the left front quadrant of a strong 300 mb jet moving up the east-side of the closed upper low. A strong vorticity center at 500 mb was also located over the area. The thunderstorms developed in an area of strong mid-level cyclonic curvature and shear, similar to a case described by Byrd (1988). Figure 3 shows the profiler winds at 700 mb overlayed with the radar summary chart around the time the tornadoes were occurring.

Destabilization due to surface heating was also taking place as a mid-level dry slot was nosing up into the area from northern Kansas. Soundings from North Platte and Omaha at 0000Z, were stable. However, based on interpolation (not shown), there was a lifted index of -3 to -4 at Grand Island at the time the tornadoes occurred. Satellite imagery for 2031Z (Figure 4a) and 2231Z (Figure 4b) show the dry slot, as well as cyclonically curved convective bands. A hook-like appearance is also evident in the IR imagery. This coincides well with location of the vorticity center.

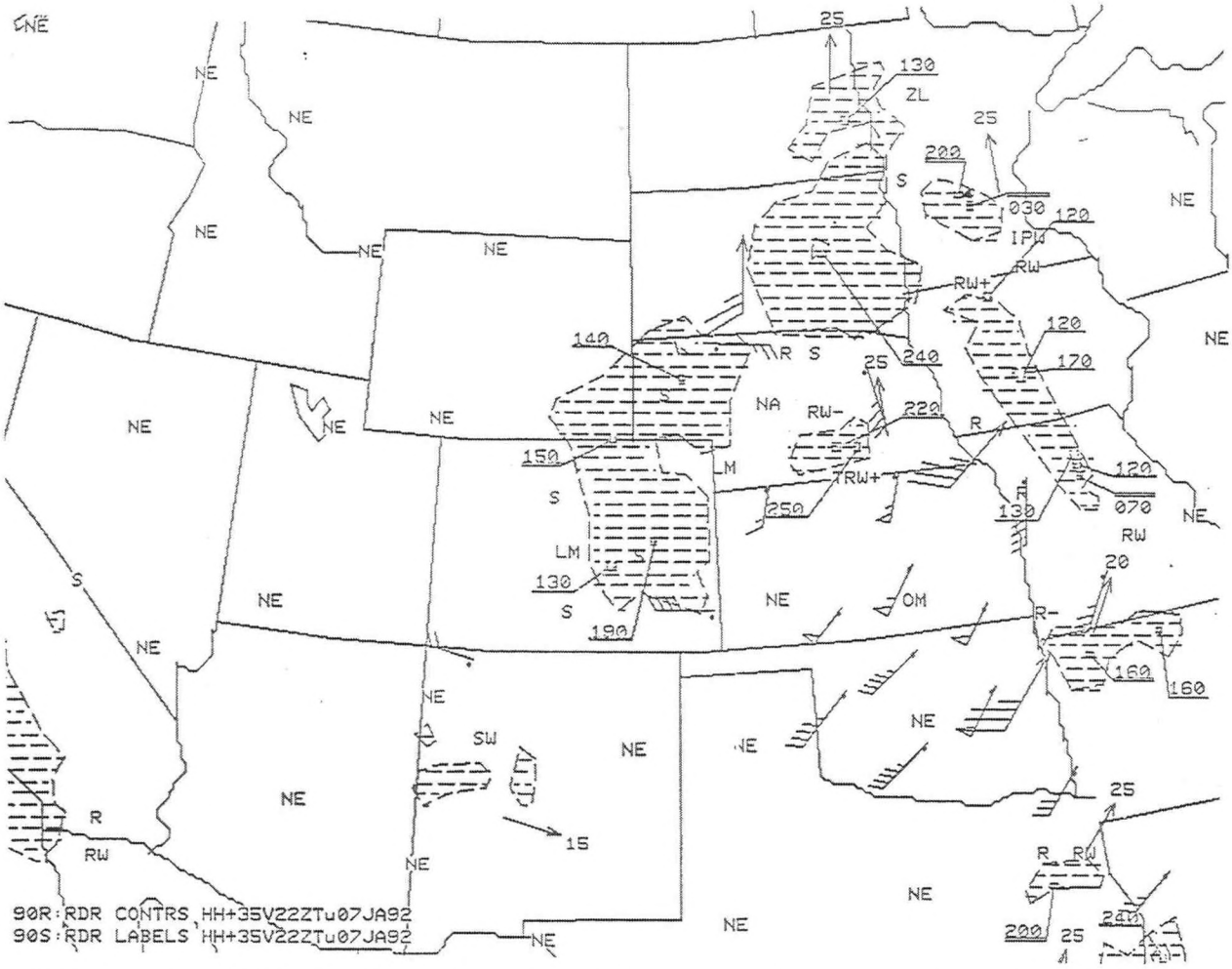

Figure 3. 700 mb profiler winds at 2300Z overlaid with radar summary chart from 2235Z, January 7, 1992. The thunderstorms developed in an area of high mid-level vorticity due to curvature and cyclonic shear.

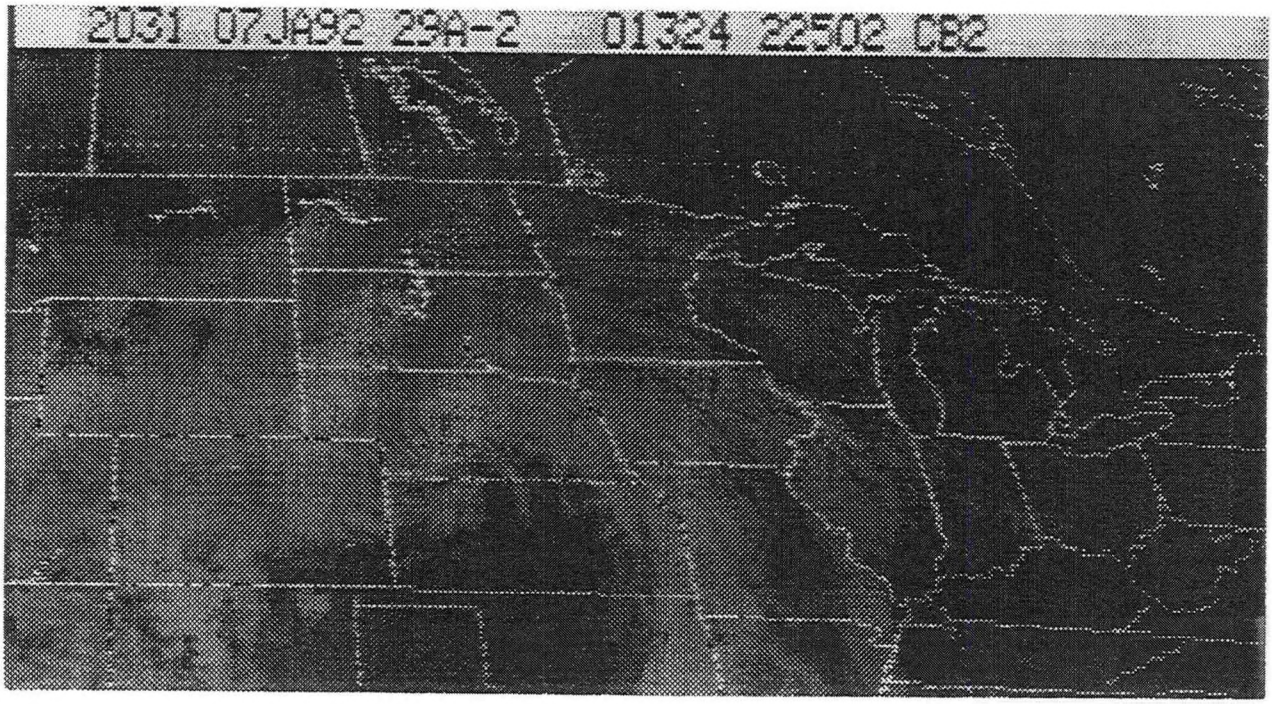

Figure 4a. Visible imagery at 2031Z.

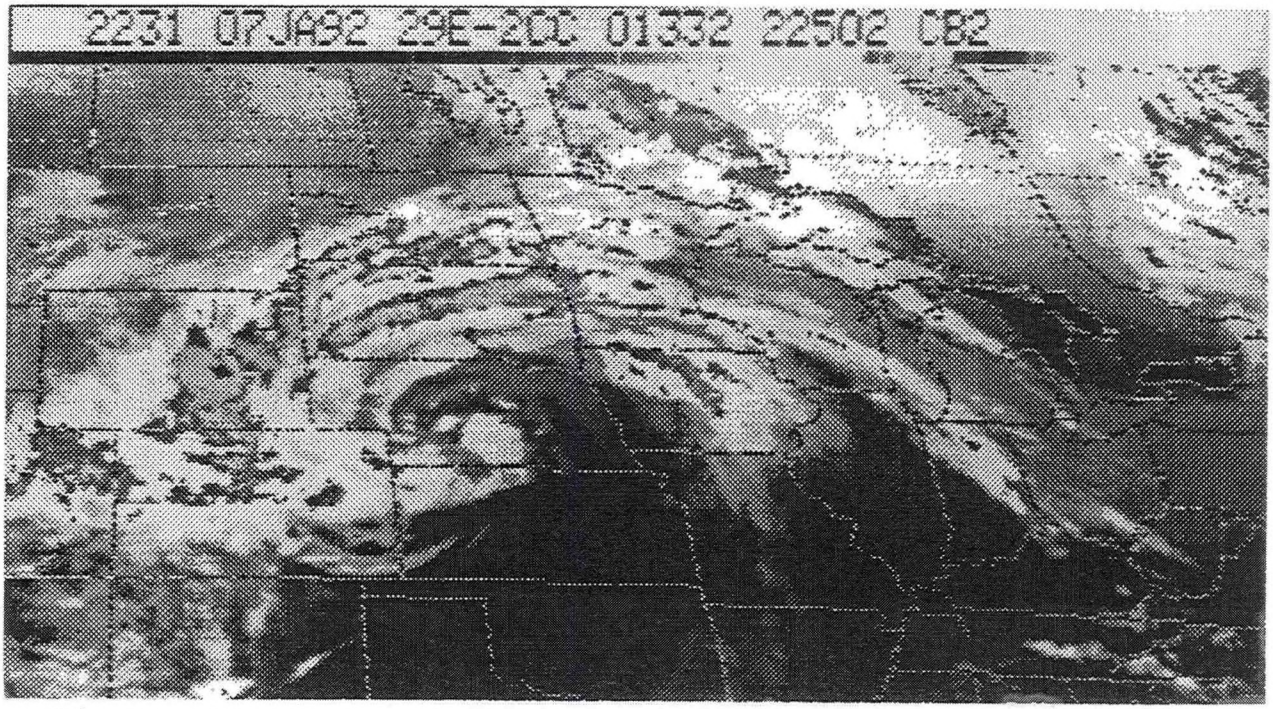

Figure 4b. IR imagery at 2231Z. Notice the dry slot and the cyclonically curved convective bands.

3. Conclusion

These tornado and funnel cloud events are rare for central Nebraska in January. It is unclear whether there has been a previous event like this. The tornadoes were not associated with typical supercell thunderstorms. In this and other cases, it is apparent that the vertical vorticity component is the main contributor to storm rotation and resulting tornadic development (Byrd 1992). Forecasters should consider the possibility of funnel clouds and even tornadoes when convection occurs in cyclonically curved bands associated with what could be called a "satellite hook" signature associated with a well-developed wintertime low pressure system.

4. Acknowledgements

The author would like to thank Steve Byrd, Lead Forecaster at WSFO Omaha, NE for reviewing this manuscript and for his suggestions.

5. References

Byrd, S., 1988: A Case of Mid-Level Vorticity Contribution to Tornadic Development. NWS, Central Region Technical Attachment CR 88-09, March.

Byrd, S., 1992: The January 7th Winter Storm - with Tornadoes. WSFO Omaha Technical Newsletter.

CENTRAL REGION APPLIED RESEARCH PAPER 9-8

A COMPREHENSIVE EVALUATION OF THE LOCAL FORECAST PRODUCT (LFP)

Thomas L. Magnuson
National Weather Service Forecast Office
Minneapolis, Minnesota

1. Introduction

Local forecasts are issued at WSOs and WSFOs by Weather Service Specialists, Meteorologist Interns and Forecasters. An evaluation has been developed for the local forecast product at Indianapolis. While numerous LFP evaluations have been used at NWS offices in the continental United States, it is hoped that this evaluation will be utilized as a framework to standardize the evaluation of LFPs nationwide. This LFP evaluation is a rather detailed exercise, addressing nearly all aspects of the forecast: precipitation, temperature, sky condition and wind direction and speed. In many ways it is a more demanding evaluation than that used to scrutinize the WSFO public forecasters. It forces the writer of the LFP to carefully look at each weather element to be forecast, acting not only as an evaluation, but as a checklist while developing the LFP.

2. Discussion

The local forecast should be as accurate a weather forecast as possible for the community or metropolitan area for which it is prepared. It should be updated quickly, responding to changes in meteorological conditions in the local area. Of primary concern is the timing of events, (most notably precipitation) into and out of the local area.

The WSFO public forecaster often, out of necessity, generalizes or averages expected weather conditions when compiling a set of zone forecasts. The writer of the LFP must not only attempt to time weather events during the first period of the forecast, but also fine-tune sky condition, temperature range, wind direction and speed and probability of precipitation for the local area as appropriate.

3. Overview of the Evaluation

This LFP evaluation is intended to give the writer of the LFP and the supervisor insight into how he/she can improve future forecasts, by reviewing past mistakes and forecasting biases. This Indianapolis LFP evaluation deals with the early morning and afternoon forecasts and consists of 20 possible base points.

Points are earned by the accuracy of the first period forecast of sky condition, temperature, wind direction and speed and probability of precipitation. There are key differences between this LFP evaluation and the public forecaster's evaluation. Forecasters are evaluated by comparison with NMC guidance. LFP writers are evaluated by comparisons with the observed weather conditions at the site in question and by their deviations from the forecaster's numbers during the first period.

Bonus points are earned by the LFP writer for being closer to the observed weather conditions than the forecaster. Fine-tuning the zone forecast for the local vicinity is the basic reason for the LFP product, and in this evaluation the writer is rewarded or penalized for acccomplishing or failing to attain that goal. In addition, one or two bonus points can be given subjectively by the grader of the forecast for: 1) the accurate forecasting and timing of weather events through the local area, 2) measurable precipitation occurrences in the local area away from the official bucket (which could make a POP forecast look better), and 3) taking an unusually bold deviation from the forecaster's values. It was decided to award bonus points for the timing of precipitation events because this timing is not a daily occurrence. Therefore, an LFP writer will not lose timing points just because he/she is on shift during dry weather.

Allowances are also given for timely updates of the LFP product, rewarding the writer for recognizing a forecast going or gone sour, and doing something about the problem.

The total possible base and bonus points an LFP product can earn in a best case scenario is 26. However, recall there are only 20 base points, so that would be 26 out of 20 points, a truly phenomenal effort!

4. Details of the Evaluation

A. Sky Condition

Numerous descriptions of the state of sky are possible in a NWS LFP. A number of word possibilities are included on the LFP evaluation sheet (APPENDIX A). All these states of sky were pigeon-holed into one of three base categories. Some recognized definitions were stretched a bit, others were arbitrarily assigned to what was thought the best category based on experience. Others fit right into the appropriate category of total opaque sky cover during the first forecast period.

It was decided not to use percent of possible sunshine for sky cover verification because during one LFP period (the afternoon forecast) the sun is mostly below the horizon, and during

some verification hours of the early morning forecast (7am - 7pm at IND) the sun is not always above the horizon. In other instances, clouds may persist in a part of the celestial dome where the sun's disk is not located; especially true in the cold season with low sun elevations.

The first base sky cover category consists of an average opaque sky cover during the forecast period (13 aviation observations) of 0 to 2.9 tenths. The average opaque sky cover is readily available on Form B (col. 36). Sky conditions in this category are Sunny, Clear, Mostly Sunny, Mostly Clear and Fair (fair is recognized as 0 to 4 tenths).

The second base sky cover category includes average opaque sky cover during the forecast period from 3.0 to 6.9 tenths. Sky conditions assigned to this category are Partly Cloudy, Partly Sunny, Variable Cloudiness, Decreasing Cloudiness and Increasing Cloudiness.

The third category includes average opaque sky cover during the forecast period of 7.0 tenths and greater. Sky conditions in this category are Mostly Cloudy, Considerable Cloudiness, Cloudy and Overcast.

There will obviously be situations that are more difficult to evaluate when multiple sky conditions occur in the first period (e.g.: becoming clear, partial clearing, etc.). This may force the LFP writer to break up the forecast into two subperiods or to give a specific time, (either in the forecast or on the evaluation sheet) when the expected change will occur. This detail will make for easier grading later.

To evaluate the LFP (Appendix B) with one sky condition forecasted, add the 13 opaque sky covers during the forecast period and divide by 13. If the forecast words fall into the same category as observed, 4 points are earned, if one category off, 2 points are earned and if an "egg is laid" (2 categories off), no points are earned.

In addition, if the sky condition is updated before the writer goes home (A shift), some face can be saved, but the maximum points earned are fewer than if the forecast had been correct in the first place (3 points versus 4). If the update is worse than the original forecast, 1 point is earned. Finally, if the LFP writer is one or two categories better or worse than the forecaster, then one point is either earned or lost.

B. Temperature

At WSFO Indianapolis, temperature is considered to be the most important daily recurring forecast element. Therefore, it is assigned 6 out of the 20 base points. Normally in an LFP, one range of temperature is used for the first period maximum or

minimum forecast temperature. For example, in the 50s: lower means 50-54, middle is 53-57 and upper indicates 56-59. Generally, between about 0 and 100 degrees, a forecast can be made using one number ending with a 0 or 5. For example, around 50 covers 48 to 52 degrees and around 55 covers 53 to 57 degrees. Given these basic NWS and perhaps local definitions, a temperature forecast is fairly simple to evaluate (Appendix B).

The LFP writer's specific number is recorded on the evaluation sheet, along with the forecaster's number from the CCF (or for WSOs not included in the state's CCF, a number obtained from a friendly chat with the public forecaster). The LFP writer's predicted temperature is compared with the observed maximum or minimum. The error is then assigned a point value. It is the feeling of the author that to hit the high or low temperature on the head (with the plus or minus 2.0°F accepted error tolerance of HO-83's) is luck. Therefore, 6 points are awarded for a direct hit **and** a 1 degree miss in either direction. A plus or minus 2 degree miss is awarded 5 points. It is felt that a plus or minus 3 degree miss (beyond the accepted error tolerance of HO-83's) begins to reflect on the forecast judgment of the LFP writer. Therefore, a plus or minus 3 degree miss is given only 3 points instead of 4 points. This line of reasoning follows for misses of plus or minus 4 degrees and plus or minus 5 degrees and worse misses. The LFP writer can either gain or lose one point in the bonus category by being better or worse than the forecaster.

As an example for a temperature forecast, the LFP writer predicts lower 50s and commits to 52 degrees. The public forecaster indicates lower 50s and puts down 51 in the CCF. If the observed high is 53 degrees, the LFP writer earns 6 points for being only 1 degree off and earns 1 bonus point for being better than the forecaster, for a total of 7 points.

An LFP writer can salvage points by updating the temperature forecast, but it has been found through experience that this is a difficult task before going off shift.

C. Wind Direction and Speed

The wind elements in the LFP can often be difficult to predict and evaluate. A wind forecast often needs to be broken up in the first period. One problem that this evaluation remedies is the "winds becoming" prediction. Many times a zone forecast will state that wind direction or speed will become something in the afternoon or after midnight, without giving the previous direction or speed. This LFP evaluation forces the writer to state, in the LFP, what the initial conditions will be. For example, southwest wind 10 to 15 mph, becoming northwest around 5

mph after midnight. While this makes for a wordier forecast, it does give the full wind picture for those who want or need the information.

After the LFP is written, the forecast wind direction and speed of the writer and the public forecaster are recorded on the evaluation sheet. At Indianapolis, a direction forecast of south to southwest or north to northeast is normally not permitted. One direction needs to be chosen or "becoming" or "shifting to" term applied for changing winds in the first period. Similar rules or guidelines are observed at other offices across the country. The wind speed is usually given with either a specific number or a 5 mph range for lower speeds (5-10) and a 10 mph range for higher speeds (10-20, 15-25 or 20-30). When wind speeds are higher, gusts are frequently included in the forecast. This LFP evaluation does **not** take gusts into account. The average observed wind speed recorded is the average of the 13 observed sustained wind speeds during each hourly observation (specials are not included). The average wind direction is the average of the 13 observed wind directions (specials are not included).

In order to gain the maximum points for wind direction, the LFP writer must be within 45 degrees of the observed direction. For example, a prediction of West (270 degrees) would earn 2 points with an average observed direction of 310 degrees or 240 degrees. If the forecast is in error by more than 45 degrees, only 1 point is earned. If the forecast is in error by more than 90 degrees, the LFP writer comes up empty. The evaluation of wind speed is more involved. If one number is chosen for the LFP product wind speed, the writer must be no more than 2.5 mph from the average observed wind speed to earn the maximum of 2 points. If the writer is 2.6 to 5.0 mph off, 1 point is earned, and if he/she is 5.1 mph or more in error from the average observed wind speed, no points are earned. If a range is used to describe the wind speed, the maximum of 2 points is earned when the average observed wind speed is in the range. In Indianapolis, 10 mph ranges are generally acceptable when average sustained wind speeds are expected to be at or above 15 mph, due to the gustiness of such days. If the average observed wind speed is 0.1 to 5.0 mph outside of the LFP forecasted range, 1 point is earned, and 5.1 mph or more outside of the LFP range, 0 points.

If the LFP writer updates the wind forecast before going off shift and the new numbers are correct in **both** direction and speed, 3 out of 4 points can be salvaged. However, if that updated wind forecast is wrong, no points are tallied. Again, the LFP writer can gain or lose another point if his/her forecast is better or worse than that of the forecaster. Of course, wind

speeds need to be converted from knots to miles per hour before the LFP evaluation can proceed (Appendix B).

D. Probability Of Precipitation (POP)

Precipitation probability is broken up into the following categories:

1) 0%-20% (no mention to slight chance, including the words isolated and widely scattered)
2) 30%-50% (chance)
3) 60%-70% (likely)
4) 80%-100% (unqualified)

Some explanation is in order regarding point assignments in this POP section. The point scheme devised generally tries to force the LFP writer to say "yes" or "no" to measurable precipitation in the local area, unlike the verification skill score scheme by which forecasters are evaluated. The feeling is that the forecast should nearly be a "yes-or-no" proposition regarding measurable precipitation in the local area. In large metropolitan areas this line of thinking, of course, is on shakier ground.

The greatest problem with the verification of precipitation is that it occurs at one 8-inch diameter circle. In the next section of this evaluation bonus points can be earned if measurable precipitation is verified in the local area, but not in the official bucket.

In this evaluation, the maximum of six points is earned in the 0% to 20% and 80% to 100% categories. The 30% to 40% and 60% to 70% categories can earn five out of six possible points. A 50% chance for measurable precipitation in a local context is considered a hedge forecast and earns three points no matter what is observed. If the public forecaster goes with 50%, the LFP writer is forced to forecast either 30% to 40% (chance) or 60% to 70% (likely) to gain an extra 2 points.

On the other side of the coin, it was thought a wet 0% to 20% forecast or a dry 80% to 100% forecast should earn no points. However, LFP forecasts in the 30% to 40% and 60% to 70% categories were thought to be less "cut and dry", therefore, three out of six points is earned for an incorrect forecast.

Finally, if the LFP writer updates the POP from 50% or from one side of 50% to the other and is correct he/she salvages four points. A point can also be earned or lost if the LFP writer's POP is in a better or worse category than that of the forecaster.

E. Final Evaluation Section

Up to two additional bonus points can be earned for the following:

1) Timing and forecasting of precipitation events into and out of the vicinity
2) For verifying measurable rain or snow in the vicinity away from the official bucket, which makes the POP forecast look better
3) Timing of sky condition change in the vicinity
4) Bold deviations from forecaster's numbers or conditions

Finally, one point can be lost if there is a technical mistake in the LFP and it is not corrected within ½ hour. A technical mistake can be a 50% POP with rain likely, not includ-ing a sky condition with a POP of 50% or lower, an incorrect date, etc. Of course, if a technical mistake is found after the ½ hour time frame, the correction should be made, regardless.

5. Summary and Conclusions

This LFP evaluation has been in experimental use at WSFO Indianapolis since June 1991, and in operational use since November 1991. Most individuals have found it easy to fill out and have had little trouble verifying their performance.

The evaluation had addressed the key issues raised at Indianapolis:

1) Too much subjectivity in evaluation
2) Not receiving due credit for timely and accurate updates
3) Too few forecasts being evaluated

There is almost no subjectivity in this evaluation (two additional bonus points). Verification is just a matter of checking the numbers and circling and adding up points earned. Important LFP updates are given recognition in this evaluation. With the ease of evaluation, more LFPs can be evaluated, giving a more representative average forecast score in a monthly or yearly time frame.

An aspect of forecasting which this evaluation does not, nor, in the opinion of the author, can directly discover, is overall "forecasting" competence. Given computer guidance and an almost made-to-order zone forecast, who is to say whether a near-perfect LFP was due to a very busy person copying the zone or a motivated and knowledgeable individual who had time to look over the weather situation and accepted the fact that the zone was

nearly perfect. However, forecasts will present themselves to separate the different levels of skill amongst individuals. Those tell-tale forecasts should be pointed out and specially archived by supervisors.

Additionally, this evaluation does not take into account updates made on LFPs generated during the previous shift. These forecast updates can be brought to light, however, by simply attaching them to the evaluation.

This evaluation scheme (Appendix C) cannot penetrate into the mind and soul of the LFP writer every time. It is the responsibility of the SMT, OIC, DMIC and MIC of each respective office to make determinations of differing competences of employees through his/her daily dealings with each individual.

It is hoped that this evaluation will, at the very least, serve as a solid framework for an LFP evaluation scheme at a NWS office that is currently searching for a better manner in which to evaluate LFPs. Of course, local conditions may necessitate the altering of certain criteria in this Indianapolis LFP evaluation to better suit weather situations unique to other offices. Thus, subtle variations on the main theme of this LFP evaluation are understood and welcomed by the author.

6. Acknowledgments

Craig Edwards, former DMIC WSFO Indianapolis, now MIC/AM WSFO Minneapolis, for help in initiating this project and encouragement during its development. John Curran, MIC/AM WSFO Indianapolis, for review of the manuscript and encouragement with valuable suggestions for its improvement. Michael Sabones, DMIC WSFO Indianapolis, for review of the manuscript and encouragement with valuable suggestions for its improvement. Joel Donner, SMT WSFO Indianapolis, for helpful "brainstorming" sessions while the project was underway. Dave Elson, forecaster WSFO Indianapolis, for review of the manuscript and helpful suggestions for its improvement. All the WSS's at WSFO Indianapolis, for suggestions to fine-tune the evaluation while in experimental use.

7. References

Curran, J., 1990: Memorandum to WSFO Indianapolis concerning LFPs, March 16.

Federal Meteorological Handbook No. 1, Chapter 12, p A12-30, 6.8.5.

APPENDIX A

Date_____
400 am 400 pm

LFP Evaluation Form

Sky Condition (Verify by opaque from 7am (7pm) to 7pm (7am) from form B) (If not included in words on LFP, include on this form)

Sunny	Partly Cloudy	Mostly Cloudy	your fcst	correct 4
Clear,Fair	Partly Sunny	Con. Cldness.		1 cat. off 2
M. Sunny	V/C, Dcr. Cld.	Cloudy	_____	2 cat. off 0
M. Clear	Incr. Cld.	Overcast		
				updated and correct 3
0 to 2.9	3.0 to 6.9	7.0 to 10.0	met. fcst	wrong 0

Remarks:

_____ better/worse than met. +1 -1

Temperature

	Observed Temp.	your fcst	Error	
Remarks:	_____	_____	-1 0 +1	6
			-2 +2	5
			-3 +3	3
	met. fcst	_____	-4 +4	1
			±5 or worse	0

If updated by your and:

-1 0 +1	5
±2 or worse	3
better or worse than met.	+1 -1

Wind Direction and Speed (verify from form A from 7am (7pm) to 7pm (7am))

Obsvd D & S	your D & S		
_____	_____	dir. 0-45 off	2
		dir. 45.1-90 off	1
met. fcst	_____	dir. >90 off	0

Remarks:

_____

in range or ≤ +2.5 from #	2
.1-5 outside range or 2.6-5.0 away from #	1
>5 outside range or away from #	0

If updated by you and correct in direction and speed 3
update wrong 0

better or worse than met. +1 -1

APPENDIX A (CONT).

Probability of Precipitation

your POP _____

met. POP _____

precipitation obsvd _____

Remarks:

0-20% and: (includes isold and wdly sct)	
does not rain (snow)	6
rains (snows)	0
30-40% (chc) (incl sct) and:	
does not rain (snow)	5
rains (snows)	3
50% (chance)	3
60-70% (likely) and:	
rains (snows)	5
does not rain (snow)	3
80-100% (unqualified) and:	
rains (snows)	6
does not rain (snow)	0

If you update from one side of 50% to the other or from 50% and correct 4
wrong 0

If your category better or worse than met. +1 -1

Subjective

Timing of weather elements in the local vicinity, measurable precipitation in the area away from ob. site, exceptional forecast deviation from forecaster up to 2

your remarks: graders remarks:

LFP had technical mistake(s) -1
corrected within 30 min. 0

FURTHER REMARKS:

TOTAL POINTS (20 base points possible) _____

Staple all LFPs and appropriate zone to this form and submit

APPENDIX B

Evaluation of the LFP

Sky Condition - for one condition in the first period

1) add 13 opaque sky conditions from 7 to 7 and divide by 13.
2) write down average observed opaque sky condition from (1), and circle points earned.
*3) if updated and correct, circle 3 points.
4) if your forecast better or worse than forecaster, circle +1 or -1.

Temperature

1) write down observed maximum or minimum temperature.
2) note error and circle appropriate point total.
*3) if updated, circle appropriate points.
4) if your forecast better or worse than forecaster, circle +1 or -1.

Wind Direction and Speed - for one condition in first period

1) add 13 directions from 7 to 7 and divide by 13.
2) write down average direction observed from (1) and circle points earned.
3) add 13 speeds from 7 to 7 and divide by 13.
4) write down average speed observed from (3) and circle points earned.
*5) if entire wind forecast updated and correct, circle 3 points.
6) if your forecast better or worse than forecaster, circle +1 or -1.

Probability of Precipitation

1) write down POP from your forecast and appropriate zone.
2) write down "yes" or "no" for a measurable amount at station site.
*3) if updated and correct, circle 4 points.
4) if your forecast better or worse than forecaster, circle +1 or -1.

Subjective

grader looks at overall quality of the LFP compared to observed weather and LFP writer's deviation from forecaster.

APPENDIX C

Rating of LFP	Total points
Outstanding	19, 20
Commendable	15, 16, 17, 18
Fully Successful	11, 12, 13, 14
Marginal	7, 8, 9, 10
Unacceptable	<7

CENTRAL REGION APPLIED RESEARCH PAPER 9-9

A CONCEPTUAL MODEL OF POSTFRONTAL DOWNSLOPE WINDS BASED ON ISENTROPIC DATA FROM THE MESOSCALE ANALYSIS AND PREDICTION SYSTEM (MAPS)

Mike R. Baker
National Weather Service Forecast Office
Denver, Colorado

1. Introduction

Forecasters at the National Weather Service Forecast Office (WSFO) in Denver must often deal with the problem of forecasting postfrontal downslope winds along the eastern slope of the Rocky Mountains. These small scale, sometimes intense wind storms of normally short duration pose a significant impact on human activity, ranging from disruptions in communication and transportation to serious property damage and loss of life. This paper will present a conceptual model of conditions favoring postfrontal downslope winds along the east facing slope of Colorado's Front Range. The wind model is based on isentropic data from the new Mesoscale Analysis and Prediction System (MAPS) being evaluated at the Denver WSFO. Isentropic data were collected during twelve postfrontal downslope wind events observed along the Front Range between January 1990 and September 1991. The model combines observational and theoretical results and uses data from new sources which will soon be available throughout the National Weather Service (NWS).

2. Study Area and Data Used

The Front Range and adjacent high plains of northeast Colorado are uniquely prone to postfrontal downslope winds. Referred to hereafter as the "Front Range High Wind Zone" (Figure 1), this transition zone between mountains and plains is bordered on the west by the Continental Divide, on the north by the Cheyenne Ridge, on the south by the Palmer Divide, and on the east by the high plains of northeast Colorado. The east facing slope of the Front Range rises most abruptly northwest of Boulder from an elevation of 5300 ft MSL to nearly 13200 ft MSL along the Continental Divide; a distance of slightly less than 25 miles. The region is home to nearly half (49%) of the state's 3.2 million population, encompassing the cities of Denver (DEN), Aurora (AUR), Fort Collins (FOR), Lakewood (LAK), Arvada (ARV), Boulder (BOU), Longmont (LGM), and Loveland (LVE) (U.S. Dept. of Commerce 1991).

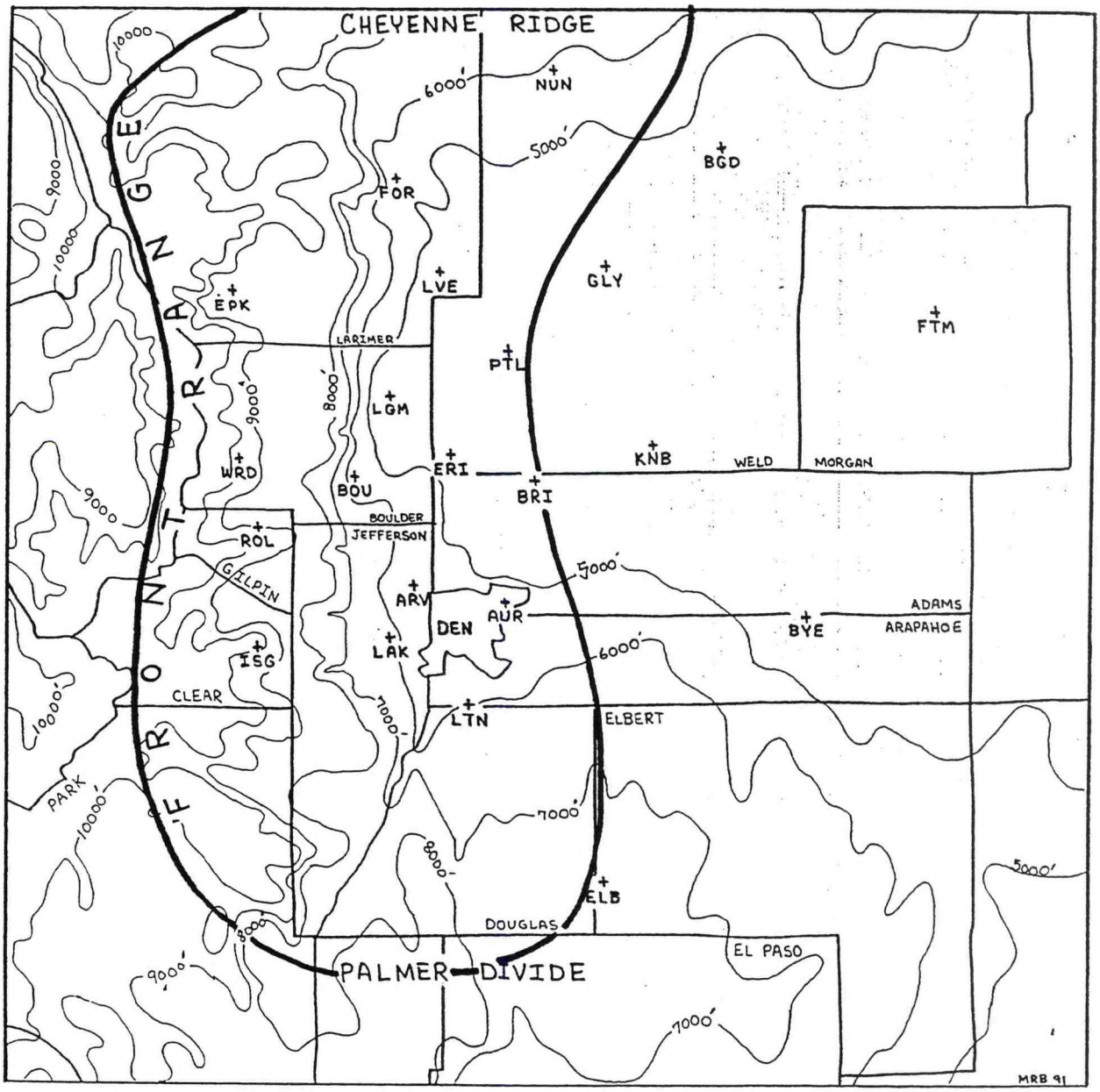

Figure 1. Terrain of northeast Colorado with outline of Front Range High Wind Zone. Mesonet sites located within this zone include Arvada (ARV), Aurora (AUR), Brighton (BRI), Estes Park (EPK), Erie (ERI), Fort Collins (FOR), Idaho Springs/Squaw Mountain (ISG),Lakewood (LAK), Longmont (LGM), Littleton (LTN), Loveland (LVE), Nunn (NUN), Platteville (PTL), Boulder (BOU), Rollinsville (ROL), and Ward (WRD).

Postfrontal downslope winds (or Bora) typically occur more often and with greater intensity during the cool season months of October through April. Surface wind speeds may exceed 60 kt and normally decrease expeditiously 40 to 50 miles east of the Front Range in all but the most intense downslope wind events.

Isentropic data were used to develop a conceptual model of conditions favoring postfrontal downslope winds. Data output was from the Mesoscale Analysis and Prediction System (MAPS) currently in real-time use at the Denver WSFO. The MAPS model provides a complete surface and upper air analysis and very short term forecast every three hours on both isentropic and isobaric surfaces. The analysis incorporates many advanced observing systems such as wind profiler and ACARS data (Benjamin 1991). The data are available in gridpoint form which allows for easy manipulation and display. MAPS is scheduled for real-time application throughout the NWS in the near future.

3. Theoretical Basis of the Conceptual Model

In an early study of conditions favoring downslope winds in the lee of the Rocky Mountains, Queney et al. (1960) note the formation of high amplitude mountain waves over barriers with gentle windward slopes and steep leeside slopes just prior to the onset of downslope wind events. With a high amplitude mountain wave in place, the report concludes that strong downslope winds are likely to develop (a) when the prevailing flow aloft is aligned within roughly 30° of perpendicular to the ridge line, (b) when the prevailing flow extends throughout a deep layer of the troposphere, and (c) when wind speed just above ridge top level exceeds at least a "terrain-dependent" value of 15 to 30 kt and shows a tendency to increase steadily with height. Strong static stability, or rather, the presence of a mountaintop inversion, is believed to be just as important, with decreasing stability found in layers above and slightly downstream of the mountain barrier.

Durran (1986) adds that if the prevailing flow aloft passes through a stably stratified layer (inversion) just above mountaintop level, air flow tends to deflect downward below ridge top level just east of the mountain barrier. The amount of downward tilt is believed to be largely dependent on the degree of static stability present within the mountaintop inversion. The greater the amplitude of the mountain wave (terrain dependent flow), the greater the potential for downward transport of upper level momentum along these arched streamlines.

In yet another study, Scheetz et al. (1976) note that Bora (katabatic) winds developing shortly after passage of standup (north-south oriented) cold fronts usually last less than an

hour. However, following a lull of no more than a few hours, winds usually increase again with onset of the so-called "frontal inversion" phase of the wind storm. This second surge of post-frontal downslope winds often develops just prior to passage of a 500 mb trough axis across the Continental Divide and normally with the surface and upper level low centers positioned north or northeast of Colorado. A strong jet (streak) maximum is usually north of the State with possibly several relatively weak short wave troughs embedded within the mid-level jet flow. Yet, the onset of downslope "high winds" may be delayed or actually prevented even after passage of both the standup cold front and 500 mb trough if a shallow inversion or pocket of cold arctic air is present on the plains adjacent to the Front Range (Brown 1986).

4. Observational Basis of the Conceptual Model

Unlike isobaric analyses, isentropic analyses allow the forecaster to approximate vertical motion with a fairly high level of accuracy. To assess the relative motion along a frontal surface, one may choose to examine a MAPS vertical cross section containing isentropes (constant potential temperature surfaces) and tangential winds (the component of the wind along the cross section) drawn normal to the front. In the absence of diabatic effects, isentropic surfaces act as material surfaces, i.e., air parcels remain confined to a specific isentrope. By examining the flow along these sloped isentropes, the forecaster can quickly and subjectively assess the amount of upglide and down-glide flow present with respect to the frontal surface. Frontal zones displaying upglide flow (ascending motion along the frontal inversion) are known as anafronts, while fronts exhibiting downglide flow (descending motion) are referred to as katafronts (Moore 1988; Moore and Smith 1989).

In general, frontal zones are statically stable regions. On a cross section stable regions are depicted as areas of vertically compact isentropes in unsaturated air and by vertically compact equivalent potential temperature surfaces under saturated conditions. Isentropes normally lie parallel to or coincident with frontal or baroclinic zones and slope significantly in regions of strong thermal contrast. The vertical depth of a frontal zone, and to what extent it is vertically coupled with the upper level flow, may be determined with a vertical cross section of isentropic surfaces as well (Moore, 1988).

Figures 2a and 2b depict cross sectional views of a standup Pacific cold front as it crosses nearly perpendicular (northwest to southeast) to the Colorado Front Range just prior to the onset of strong downslope winds. In Fig. 2a, the observed wind field is depicted by wind barbs and isotachs drawn at 10 kt intervals.

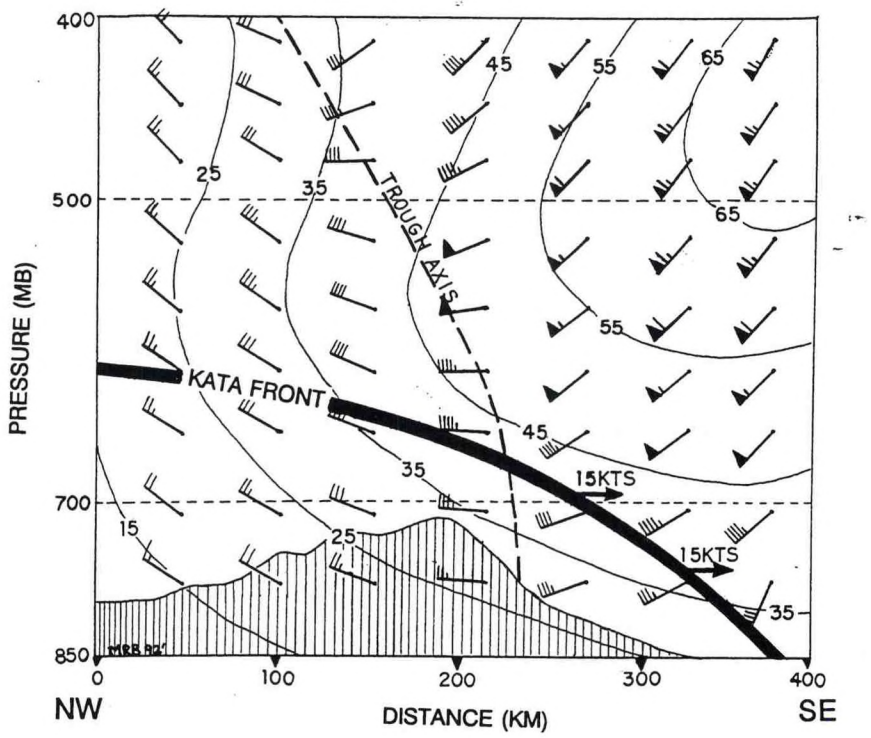

Figure 2a. Cross sectional view of a standup Pacific Cold frontpassing at a right angle to the Front Range. The wind field isdepicted by wind barbs and isotachs drawn at 10 kt intervals. The vertically dashed line represents 500 mb trough axis, and heavy arched line the frontal surface of a Katafront.

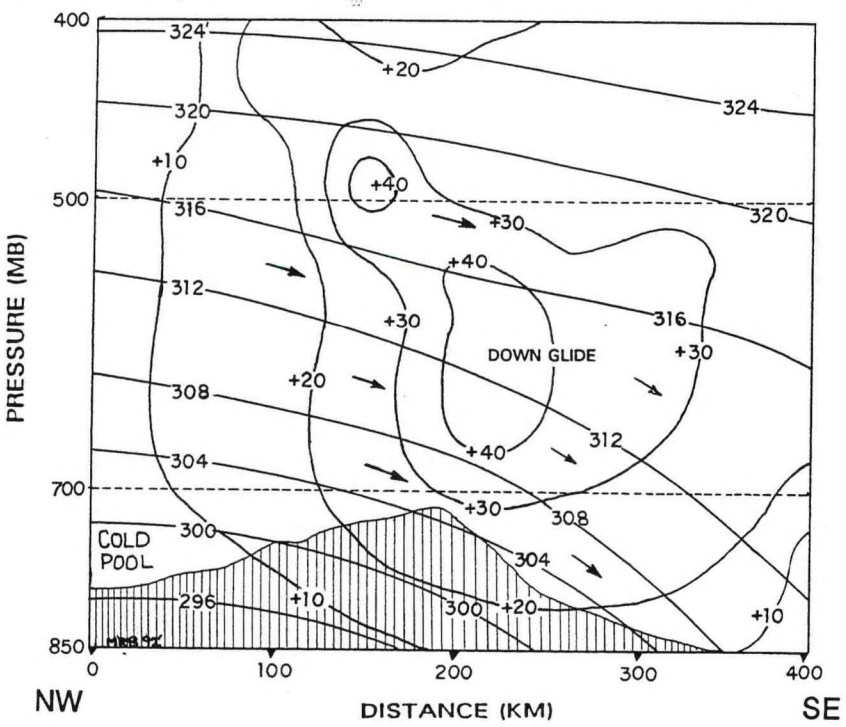

Figure 2b. Cross sectional view of isentropes (at 4° Kintervals) and isotachs of the tangential wind component (kt), drawn normal to surface front. The positive wind component values indicate flow from left to right (northwest wind). The small arrows represent the adiabatic flow down along the frontal surface.

The vertically tilted dashed line in the center of the diagram represents the preferred position of the 500 mb trough axis; and the heavy arched line denotes the leading edge of the surface based cold air (cold front). The hatched area denotes the model terrain through the cross section.

Figure 2b depicts a cross section of arched isentropes (at intervals of 4°K) and isotachs of the tangential wind component (in kt). The tangential wind in this figure, due to the orientation of the cross section, is normal to the front. Positive values indicate flow from left to right (northwest to southeast). Since the overall tangential wind component exceeds the front's translational speed of 15 kt, a katafront is present. In this case, air flow is down the sloped frontal inversion just above and to the east (right) of the mountain barrier where we find the tightest packing of the isentropic surfaces.

In approximately one-third of the postfrontal wind cases studied, strong frontal inversions (6 to 8 K per 100 mb) appeared on MAPS cross sections just above and slightly downstream of the Continental Divide just prior to the onset of ridge top winds of 50 kt and greater. In all four cases, front-normal wind maxima of 36 to 48 kt appeared on or slightly above the frontal inversion (between 450 and 600 mb) immediately downstream of the 500 mb long wave trough axis. As the wind maxima propogated downward along frontal inversions below ridge top level, wind speeds of 50 kt and greater developed immediately east of the Front Range and usually persisted for five to eight hours following passage of a strong standup cold front. However, during one event, strong postfrontal downslope winds persisted for 18 to 24 hours as unusually strong cold air advection persisted at mountaintop level throughout the period.

In the remaining eight cases, tangential wind maxima of 30 to 42 kt were found embedded within frontal inversions near ridge top level (between 600 and 700 mb) and slightly downwind of the Front Range ridge line. Wind speeds at ridge top level rarely exceeded 50 kt under these conditions. As the tangential wind maximum translated downward along the frontal inversion below ridge top level, surface wind speeds of 25 to 50 kt developed at the base of the Front Range, but rarely persisted for more than five hours after passage of the surface front

In all twelve cases studied, winds speeds typically decreased an hour or two after passage of the surface front. However, speeds increased again after a lull of one to two hours, often with greater intensity, with passage of the frontal inversion wind maxima.

5. Validation of the Conceptual Model -- Case Studies

A. 4 December 1990

Figure 3 illustrates a Salt Lake City (SLC) to Goodland (GLD) cross section of potential temperature and relative humidity just prior to the onset of strong postfrontal downslope winds east the Front Range at 1200 UTC, 14 December 1990. A deep pool of cold maritime Pacific air (284 K to 300 K) is depicted in the lower left corner of the diagram. The surface front (denoted as steeply sloped and tightly packed isentropes) is located near Leadville (LXV). The prevailing flow aloft (not shown) is from left (west) to right (east) normal to the front. Assuming the flow to be adiabatic, the tangential wind flow down the frontal surface (inversion) signifies the presence of a katafront.

During the predawn hours on 14 December 1990, Colorado's northwest plateau and northern mountains became engulfed in heavy snowfall, northwest winds of 40 to 60 kt and bitter cold temperatures shortly after passage of a strong, fast moving standup Pacific cold front. The front raced across the Continental Divide and by 1000 UTC, was detected with mesonet data in the Front Range foothills west of Denver and Boulder. Gusty west to northwest winds of 40 to 70 kt developed in the higher foothills (above 7000 ft) shortly after frontal passage (FROPA). On the plains in advance of the front, weak upslope conditions (fog, drizzle, and light northeast winds) were prevalent throughout the night. The shallow pool of cold Canadian air (288 K to 296 K) east of the Front Range was forecast by MAPS, and is represented in the lower right hand corner of Figure 3 by a slight upward bulge in the isentropic surfaces.

By 1500 UTC, the moist, cold air mass on the northeast high plains was quickly replaced by drier, warmer air from aloft with erosion of the surface based inversion. The event was marked by a sudden increase in temperature at Denver's Stapleton Airport (AUR), although surface winds remained unchanged. Shortly after 1600 UTC, west winds of 60 to 90 kt developed at the foot of the Front Range, and by 1700 UTC had spread across remaining portions of the Front Range High Wind Zone. After an initial temperature rise of 3°F to 5°F, temperature readings dropped 5°F to 10°F within minutes after onset of strong winds. Bora winds persisted throughout the day along the Front Range, but by evening (0400 UTC) had subsided in all but the higher elevations (above 7000 ft) west of Denver, Boulder and Fort Collins. The decrease in wind speed at lower elevations coincided with displacement of the postfrontal cold pool axis onto the high plains east of the Front Range High Wind Zone.

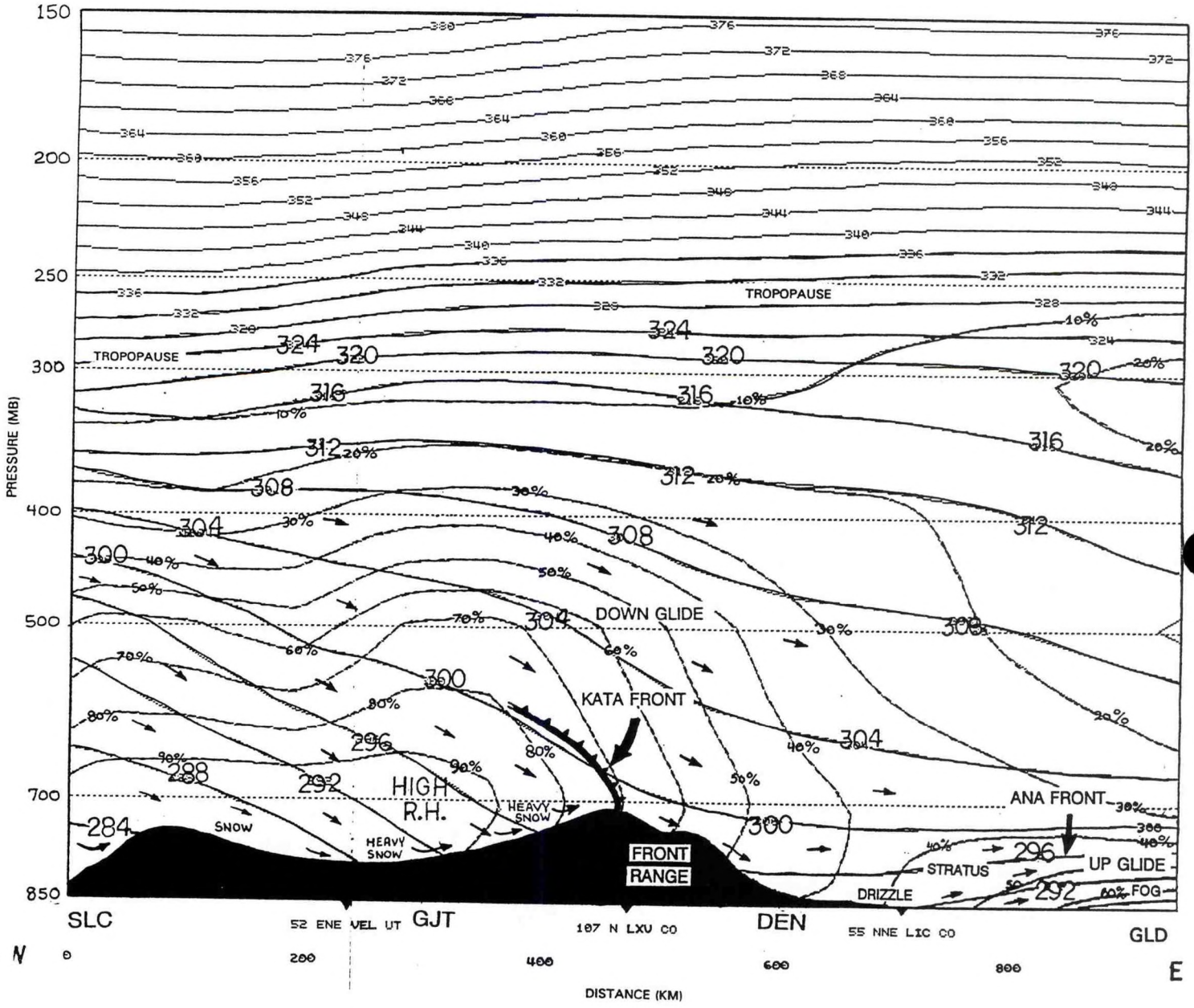

Figure 3. Cross sectional view of potential temperature (°K) and relative humidity (percent) between Salt Lake City (SLC) and Goodland (GLD) at 1200 UTC, 14 December 1990. Strong Pacific coldfront in the vicinity of Leadville (LXV) at lower center of diagram.

B. 8 September 1991

Forecast models and numerical weather guidance gave forecasters at WSFO Denver little indication of a potential downslope wind event along the Colorado's Front Range during the afternoon of 8 September 1991. Yet, 1200 UTC upper air plots revealed a weak short wave trough and cold air advection at 700 mb approaching the State from Utah. Ahead of this system, gusty southwest winds of 20 to 40 kt had already developed in the higher foothills (above 7000 ft) west of Denver as of 1200 UTC, the result of lee troughing.

Forecasters late that morning turned to MAPS for additional guidance. Figure 4 shows 6-, 9- and 12-hour forecast cross sections from Salt Lake City (SLC) to Goodland (GLD) of isentropes and tangential wind components. At 1800 UTC (Fig. 4a), the 6-hour forecast placed the tangential wind maximum (26 to 30 kt) east of the Continental Divide near Leadville (LXV) with the tightest isentrope packing (mountain top inversion) found near 670 mb. The thermal trough at 700 mb was forecast to move near Vernal (VEL), and by 2100 UTC, just west of LXV (Fig. 4b) with only slight eastward shift in the tangential wind maximum. Front Range mesonet sites (above 8000 ft) began reporting west to northwest winds of 20 to 30 kt shortly after passage of the 700 mb trough (around 2200 UTC).

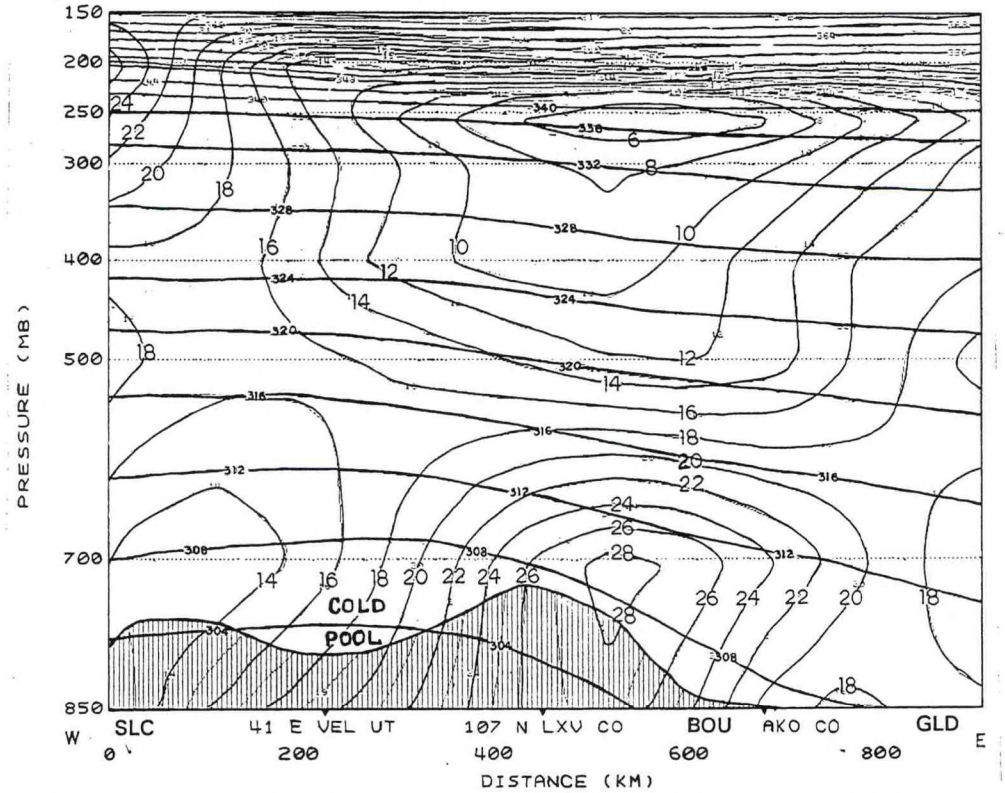

Figure 4a. Cross sectional view of standup Pacific cold front crossing the Front Range from 280°. Six-hour forecast valid 1800 UTC, 8 September 1991.

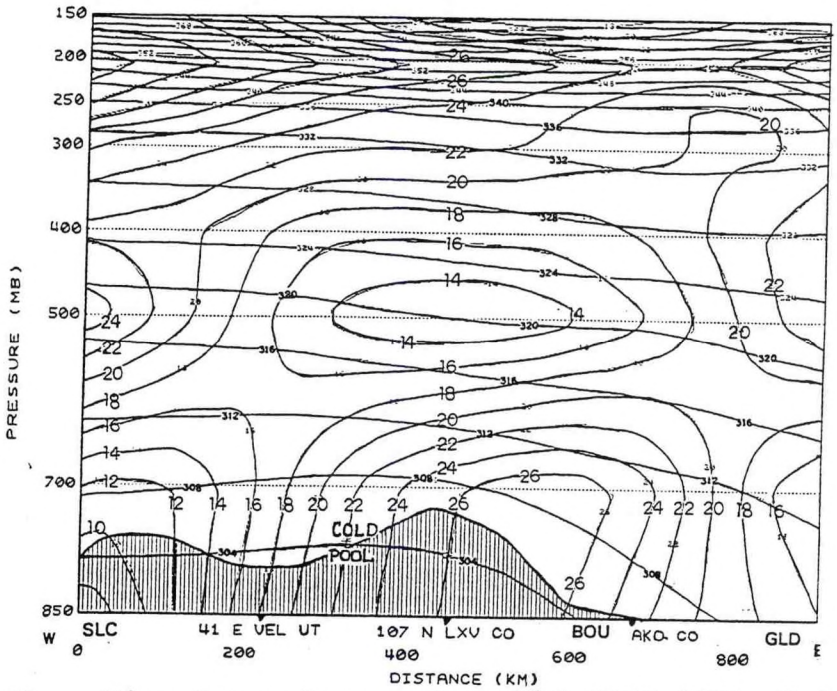

Figure 4b. Nine-hour forecast valid 2100 UTC, 8 September 1991.

The tangential wind maximum was forecast by MAPS to move east near BOU by 0000 UTC (Fig. 4c), with the cold pool just east of the Continental Divide (near LXV). At 0000 UTC, nearly every mesonet site within the Front Range High Wind Zone reported 5-minute average peak wind gusts of 25 to 40 kt. Note the position of 304 K and 308 K theta surfaces as they intersect the ground just east of the Front Range in Fig. 4c; a pattern often observed on cross sections during strong downslope wind events.

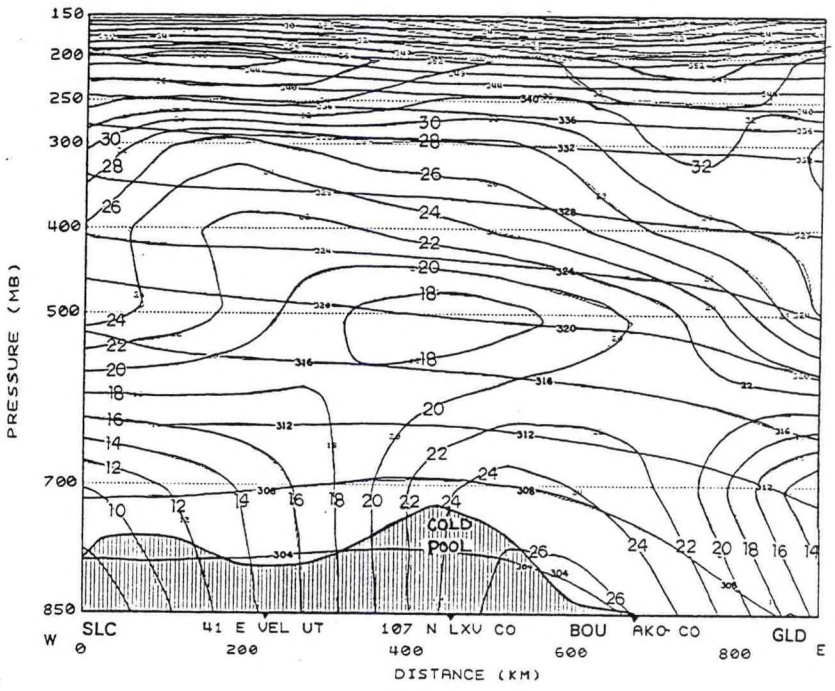

Figure 4c. Twelve-hour forecast valid 0000 UTC, 9 September 1991. Noteshift in cold pool to just east of the Continental Divide, and thetangential wind maximum to near foot of Front Range. This was periodof strongest downslope winds.

In Table 1, note the eastward progression of frontal inversion winds (of 25 kt and greater) from upper Front Range mesonet sites (EPK, ISG, ROL, WRD) to mesonet sites (AUR, BOU, FOR, LAK, LGM, LVE AND NUN) at lower elevations. Wind speeds at all mesonet sites quickly decreased to less than 25 kt soon after passage of the cold air pool axis around 0100 UTC (not shown).

TTAA00 KEDF 081502
FSL EXPERIMENTAL 3-HR WEATHER SUMMARY
8-SEP-1991 15:00 GMT

STA	TX	TX TIME	TN	TN TIME	ACC PCP	PK WIND	PK DIR	PKWD TIME	PCT OBS
ARV	73	1500	56	1305	0.00	9	241	1430	100
AUR	67	1500	56	1245	0.00	16	213	1420	100
BYE	72	1455	55	1235	0.00	10	208	1205	100
ELB	66	1500	57	1315	0.00	22	249	1205	100
EPK	58	1500	55	1205	0.00	●28	267	1230	100
ERI	74	1500	62	1235	0.00	7	171	1350	100
FOR	66	1500	60	1205	0.00	7	337	1435	100
FTM	62	1500	55	1255	0.00	9	236	1220	100
GLY	63	1500	55	1215	0.00	7	102	1450	100
ISG	42	1500	37	1205	0.00	●48	267	1440	100
KNB	68	1455	58	1255	0.00	16	216	1215	100
LAK	72	1500	63	1235	0.00	20	234	1300	100
LGM	73	1450	64	1205	0.00	●29	279	1300	100
LTN	65	1450	62	1220	0.00	15	173	1350	100
LVE	71	1445	59	1235	0.00	21	253	1440	100
NUN	67	1500	57	1205	0.00	8	22	1225	100
PTL	67	1455	56	1240	0.00	6	183	1245	100
BOU	69	1500	60	1250	0.00	8	263	1215	100
ROL	52	1500	48	1205	0.00	●50	263	1335	100
WRD	50	1500	46	1205	0.00	●43	70	1240	100

TTAA00 KEDF 081802
FSL EXPERIMENTAL 3-HR WEATHER SUMMARY
8-SEP-1991 18:00 GMT

STA	TX	TX TIME	TN	TN TIME	ACC PCP	PK WIND	PK DIR	PKWD TIME	PC OB
ARV	82	1735	72	1505	0.00	19	277	1710	1(
AUR	79	1750	67	1505	0.00	19	252	1720	1(
BGD	79	1725	66	1505	0.00	12	273	1710	1(
BRI	80	1755	69	1505	0.00	10	29	1715	1(
BYE	80	1710	71	1535	0.00	15	227	1645	1(
ELB	75	1800	66	1505	0.00	●26	285	1615	1(
EPK	65	1745	58	1505	0.00	●30	282	1545	1(
ERI	80	1800	74	1525	0.00	8	65	1620	1(
FOR	75	1800	65	1505	0.00	11	133	1735	1(
FTM	83	1800	62	1505	0.00	10	324	1730	1(
GLY	81	1800	63	1505	0.00	7	127	1525	1(
ISG	50	1645	41	1505	0.00	●47	267	1510	1(
KNB	78	1800	67	1505	0.00	13	201	1545	1(
LAK	79	1720	70	1530	0.00	20	350	1750	1(
LGM	82	1755	71	1505	0.00	16	250	1530	1(
LTN	81	1755	65	1505	0.00	13	249	1730	1(
LVE	78	1655	65	1505	0.00	15	343	1525	1(
NUN	79	1750	67	1505	0.00	●32	273	1730	1(
PTL	79	1800	66	1505	0.00	10	124	1800	1(
BOU	79	1755	69	1505	0.00	10	46	1540	1(
ROL	62	1755	52	1505	0.00	●50	313	1605	1(
WRD	55	1725	50	1505	0.00	●37	301	1530	1(

TTAA00 KEDF 082102
FSL EXPERIMENTAL 3-HR WEATHER SUMMARY
8-SEP-1991 21:00 GMT

STA	TX	TX TIME	TN	TN TIME	ACC PCP	PK WIND	PK DIR	PKWD TIME	PCT OBS
ARV	86	1920	80	1855	0.00	21	239	1920	100
AUR	82	2030	79	2005	0.00	23	306	1945	100
BGD	83	2020	77	1805	0.00	13	224	1950	100
BRI	86	2010	79	1805	0.00	22	271	1955	100
BYE	85	2025	79	1805	0.00	15	253	2030	100
ELB	79	2010	74	1805	0.00	●29	293	2055	100
EPK	67	1825	53	1925	0.02	●26	273	1845	100
ERI	84	1940	80	2020	0.00	24	233	1900	100
FOR	80	1905	73	2040	0.00	●30	265	2030	100
FTM	86	2025	82	1840	0.00	11	14	1840	100
GLY	86	2030	80	1805	0.00	11	80	1910	100
ISG	52	2030	47	1805	0.00	●29	251	2040	100
KNB	83	2025	78	1810	0.00	18	242	2100	100
LAK	82	2025	77	1810	0.00	24	271	1840	100
LGM	85	1910	81	2100	0.00	●30	289	1940	100
LTN	83	1825	78	1955	0.00	18	226	2035	100
LVE	86	2030	77	1805	0.00	●30	304	2040	100
NUN	80	1940	77	1850	0.00	22	283	1805	100
PTL	86	2045	79	1805	0.00	18	253	2100	100
BOU	80	1825	75	1920	0.02	●28	249	2015	100
ROL	64	1950	59	1830	0.00	●37	261	2010	100
WRD	53	2045	51	2015	0.00	22	195	1820	100

TTAA00 KEDF 090002
FSL EXPERIMENTAL 3-HR WEATHER SUMMARY
9-SEP-1991 00:00 GMT

STA	TX	TX TIME	TN	TN TIME	ACC PCP	PK WIND	PK DIR	PKWD TIME	PC OB
ARV	83	2155	74	0000	0.00	●27	256	2220	1(
AUR	81	2120	75	0000	0.00	●26	294	2305	1(
BGD	85	2130	65	2355	0.01	●25	172	2140	1(
BRI	85	2105	75	0000	0.00	●25	291	2240	1(
BYE	82	2110	70	2325	0.01	●26	220	2150	1(
ELB	78	2110	72	2335	0.00	●30	257	2140	1(
EPK	64	2105	55	2230	0.00	●28	287	2215	1(
ERI	84	2110	71	0000	0.00	●26	258	2125	1(
FOR	78	2235	73	2335	0.00	●36	284	2300	1(
FTM	85	2155	75	0000	0.00	14	5	2140	1(
GLY	85	2110	73	2355	0.00	24	340	2255	1(
ISG	51	2105	44	2330	0.00	●35	253	2315	1(
KNB	82	2120	74	0000	0.00	22	234	2120	1(
LAK	80	2150	72	0000	0.00	24	295	2235	1(
LGM	82	2200	71	2355	0.00	●30	282	2250	1
LTN	79	2245	74	0000	0.00	21	224	2210	1(
LVE	82	2105	74	0000	0.00	●31	299	2215	1(
NUN	76	2105	57	2130	0.67	●32	263	2115	1(
PTL	85	2105	74	2345	0.00	21	227	2115	1(
BOU	78	2110	70	0000	0.04	●29	247	2240	1(
ROL	61	2205	52	0000	0.00	●41	266	2235	1(
WRD	54	2145	44	2315	0.02	●28	80	2125	1(

●-- MESONET STATION REPORTING A 3-H PEAK WIND GUST OF 25 KTS OR GREATER

Table 1. Front Range mesonet sites above 7000 ft: EPK, ISG, ROL,and WRD. Other sites located within the Front Range High Wind Zone: ARV, AUR, BRI, ERI, FOR, LAK, LGM, LTN, LVE, NUN, PTL, and BOU. Mesonet site recording a 3-hr peak wind gust of at least 25 kt aremarked with a dot.

C. 14 September 1991

A 500 mb long wave trough and strong standup Pacific cold front raced southeast across northern Colorado and southern Wyoming during the afternoon and evening of 14 September 1991. Most of the Front Range High Wind Zone was spared the blast of

strong (50 to 75 kt) northwest winds which developed shortly after passage of the surface cold front. Unlike the 8 September downslope wind event where the surface front crossed the central Front Range at nearly a right angle, movement of this front was oriented more northwest to southeast. The front crossed the Cheyenne Ridge and northern Front Range around 2200 UTC. The prevailing northwest flow aloft was within roughly 30° of perpendicular to the Cheyenne Ridge.

Figure 5 depicts a plan view of isobars and wind barbs on the 312 K isentropic surface at 0000 UTC, 15 September 1991. This theta surface was selected because it best represented boundary layer conditions (850 to 650 mb) over northeast Colorado. Note the tight isobar packing along the surface cold front. Model winds along this steeply sloped (250 mb/100 km) katafront were northerly in direction, and directed downward along the frontal surface.

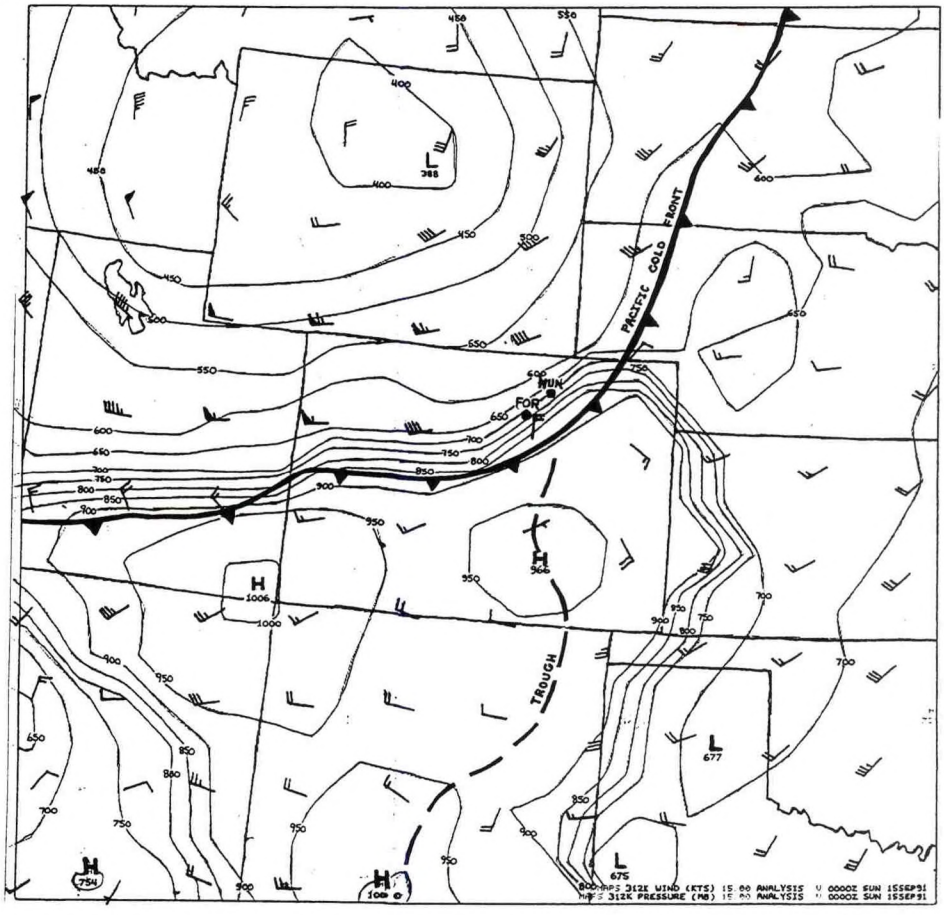

Figure 5. MAPS 312 K surface plotted with wind (kt) and pressure (mb) at 0000 UTC, 15 September, 1991. Tight packing of isobars indicates steep slope to frontal surface. Note downglide flow immediately behind front near FOR and NUN.

Temperatures plunged by as much as 20°F in less than an hour (from 2200 and 2300 UTC) at many northern Front Range and northeast plains mesonet sites shortly after FROPA. At the same time, wind speeds increased by as much as 25 to 40 kt within minutes after FROPA at the FOR and NUN mesonet sites (Fig. 6). The NUN mesonet site recorded wind gusts of 40 to 70 kt for nearly two hours following FROPA, with similar speeds recorded at FOR. Note the almost two hour lull in wind speed between wind peaks; a common pattern identified by Scheetz et al. (1976).

During the period of maximum surface wind speeds, MAPS cross sections (Figs. 7a and 7b) revealed tangential wind maxima (36 to 42 kt) centered within the frontal inversion near 500 mb and slightly upstream (northwest) of the Cheyenne Ridge. As the surface front moved southeast across Colorado's northeast plains, the frontal inversion wind maximum decreased in strength, but remained nearly stationary over the Cheyenne Ridge for about four hours. Strong postfrontal downslope winds continued to rake northern portions of the Colorado Front Range High Wind Zone throughout the evening.

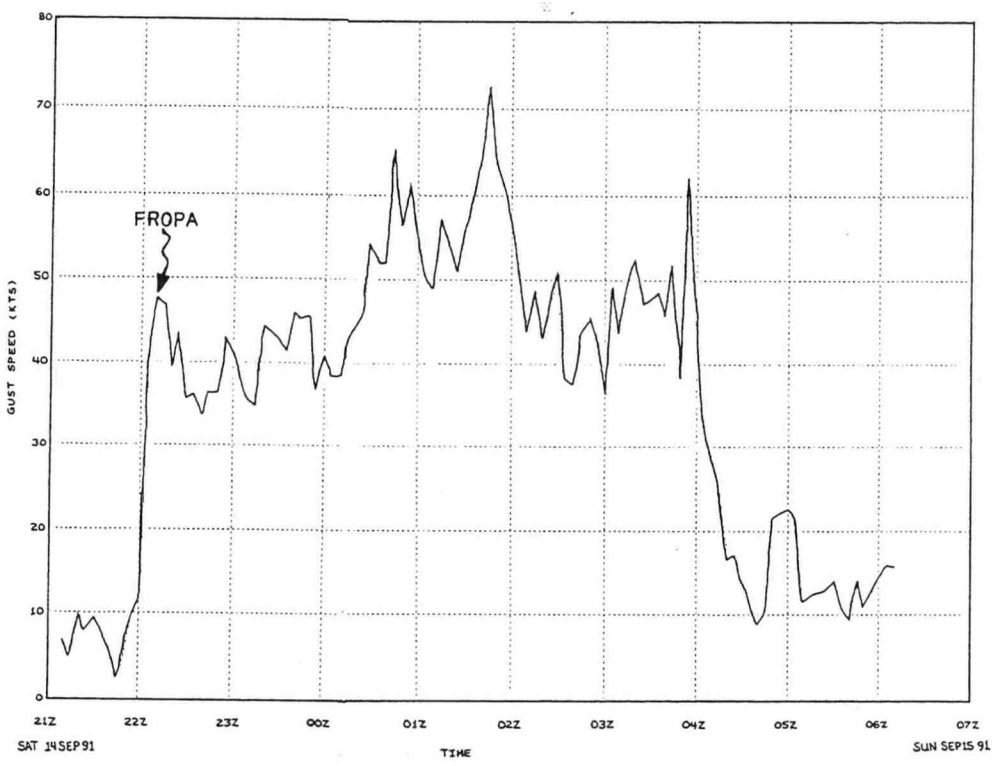

Figure 6. Peak wind gust time series for FOR from 2100 UTC, 14 September to 0700 UTC, 15 September 1991. Gust speeds in kt.

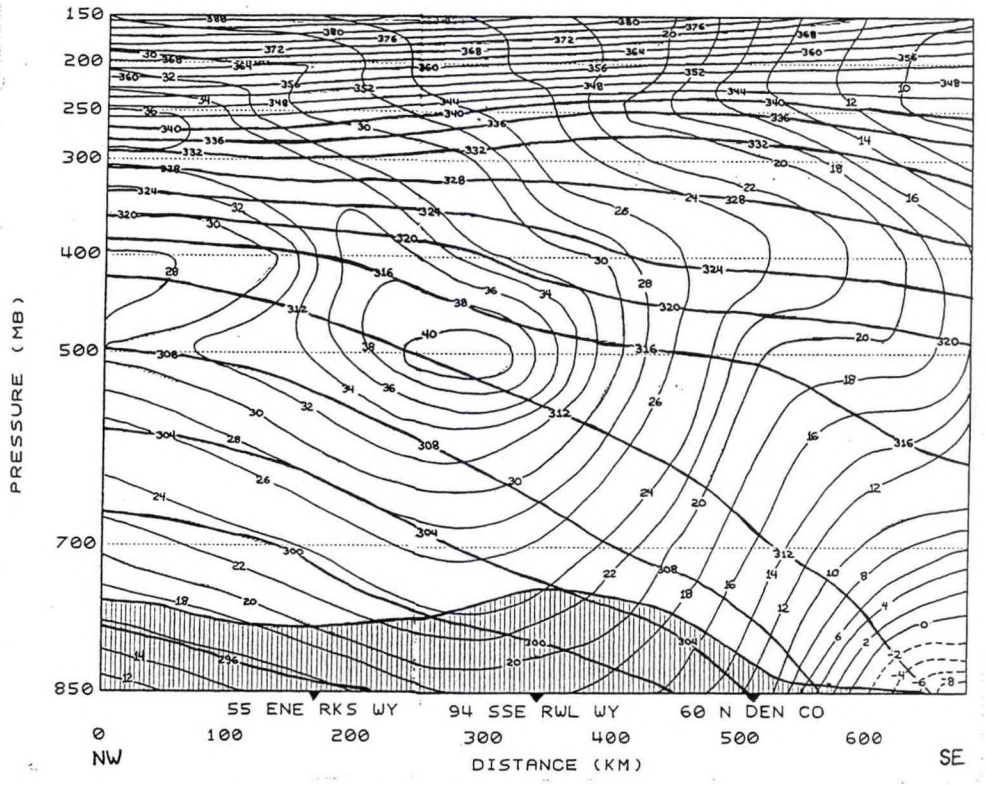

Figure 7a. A cross sectional view of a strong Pacific cold frontcrossing the northern Front Range and Cheyenne Ridge at 0000 UTC, 15 September 1991. Cross section is drawn from 20 SW of Big Piney, WY to 51 NE of Limon. Tangential wind speed in kt.

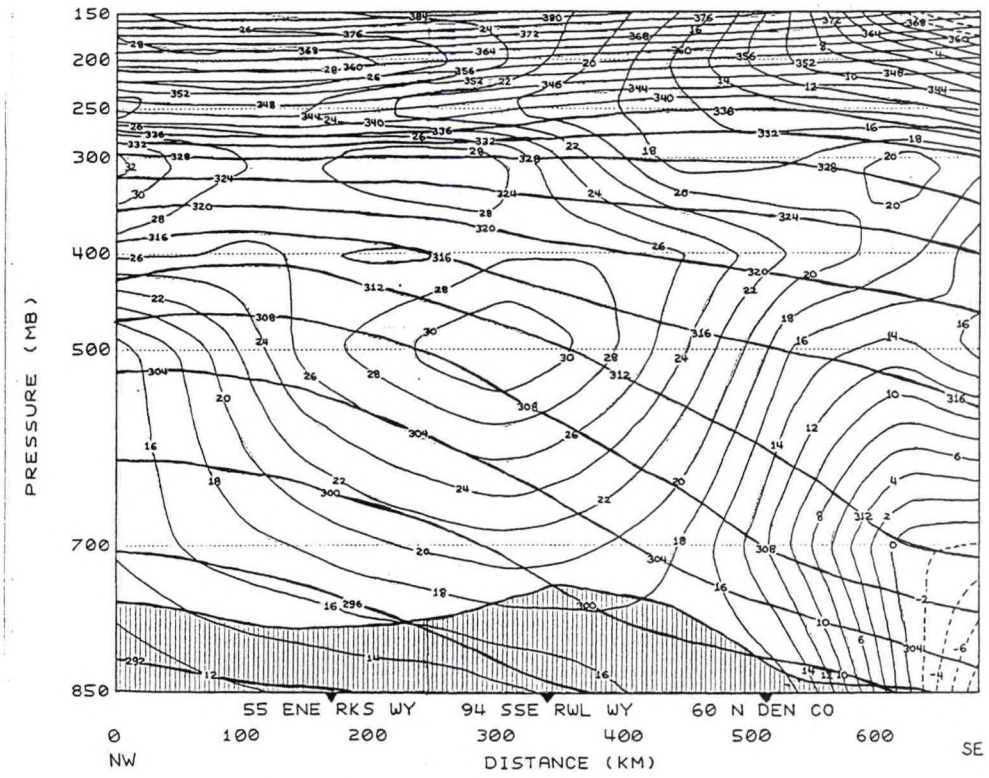

Figure 7b. Surface cold front as of 0300 UTC, 15 September 1991, southeast of Denver. Negative tangential wind speed values in lower right corner of diagram indicates a slight upglide flow ahead of front.

6. Conclusion

MAPS isentropic cross sections will add a new dimension to forecasting short term, mesoscale weather phenomena, but should not be thought of as the final solution to every downslope wind forecast situation. MAPS isentropic data have been used to develop a conceptual model of favorable postfrontal downslope wind conditions along Colorado's Front Range. The model was based on only 12 postfrontal downslope wind events. Nevertheless, the summary offered below should provide forecasters with some idea as to how they may use the MAPS model to forecast the onset, duration and intensity of postfrontal downslope winds along Colorado's Front Range.

The following guidelines pertain to postfrontal downslope winds of 25 to 50 kt:

(a) Postfrontal downslope winds normally develop within two hours after passage of standup surface fronts and/or 700 mb short wave troughs.

(b) Postfrontal downslope winds rarely persist for more than five hours.

(c) A strong stable layer or frontal inversion (6 to 8 K per 100 mb) is normally present just above and slightly downwind of Front Range ridge line.

(d) A tangential wind maximum of 30 to 42 kt is normally embedded within the frontal inversion just above mountain top level (600 to 700 mb.)

(e) Onset of winds at base of Front Range foothills usually occur within a couple of hours after passage of "cold pool" axis across the Continental Divide.

(f) Winds may be delayed or prevented all together if a shallow inversion or pool of cold stable air overlays the high plains adjacent to the Front Range.

(g) The northern one-third of the Front Range High Wind Zone is more susceptible to postfrontal downslope winds when ridge top winds are from 290° to 340°.

(h) Central and southern portions of the Front Range High Wind Zone are more susceptible to postfrontal downslope winds when ridge top flow is from 260° to 300°.

(i) Wind speeds are likely to decrease shortly after displacement of the cold pool axis east of the Front Range High Wind Zone.

The following guidelines pertain to postfrontal downslope winds of 50 kt and greater:

(a) Downslope wind storms of this intensity have an average duration of six to ten hours; but may last as long as 18 to 24 hours with very strong cold air advection present at mountain top level.

(b) Strong winds develop usually within an hour after passage of a strong standup Pacific cold front and before passage of the 500 mb long wave trough axis.

(c) Downslope winds may be delayed for an hour or two (but not prevented) if an inversion overlaying a shallow pool of cold air is present on the high plains adjacent to the Front Range.

(d) Tangential wind maxima of 36 to 48 kt are usually found on or slightly above strong frontal inversions (6 to 8 K per 100 mb) between 450 and 600 mb, above and slightly east of the Continental Divide.

7. References

Benjamin, S.G., 1991: Short-range forecasts from a 3-hourly isentropicsigma assimilation system using ACARS data. *Preprints, 4th International Conference on Aviation Weather Systems*, Amer. Meteor. Soc. (in press), Paris, France.

Brown, J.M., 1986: A decision tree for forecasting downslope windstorms in Colorado. *Preprints, 11th Conference on Weather Forecasting and Analysis*, Amer. Meteor. Soc., 83-88, Kansas City, Missouri.

Durran, D.R., 1986: Mountain waves. *Mesoscale Meteorology and Forecasting*. Amer. Meteor. Soc.,472-492.

Moore, J.T., 1988: Isentropic analysis and interpretation: Operational applications to synoptic and mesoscale forecast problems. St. Louis University, St. Louis, Missouri.

Moore, J.T. and K.F. Smith, 1989: Diagnosis of anafronts and katafronts. *Wea. & Forecasting*, **4**, 61-72.

Queney, P., G. Corby, N. Gerbier, H. Koschmieder, and J. Zierep, 1960: The airflow over mountains. WMO Technical Note 34.

Scheetz, V.R., J.F. Henz and R.A. Maddox, 1976: Colorado severe downslope windstorms: A prediction technique. Final Report under Contract No. 5-35421 to TDL/SDO/NWS from Geophysical Research and Development Corporation.

U.S. Department of Commerce, 1991: Population of Colorado, 1990. Bureau of the Census, Washington, D.C.

CENTRAL REGION APPLIED RESEARCH PAPER 9-10

EXAMPLES OF SIGNIFICANT THUNDERSTORM INITIATION IN IDENTIFIABLE LOW LEVEL THETA-E PATTERNS

Jeffrey K. Last
National Weather Service Forecast Office
Milwaukee/Sullivan, Wisconsin

1. Introduction

Equivalent potential temperature (theta-e) has become an increasingly examined variable in recent years. Low-level theta-e analyses have been shown to be useful in identifying areas of thunderstorm development, propagation, and flood-producing rainfall (e.g., Cylke 1992, Kusselson 1990, Scofield and Robinson 1989). The advent of personal computer-based software that computes and contours theta-e and theta-e advection (Last 1991) has allowed for quick analysis of such parameters in an operational environment.

This paper examines three cases of explosive thunderstorm development over the Central United States and the associated theta-e patterns. First, a brief overview of theta-e is presented in Section 2. Satellite imagery of the three Mesoscale Convective Systems (MCSs), along with theta-e analyses are shown in Section 3. Section 4 is a discussion of the examples and theta-e forecast possibilities. Finally, a brief summary is provided in Section 5.

2. Equivalent Potential Temperature and Theta-e Analysis

Simply stated, theta-e is a measure of the amount of heat and moisture an air mass contains. More technically, equivalent temperature represents essentially the sum of a parcel's actual air temperature and the temperature increment corresponding to the heat latent in the water vapor contained in the parcel (Saucier, 1989). Compressing the parcel dry-adiabatically to 1000 mb results in equivalent potential temperature, or theta-e.

A large value of theta-e indicates greater convective available potential energy (CAPE), energy released if the environmental lapse rate is greater than the moist adiabatic lapse rate. The resultant positive buoyancy allows the parcel to be accelerated upward, releasing the energy for thunderstorm formation and maintenance. Of course, lifting of unstable air by a surface boundary, an upper level short wave, insolation, etc., must occur in conjunction with high levels of CAPE (high theta-e) before thunderstorms will develop.

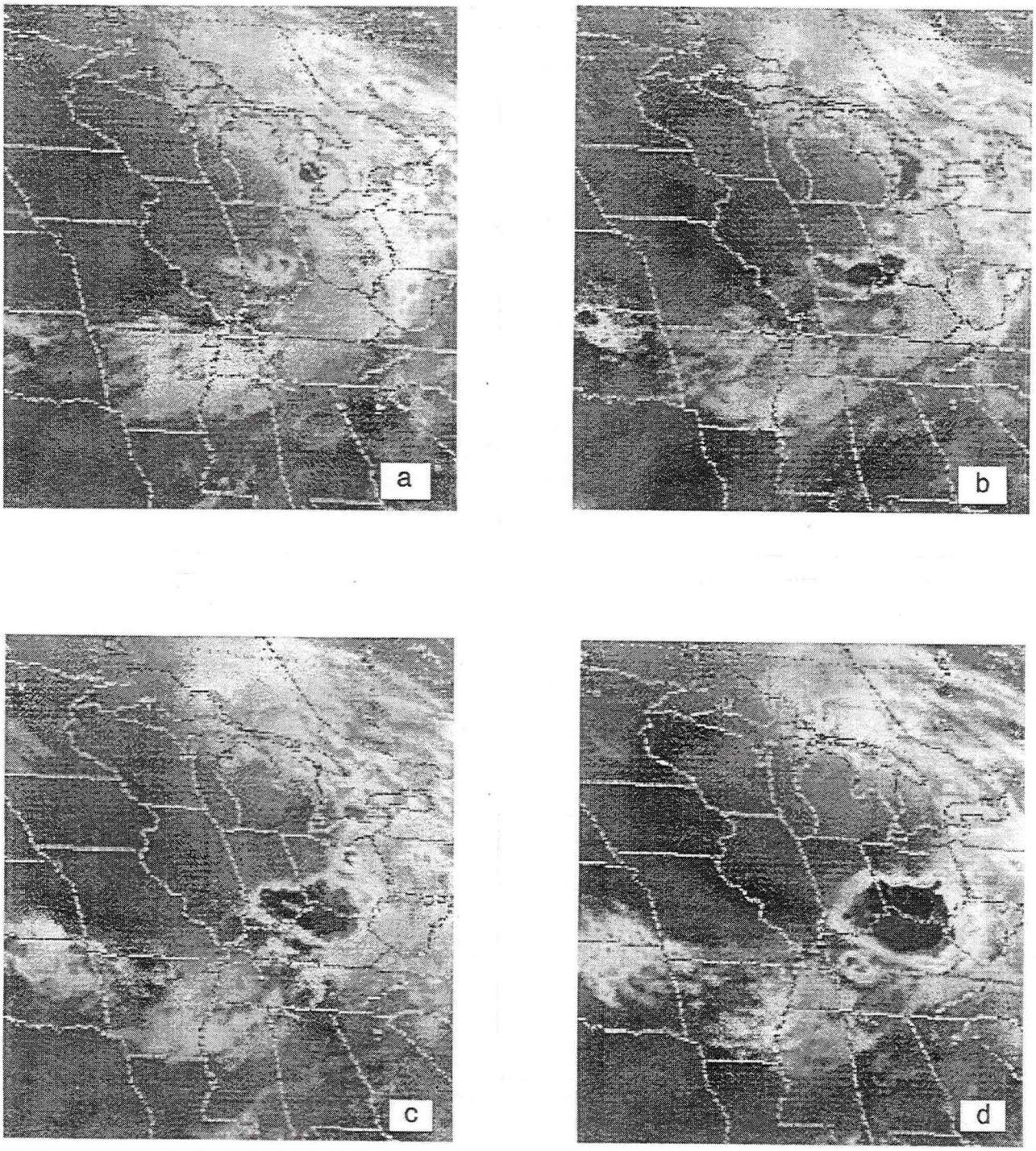

Figure 1. GOES enhanced infrared satellite imagery (MB curve) of the central United States for 8 August 1992 at: (a) 0801 UTC, (b) 1001 UTC, (c) 1201 UTC, and (d) 1401 UTC.

Usually 850 mb (or 700 mb in the western United States [Campbell 1991]) theta-e analyses are performed to locate areas of high CAPE. Scofield (1990) noted three patterns of low-level theta-e that were associated with MCSs:

(a) theta-e ridge axes,
(b) near areas of theta-e maxima, or
(c) within areas of theta-e gradients north of theta-e ridge axes.

In the examples presented in this paper, all three patterns will be examined.

3. Examples of Theta-e Patterns

A. MCS development along a theta-e ridge axis

During the morning hours of 8 August 1992, thunderstorms produced nearly 10 inches of rain over south-central Indiana. Infrared satellite imagery during the morning hours of August 8 are shown in Figure 1. Note, the east-west orientation of the developing MCS.

Figure 2 is the 850 mb theta-e analysis for 1200 UTC, 8 August. A prominent theta-e ridge lies east-west across the Ohio River. In this case, an upper level short wave produced the necessary lift to initiate the convection. It is interesting to note the time of thunderstorm development. Often, MCSs develop and begin to organize during the evening. The 8 August storms began well after midnight local time.

B. MCS development near a theta-e maximum

Thunderstorms rapidly developed north of a stationary front during the late afternoon of 15 July 1992 over extreme southeast Nebraska and northwest Missouri. Figure 3 illustrates the explosive formation between 2200 UTC, 15 July and 0200 UTC, 16 July. The storms produced heavy rain and severe weather in Iowa, Missouri, and Kansas.

The 850 mb theta-e analysis for 0000 UTC, 16 July is shown in Figure 4. Note the very pronounced theta-e maximum over the Nebraska-Missouri state line, with a value over 357 Kelvin (K). After initial formation near the center of the maximum, the MCS developed northeast, along a theta-e ridge, and over a very tight theta-e gradient. In this case, all three theta-e patterns were identifiable.

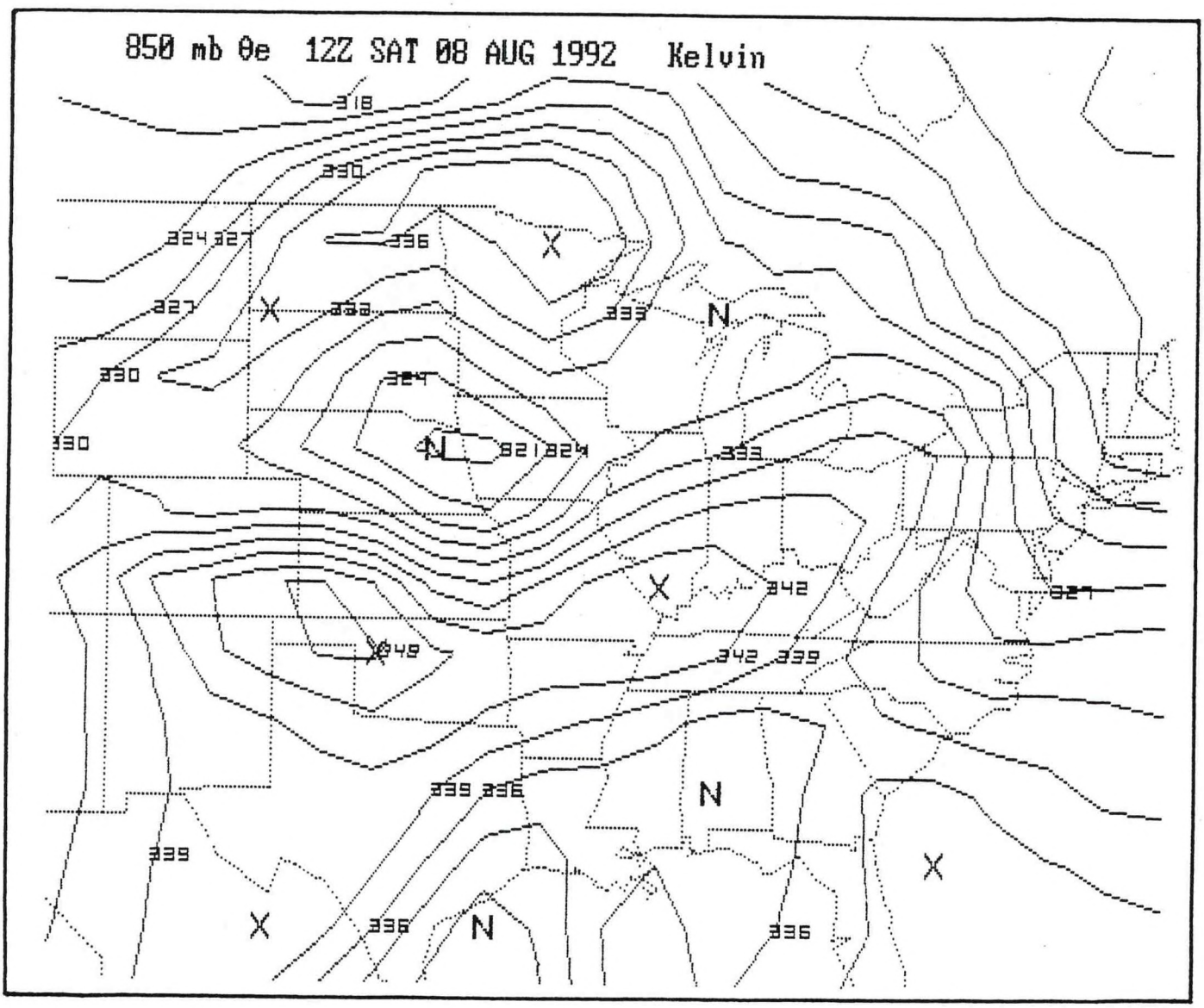

Figure 2. Theta-e analysis of the central and eastern United States for 8 August 1992 at 1200 UTC. Output is from PC-THETAE program (Last 1991).

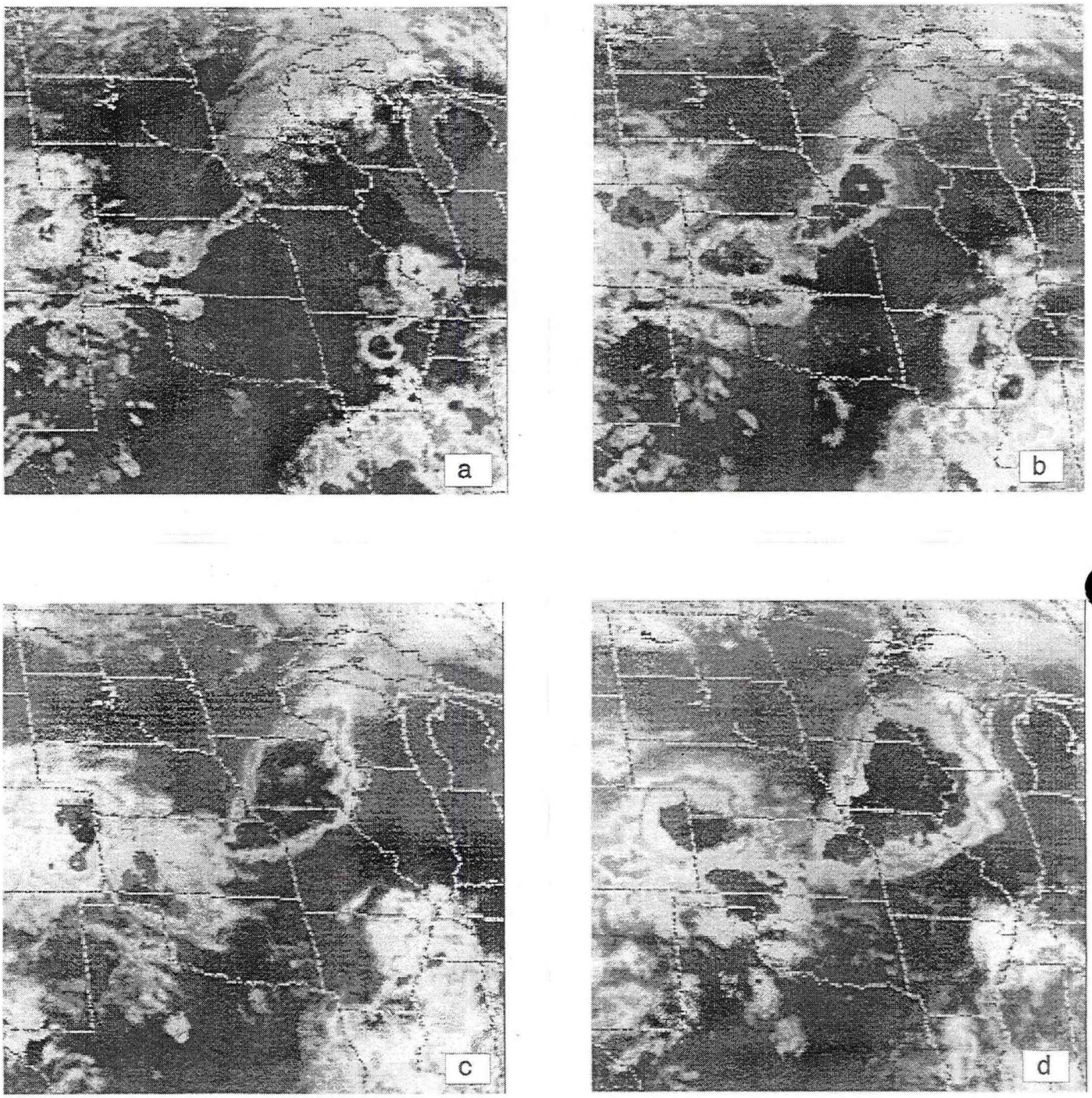

Figure 3. As in Figure 1, except for 15 July 1992 at (a) 2201 UTC, and 16 July 1992 at: (b) 0001 UTC, (c) 0201 UTC, and (d) 0401 UTC.

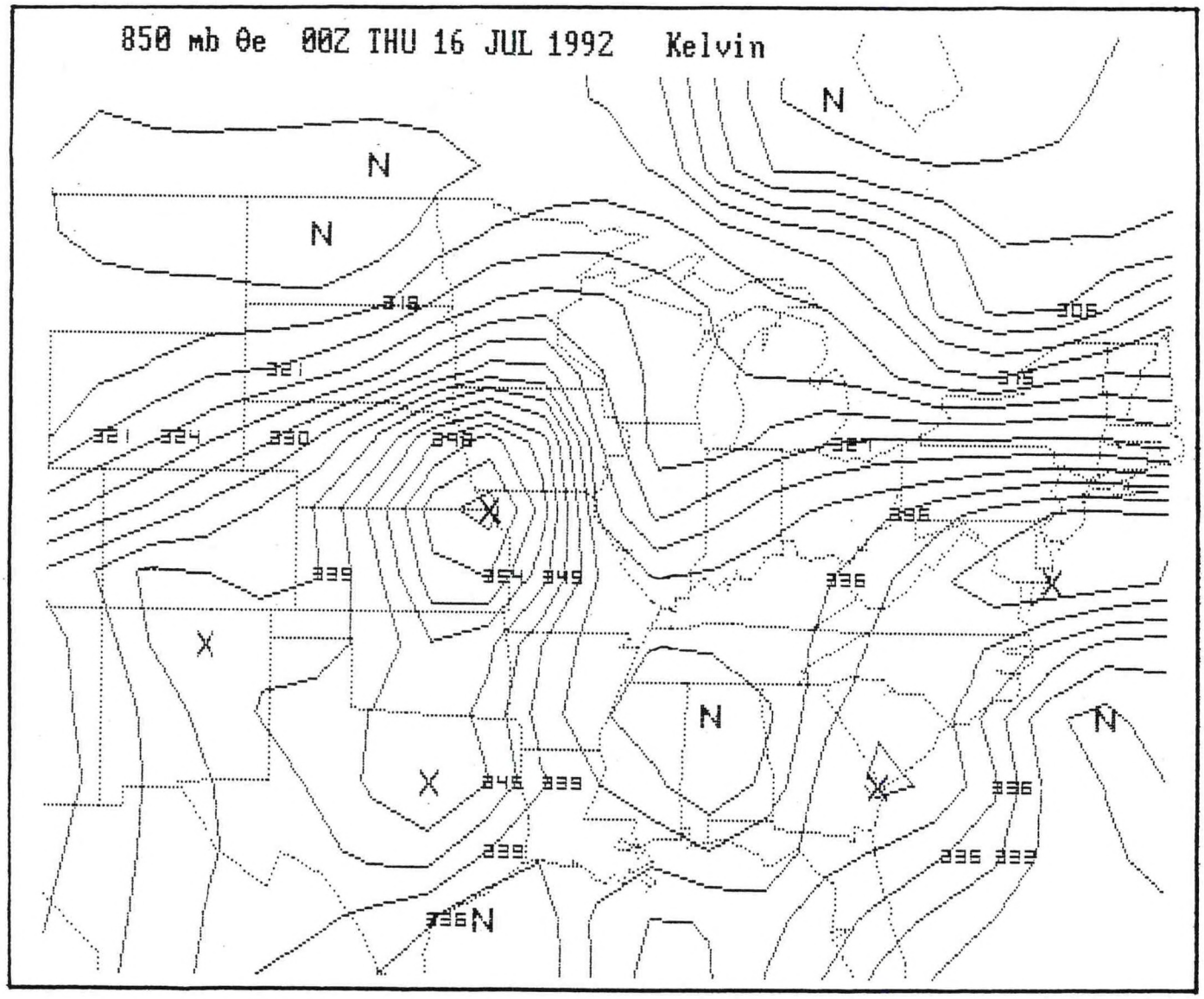

Figure 4. As in Figure 2, except for 16 July 1992 at 0000 UTC.

C. MCS development along a theta-e gradient

Late in the afternoon of 12 July 1992, thunderstorms rapidly developed along a stationary front over the central plains and midwest. Two-hourly satellite imagery between 2300 UTC, 12 July and 0500 UTC, 13 July is shown in Figure 5.

Figure 6 is the 850 mb theta-e analysis for 0000 UTC, 13 July. Note how the line of thunderstorms developed north of the theta-e ridge, along a strong gradient between high theta-e values to the south and low values to the north. What is fascinating in this example is how the storms initially "lined up" in an "S" like shape (Figure 5a-c). It is nearly identical to the S-pattern seen in the theta-e analysis. Again, severe weather and heavy rain were associated with some of the storms from Kansas to Indiana.

4. Discussion

In each of the examples of MCS development, the associated theta-e patterns were easily recognizable. Values of 850 mb theta-e exceeded 340 K in all three cases, indicating high CAPE. Fronts or upper-level short waves were also present, providing a lifting mechanism to release the instability. Unfortunately, the theta-e analyses were available only **after** thunderstorm organization was well underway, almost after the fact, and perhaps too late to be used in a **forecast**.

Is it possible to forecast these patterns? It is important to note that equivalent potential temperature is conserved in either dry adiabatic or pseudo-adiabatic displacements (Saucier 1989), and therefore is trackable over time. Poor upper-air data resolution, daytime heating over higher terrain, and vertical motion, however, make tracking significant theta-e patterns over long distances or long time periods difficult. It may be that a numerical forecast of low-level theta-e (using output from the Nested Grid Model [NGM] or Eta Model, for example) would be simpler and more accurate than attempting to estimate a theta-e pattern 12 or more hours in the future. Theta-e forecasts are available, but on a limited basis. A personal computer based program, called PCGRIDDS (Petersen 1991) allows analysis of grid point output, which includes theta-e fields, from either the NGM or Eta Model. As the availability of the gridded data increases, future work will likely focus on the accuracy of low-level theta-e model output and how it relates to MCS development.

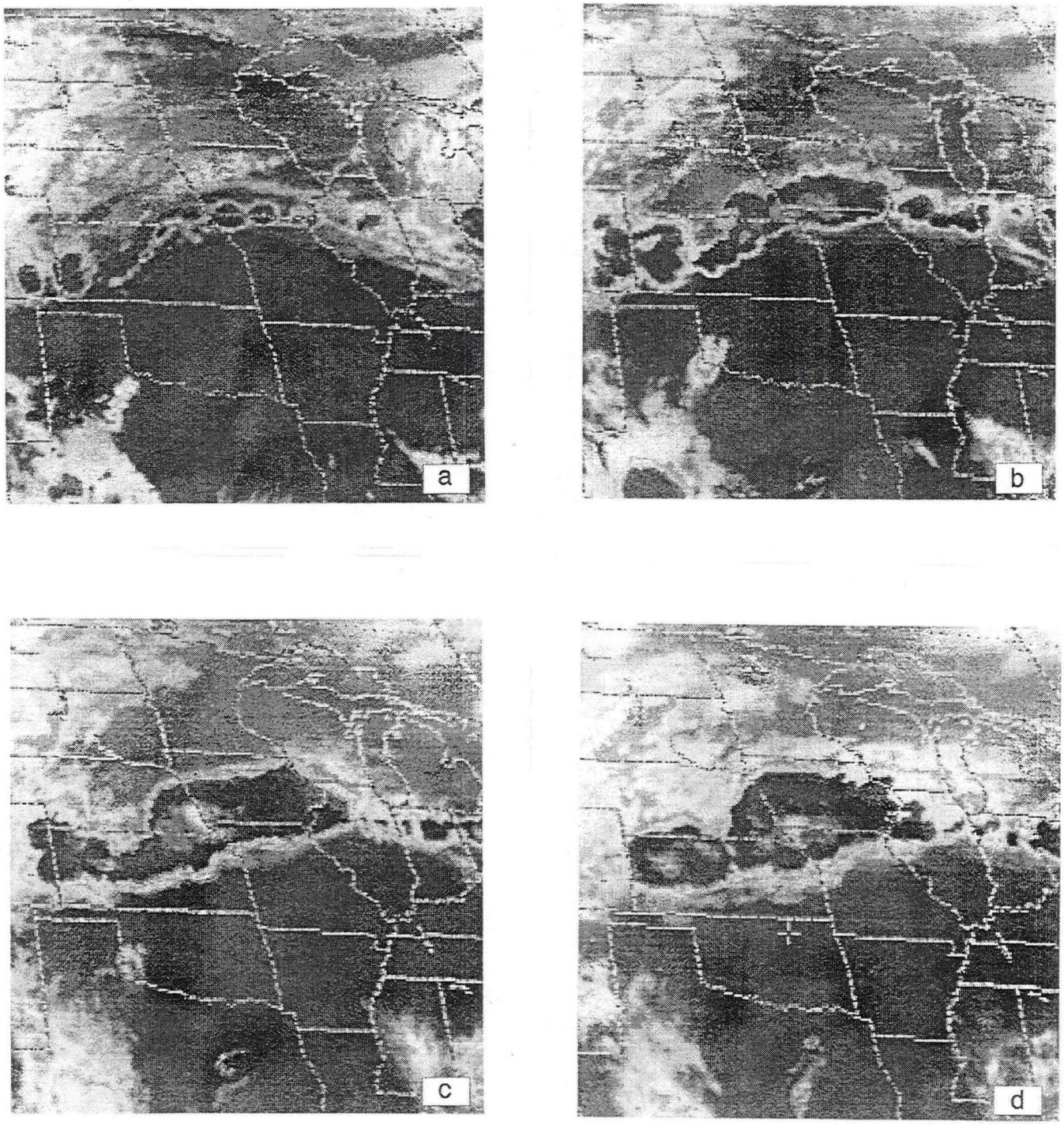

Figure 5. As in Figure 1, except for 12 July 1992 at (a) 2301 UTC, and 13 July 1992 at: (b) 0101 UTC, (c) 0301 UTC, and (d) 0501 UTC.

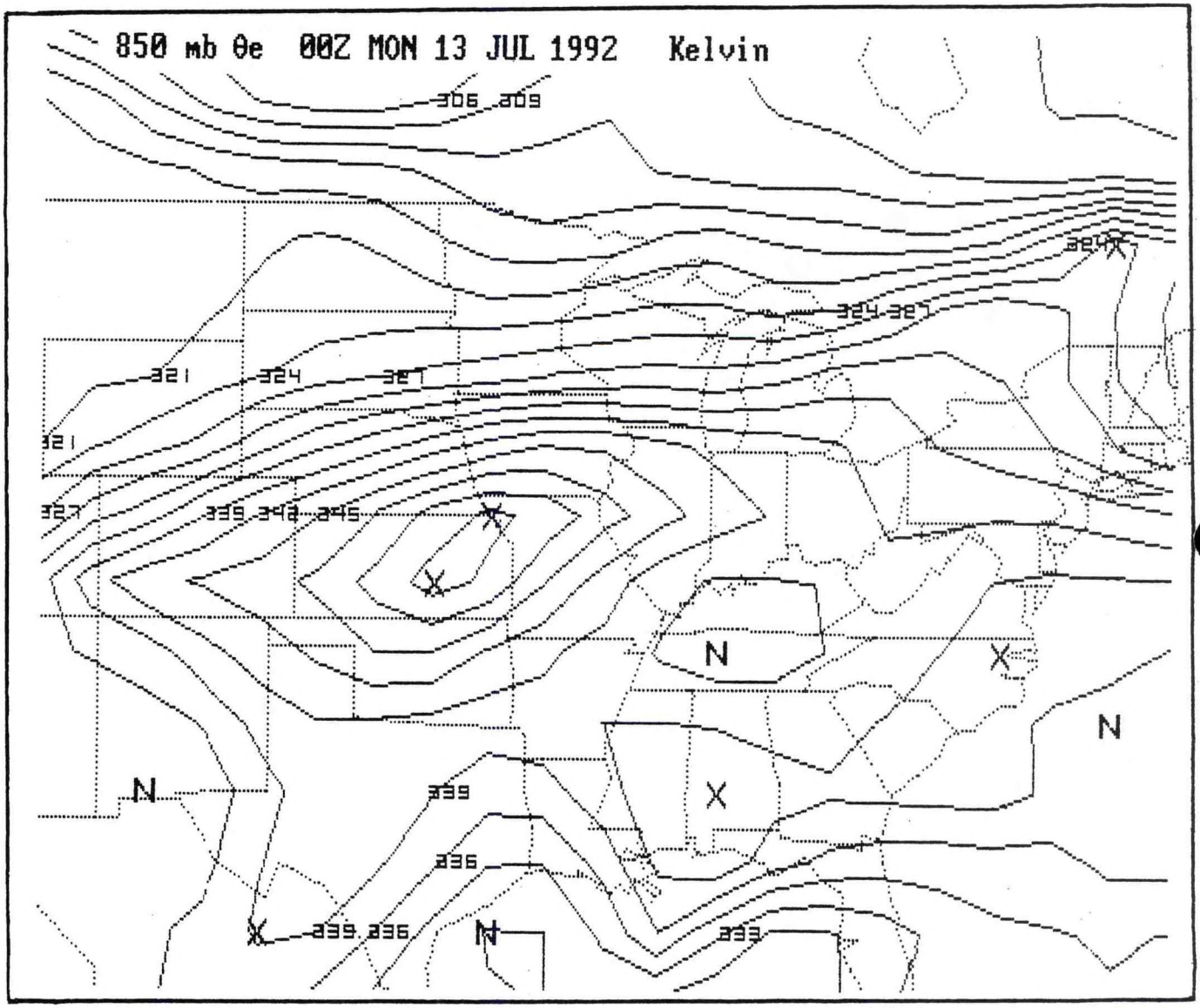

Figure 6. As in Figure 2, except for 13 July 1992 at 0000 UTC.

5. Summary

Low-level theta-e analyses have been shown to be useful in identifying areas of high CAPE and possible thunderstorm formation. Pattern recognition techniques can be used with theta-e analysis since significant thunderstorm development often occurs in three distinct patterns: theta-e maxima, theta-e ridges, and theta-e gradients north of theta-e ridges. It should be restated, however, that high theta-e values alone are not enough to produce MCSs -- a mechanism to lift the air must also be present.

6. Acknowledgments

I am grateful to Rick Ewald, NWS Central Region Scientific Services Division, for his quick response to my requests for satellite imagery used in this paper. I also would like to thank Anthony Siebers, NWS Forecast Office at Milwaukee/Sullivan, for his helpful comments.

7. References

Campbell, M., 1991: Equivalent potential temperature (theta-e) applications. Western Region Technical Attachment 91-37, NWS Western Region, Scientific Services Division, Salt Lake City, Utah.

Cylke, T., 1992: The development and evolution of flash-flood producing thunderstorms over southern Nevada on August 10, 1991. Western Region Technical Attachment 92-23, NWS Western Region, Scientific Services Division, Salt Lake City, Utah.

Kusselson, S. J., 1990: Using satellite imagery and instability bursts to forecast a wide-spread flood event in the northeastern United States. *Preprints, 8th Conference on Hyrdrometeorology*, Amer. Meteor. Soc., Kananaskis Park, Alberta, Canada, 118-123.

Last, J. K., 1991: PC-THETAE. Central Region Computer Programs NWS CRCP - No. 9MC. NWS Central Region, Scientific Services Division, Kansas City, Missouri.

Petersen, R. A., 1991: PC-GRIDDS: A P.C. based gridded informa tion display and diagnosis system. Unpublished.

Saucier, W. J., 1989: *Principles of meteorological analysis.* Dover Publications, Inc., 438 pp.

Scofield, R. A., 1990: Instability bursts associated with extratropical cyclone systems (ECSs) and a forecast index of 3-12 hour heavy precipitation. NOAA Technical Memorandum NESDIS 30, National Environmental Satellite, Data, and Information Service, Washington, D.C., 77 pp.

_____ and J. Robinson, 1989: Instability bursts and mesoscale convective system development and propagation. Satellite Applications Information Note 89/2, National Environmental Satellite, Data, and Information Service, Washington, D.C.